Age-related Differences in the Neural Mechanisms of Episodic Memory: Representational and Network Analyses

by

Lifu Deng

Department of Psychology and Neuroscience
Duke University

Date:_____

Approved:

_____
Roberto Cabeza, Dissertation Advisor

_____
Simon Davis

_____
Tobias Egner

_____
Gregory Samanez-Larkin

Dissertation submitted
in partial fulfillment of the requirements for
the degree of Doctor of Philosophy in the Department of
Psychology and Neuroscience in the Graduate School of
Duke University

2023

ABSTRACT

Age-related Differences in the Neural Mechanisms of Episodic Memory:
Representational and Network Analyses

by

Lifu Deng

Department of Psychology and Neuroscience
Duke University

Date:_____
Approved:

_____
Roberto Cabeza, Dissertation Advisor

_____
Simon Davis

_____
Tobias Egner

_____
Gregory Samanez-Larkin

An abstract of a dissertation submitted
in partial fulfillment of the requirements for
the degree of Doctor of Philosophy in the Department of
Psychology and Neuroscience in the Graduate School of
Duke University

2023

Abstract

Advanced age is associated with substantial changes in the brain. These changes can be attributed to many difference sources, such as detrimental effects of aging, brain's compensatory responses to such negative effects, and cognitive or neural resources acquired over lifespan. As a result, under the same cognitive task, healthy older adults (OAs) often show recruitment of brain regions that are different from healthy young adults (YAs). These observations have been drawn from functional magnetic resonance imaging (fMRI) studies on aging and cognition, which have been largely based on univariate analysis that relates experimental conditions to activity level in individual brain region. While univariate analysis reveals the age differences in the recruitment of brain regions, much remains unknown regarding how these regions are playing their roles. Meanwhile, recent methodological advances in cognitive neuroscience have provided the opportunities to examine 1) functional communications across brain regions, and 2) information stored in the distributed neural representation in a region. In this dissertation, I described age-related differences in these two novel perspectives in a series of fMRI studies on episodic memory, a domain of cognition that is particularly affected by aging. In these studies, healthy YAs and OAs encoded and later retrieved images of scenes or objects inside the scanner. Analyses on functional brain network and neural representations were conducted on the neuroimaging data. These analyses

revealed three main findings. First, neural representation and functional connectivity revealed reduced involvements of the core task regions in OAs. During encoding, early visual cortex (EVC) in OAs exhibited reduced representation of visual information. During retrieval, medial temporal lobe (MTL) in OAs exhibited reduced reconfiguration of functional connectivity associated with successful remembering. Second, enhanced recruitments of additional neural resources in OAs were also observed. During encoding, anterior temporal lobe (ATL) in OAs exhibited enhanced semantic representation. During retrieval, prefrontal cortex (PFC) in OAs showed enhanced functional connectivity and stronger reconfiguration of connectivity associated with successful remembering. Finally, we found that schematic knowledge affected functional communication in PFC and semantic representation in ATL differently in the two age groups, suggesting that schema-related strategies may be preferentially selected by OAs. Taken together, these studies depicted the detrimental effect of aging and brain's adaptive changes in two novel perspectives: functional communication and information processing, which may contribute to a more comprehensive understanding of episodic memory function in aging populations.

Dedication

To my Parents, for their unwavering love and supports; and to Mengdan Xie, for being my better half.

Contents

List of Tables

List of Figures

Acknowledgements

I would like to express my deep gratitude to my advisor, Roberto Cabeza, and my co-advisor, Simon Davis. I am extremely lucky to have the opportunity to work under the guidance of Roberto and Simon in an area that is truly meaningful and rewarding. I have benefited tremendously from their wisdom in synthesizing existing evidence, identifying the significance of a problem, and telling a story effectively, which will have a deep and positive impact on my career for the years to come.

I am grateful to Tobias Egner and Gregory Samanez-Larkin, who kindly offered to serve as my committee members and have provided insightful feedbacks on my research projects. I also want to thank Tobias and Greg for their efforts in fostering a supportive environment within the Center for Cognitive Neuroscience community, which makes my trainee experience in the past few years a memorable journey.

I appreciate the generous helps from current and previous members of Cabeza Lab. My early projects have received substantial supports from lab alumni Erik Wing, Benjamin Geib, Matthew Stanley, and Zachary Monge. In specific, Chapter 3 is the fruition of Zach's pioneering work. Margaret McAllister and Erin Welch helped me a lot in piloting and data collection. I also want to thank Cortney Howard, Shenyang Huang, Christina Yu, Ricardo Morales, Matthew Slayton, and Tory Worth for their helps and for being the best labmates. Besides Cabeza Lab members, I would like to thank Todd Harshbarger and Andrew Michael for providing technical supports.

1. Introduction

As we age, the anatomy and physiology of our brain deteriorate, leading to decline in multiple cognitive abilities, such as memory, attention, and processing speed (Dennis, Gutchess, & Thomas, 2020). Meanwhile, the aging brain does not endure these changes passively: across the lifespan, brain builds up various neural and cognitive reserves, and it attempts to compensate for the negative consequences of aging with additional neural resources (Reuter-Lorenz & Cappell, 2008; D. C. Park & Reuter-Lorenz, 2009; Cabeza, Albert, et al., 2018; Dennis et al., 2020; Stern et al., 2023). These factors contribute jointly to the complex picture of brain's resilience to aging.

One of the significant progresses in the field of cognitive aging has been contributed by neuroimaging studies that investigated brain activities during cognitive performance, using positron emission tomography (PET), and more recently, functional magnetic resonance imaging (fMRI). These studies revealed systematic patterns of age differences in brain regions recruited during task performance (Li et al., 2015). For example, under the same task condition, older adults (OAs) often show more recruitment of contralateral hemisphere than young adults (YAs), which is known as the hemispheric asymmetry reduction in older adults (HAROLD; Cabeza, 2002). OAs also tend to display weaker activity in posterior brain regions, but stronger activity in anterior brain regions, which is known as the posterior-anterior shift in aging (PASA) (Davis, Dennis, Daselaar, Fleck, & Cabeza, 2008).

Most of the early fMRI studies on cognitive aging are based on univariate analyses, which measure mean activity level in individual brain regions, often with regard to different experimental conditions (Poldrack, Mumford, & Nichols, 2011). Although these studies have yielded a wealth of findings and insights by linking age-related differences in the recruitment of brain regions to the cognitive processes associated with different experimental conditions, they are limited in at least two aspects. Firstly, while univariate analyses attribute task performances to activities in individual brain regions, these regions do not operate independently. Instead, individual regions are thought to perform relatively simple processes, and they need to interact closely with each other in order to fulfill a cognitive task (Cabeza, Stanley, & Moscovitch, 2018). In recent years, sophisticated network analyses have been developed to investigate many forms of biological networks, including structural and functional brain networks (E. Bullmore & Sporns, 2009; E. T. Bullmore & Bassett, 2011). This methodological advance has gained increased attention from cognitive neuroscience researchers, although applications of network analysis in aging studies have been scarce. Secondly, univariate analyses can determine if the mean activity of a region is higher in OAs or YAs but cannot assess the nature and quality of the information processed or stored in that region. Such gap in knowledge can now be bridged by recent developments in representational analyses that infer the coding of information based on the multivoxel activation patterns (i.e., neural representations; Norman, Polyn, Detre, &

Haxby, 2006; Kriegeskorte, 2008), and it has been a nascent trend in the field of cognitive aging to examine age-related changes in information processing at the representational level.

This dissertation aims to reveal the differences between healthy YAs and OAs in their functional brain network and neural representation during episodic memory, a domain of cognitive function known to be particularly affected by aging (Nyberg, Lövdén, Riklund, Lindenberger, & Bäckman, 2012). We examined the functional brain network during retrieval (i.e., remembering of the previous experiences) and the neural representation during encoding (i.e., new experiences that form later memory). In addition, we also investigated the effect of schematic knowledge on brain network and representation in the two age groups. These investigations are carried out in four separate studies, which are described in detail in Chapters 2, 3, 4, and 5. We briefly outlined these studies in the following subsections.

1.1 Age-related Differences in Large-scale Functional Network during Memory Retrieval

Many complex systems in nature and human society exhibit network-like architecture, and the brain is not an exception. The intricate network-like anatomical structure of the brain has been revealed at multiple levels – from specific cytoarchitecture at microscopic level, to the local pathway in a structure that implies certain computational function, to large white matter tracts that bridge distant parts of the brain. Such hierarchical layout allows both functional specialization and integration

(Meunier, Lambiotte, & Bullmore, 2010), which are thought to support complex behaviors that emerge from the cooperation of relatively simple processes (E. Bullmore & Sporns, 2009; Yuste, 2015; Krakauer, Ghazanfar, Gomez-Marin, MacIver, & Poeppel, 2017). This organization emphasizes the importance of the analysis on functional network. In functional network analysis, different regions are treated as network nodes, and functional coupling between the regions are treated as connections, or edges as they are known in graph theory. In fMRI network analyses, the nodes are regions-of-interest (ROIs)—of different size depending on the atlas used—and the connections are assessed based on the covariation in blood oxygenation level dependent (BOLD) signal over time. A core assumption in fMRI-based network analyses is that, if activity in two brain regions is correlated over time, then the two regions are communicating neural signals.

Early investigations on functional brain network, including early studies on aging, were almost exclusively based on resting- state fMRI. During a resting-state fMRI study, participants are instructed to relax and not to think of something in particular. The BOLD signal in resting state is believed to reflect spontaneous brain activity, and the correlation value between the BOLD signals in each pair of brain region is assigned to the corresponding edge in the brain network, which reveals the spontaneous organization of the whole brain network. The convenient setup for resting-state fMRI results in a large corpus of existing studies, and the almost uniform experimental condition also facilitates cross-study comparison and meta-analysis. An accumulating

body of literature has pointed to the biological and behavioral relevance of resting-state brain network. For example, resting-state connectivity can be predicted by white matter connections (Greicius, Supekar, Menon, & Dougherty, 2009; Goñi et al., 2014) and the activation pattern during task (van den Heuvel & Hulshoff Pol, 2010; Bertolero, Yeo, & D'Esposito, 2015; Cole, Ito, Bassett, & Schultz, 2016), and cognitive performance has been found to correlate with the topological properties of resting-state network (Heuvel, Kahn, Goñi, Sporns, & van den Heuvel, 2012). In short, resting-state network is biologically meaningful and provides a holistic view of the brain, which is suitable for data-driven, exploratory analysis.

One issue of resting-state network analysis is its limited interpretability, as it cannot directly attribute a certain network characteristic to cognitive function. This can be addressed by directly analyzing functional network during task performance. Indeed, there has been emerging evidence that the brain network reconfigures qualitatively between task and rest and between different tasks (Gallen, Turner, Adnan, & D'Esposito, 2016; Hearne, Cocchi, Zalesky, & Mattingley, 2017; Davis et al., 2018). Importantly, these changes do not necessarily occur in key 'connectivity hub' regions that are often highlighted in resting-state network studies, but rather in regions that are most relevant to the task. For example, one study showed that, during memory retrieval, hippocampus, although not being a central region in the whole brain network, exhibited greatest memory-related changes in network measures such as path length and

centrality among all brain regions in the network (Geib, Stanley, Wing, Laurienti, & Cabeza, 2017), which suggests that hippocampus becomes a more efficient and central node in the whole brain network to support successful memory retrieval, adding to the existing knowledge that hippocampus interacts with different brain regions to retrieve memory traces stored in them (Alvarez & Squire, 1994; McClelland, McNaughton, & O'Reilly, 1995; Teyler & Rudy, 2007). This study further implies the need to examine the age-related differences in functional brain network during retrieval: earlier studies using univariate analyses have reveal that, during memory retrieval, OAs showed reduced activation in the medial temporal lobe (MTL) regions, the core memory system that includes the hippocampus, while they also showed increased activation in prefrontal cortex (PFC) (Gutchess et al., 2005; Daselaar, Fleck, Dobbins, Madden, & Cabeza, 2005; Dennis, Daselaar, & Cabeza, 2007; Davis et al., 2008). This age-related increase in PFC activity is often associated with enhanced cognitive performance, suggesting that, while MTL in OAs is negatively impacted by age, neural resources in PFC are recruited to compensate for such deficit. It can be expected that, in OAs, MTL may display deficits in functional connectivity, while PFC could be in a more central position in the brain network and exhibit network measures that vary with memory performance. However, the mechanisms of such age-related deficits and compensation in functional brain network remains elusive.

To investigate this, we examined the age-related difference on the functional brain networks during episodic memory retrieval. YAs and OAs participants encoded and recalled visual scenes, and age-related differences in network topology during memory retrieval were investigated as a function of memory performance. We measured 1) changes in functional integration and 2) reconfiguration in connectivity patterns. The study yielded three main findings. First, PFC regions were more functionally integrated with the rest of the brain network in OAs. Critically, this age-related increase in PFC integration was associated with better retrieval performance. Second, PFC regions showed stronger performance-related reconfiguration of connectivity patterns in OAs. Finally, the magnitude of PFC reconfiguration increases in OAs tracked reconfiguration reductions in MTL, suggesting that PFC connectivity in OAs may be compensating for MTL deficits. These results are presented in detail in **Chapter 2**.

1.2 Age-related Differences in Neural Representation during Visual Perception

Cognitive neuroscience theories assume that cognitive tasks are accomplished by a set of interacting processing components. Each component receives information, operates on it, and sends it to other components. Different processing components are mediated by different brain regions, that information transfer and management are mediated by interactions between regions, and the information itself is represented within each region involved. In fMRI studies, univariate analyses, when combined with

proper task design, can be used to link each of these regions to the presumed processing component; network analyses can be used to investigate information transfer and control processes between the processing components. However, neither univariate analysis nor network analysis provides evidence regarding the nature of the information processed by each region, that is, the representations.

This evidence is now provided by representational analyses, which take advantage of the spatial distribution of neural activity within a region to interrogate the coding of underlying information, using different analytical techniques such as multi-voxel pattern analysis (MVPA) (Norman et al., 2006) or representational similarity analysis (RSA) (Kriegeskorte, 2008). The application of representational analyses to aging research is very recent, and hence few studies are currently available. An important and convergent finding of the existing aging studies highlights the dedifferentiation of visual representation with aging: the activation patterns in occipital and/or temporal cortices (OTC) for different visual stimuli are less distinct in older (OAs) than younger (YAs) adults, suggesting an age-related reduction of the specificity of visual information in OTC (Koen & Rugg, 2019). For example, when viewing stimuli of two different categories (e.g., faces versus houses), OAs showed reduced activation patterns specificity for the two stimuli categories (J. Park, Carp, Hebrank, Park, & Polk, 2010; Carp, Park, Hebrank, Park, & Polk, 2011; Koen, Hauck, & Rugg, 2019). Lower representation specificity during encoding was associated with lower subsequent

memory performance in OAs (Zheng et al., 2018; Koen et al., 2019), and in one study, it also predicted reduced fluid processing ability irrelevant to the visual perception task in scanner (Park et al., 2010), indicating that such dedifferentiation is detrimental. Taken together, these findings suggest that the dedifferentiation of visual representation reflects an age-related degradation of visual information in OTC, which, subsequently, lead to reduced task performances in OAs.

Despite the important advances made by these studies, one of their limitations is that they used primarily MVPA to examine representational differences between completely different kinds of stimuli, such as places or faces, meaning that such examination measures information in neural representations in a single dimension. However, even within the same kind of stimuli (e.g., pictures of animals), rich information exists among multiple feature dimensions (e.g., color, shape, physical size, animacy, taxonomy) that are processed in different brain regions (Davis et al., 2021; Hovhannisyan et al., 2021). As a solution to such complexity, model-based RSA approach can measure the processing of a certain feature (e.g., color, taxonomy) by comparing the representational structure of a brain region with that of a computational model that is sensitive to that feature dimension (Kriegeskorte et al., 2008; Kriegeskorte, 2008; Khaligh-Razavi & Kriegeskorte, 2014). In other words, RSA can attribute the variance in brain activity pattern in a region to the variance in a specific type of information of the stimuli in an explicit manner, which greatly improves the

interpretability of the data if multiple types of features/information are surveyed in the same time.

The idea of examining neural representation in separate feature dimensions is especially worth considering. This is because, although healthy aging is associated with significant visuo- perceptual deficits (Sekuler & Sekuler, 2000; Peters, Moss, & Sethares, 2001; Raz et al., 2005; Owsley, 2011), semantic knowledge continues to accumulate and is preserved in old age (D. C. Park, Polk, Mikels, Taylor, & Marshuetz, 2001; Verhaeghen, 2003; Umanath & Marsh, 2014; Spreng & Turner, 2019). Therefore, it is possible that, between healthy YAs and OAs, we may observe a dissociation of different types of representation. For example, age-related decrease may be more prominent in pure sensory (i.e., visual) representation, while the representations of semantic or categorical information may be preserved or even enhance in OAs. Furthermore, if semantic knowledge plays a role in attenuating age-related cognitive deficits, it is also possible that, the representation in brain regions that process semantic information (such as anterior temporal lobe, ATL) during perception will be reactivated during memory retrieval.

We investigate these possibilities in **Chapter 3**, in which we examined the neural representations of YAs and OAs when they were viewing (encoding) and then remembering (retrieving) naturalistic scenes. We termed the representations in the two memory phases as 'perceptual representation' and 'mnemonic representation',

respectively. First, using model-based RSA, we distinguished sensory vs. categorical features of perceptual representations. We found that, compared to YAs, low-level sensory features in early visual cortex (EVC) were less differentiated in OAs (i.e., age-related dedifferentiation), replicating previous research, whereas categorical features in ATL were more differentiated in OAs. This is, to our knowledge, the first report of an age-related hyperdifferentiation. Second, we assessed the quality of mnemonic representations by measuring encoding-retrieval similarity (ERS) in activation patterns. We found that aging impaired mnemonic representations in early visual cortex and hippocampus but enhanced mnemonic representations in ATL. Thus, both perceptual and mnemonic representations in ATL were enhanced by aging. In sum, our findings suggest that aging impairs visual and mnemonic representations in posterior brain regions but enhances them in anterior regions.

1.3 The Effect of Schema on Functional Connectivity and Neural Representations in Young and Older Adults

Network and representation analyses provide novel perspectives of the differences in neural mechanisms between YAs and OAs. These findings further highlight the necessity of understanding the underlying cognitive differences between the two age groups that drive the observed age difference in fMRI. Under the same objective task condition (e.g., encoding and retrieving visual images in our case), OAs may adopt certain cognitive processes (and hence the associated neural resources) that are available to but not employed by YAs, due to the age-related deficits in the neural

resources that typically support the task in YAs (Cabeza, Albert, et al., 2018). Empirical findings of the associations between age-related neural differences and the potential cognitive strategies may have considerable practical implications, ranging from the development of more effective intervention (e.g., cognitive training, neural stimulation) to counter negative impact of aging, to the design of user interfaces of products and software applications that are more intuitive and user-friendly to OAs.

The findings in **Chapter 2** and **Chapter 3** hinted at possible cognitive strategies in OAs that may drive the age-related differences at the network and representation levels. In specific, we are interested in the utilization of schema, which refers to a memory framework of experiences and associations that can be activated by certain context (e.g., the common actions you do and the common objects you see when you go to a restaurant). Schema often serves a supportive role in cognitive functioning, guiding decisions and predictions, and facilitating the integration of new information into long term memory (van Kesteren et al., 2013; Ghosh, Moscovitch, Melo Colella, & Gilboa, 2014; Hebscher & Gilboa, 2016). Meanwhile, there has been behavioral evidence that OAs may rely more on schematic knowledge (Mather, Johnson, & De Leonardis, 1999; Brashier, Umanath, Cabeza, & Marsh, 2017). Thus, the neural effects of schema in YAs and OAs deserve further exploration.

Schema processing has been strongly linked to PFC regions. In specific, ventral medial PFC has been thought to facilitate integration and reactivation of information

and augment the function of MTL (van Kesteren, Fernandez, Norris, & Hermans, 2010; van Kesteren et al., 2013; Preston & Eichenbaum, 2013; Ghosh et al., 2014). The role PFC plays in schema processing offers one possible explanation for the findings in **Chapter 2**, that is, an increased PFC engagement in the brain network accompanied by a reduced MTL engagement in OAs. In addition, schema is developed through lifetime and often highly semantic, meaning that an activating schema should be accompanied by the processing of semantic information. Although direct neuroimaging evidence has been lacking, such possibility may explain the age-related increase in semantic representation in ATL, as observed in **Chapter 3**. These speculations can be further testified in studies using similar encoding-retrieval paradigm that incorporates manipulation of schema availability.

Thus, in **Chapters 4 and 5**, we interrogated the effects of schema on global functional connectivity and neural representations in YAs and OAs. An experimental paradigm was designed to manipulate the congruency of schema to visual objects. In each trial, participants first viewed a scene, and after a brief pause, an object, and they were instructed to respond the likelihood of finding the object in the scene. The scenes and objects were paired in varying levels of schema congruency, such that some objects are highly congruent with the schema provided by the preceding scene (e.g., farm -> tractor), and some are highly incongruent (e.g., prison -> poker table). The memories for the objects were tested in the following day, and participants showed higher memory

for objects that fitted congruently with scene schemas, confirming that memory can benefit from a schema-related strategy.

In **Chapter 4**, we investigated the encoding neural representation of visual and semantic information about the objects in ventral visual regions in the occipital and/or temporal cortices, including EVC and ATL. We observed an age-related decrease of visual representation in early visual cortex (EVC), confirming our previous finding in **Chapter 3** on age-related dedifferentiation of visual processing. Schema congruency showed age-invariant effects on the visual representation in lateral occipital cortex (LOC) and the semantic representation in fusiform gyrus (FG), suggesting that schema influences the processing of both visual and semantic information in OTC regions. Crucially, in ATL, we found an interaction effect between age and schema congruency on semantic representation, as OAs showed an increase of semantic representation with schema congruency. This finding offers one possible explanation for the age-related difference in ATL semantic representation in **Chapter 3**, that is, such age difference may be contributed by schema-related processes that are preferentially employed by OAs.

In **Chapter 5**, we investigated the functional brain network during retrieval. We sought to link the functional connectivity in PFC and MTL to two factors: 1) memory performance (remember vs forgotten), and 2) schema congruency of the remembered items in encoding. We found that MTL in OAs was less integrated with the global functional network; while stronger MTL functional connectivity with other parts of the

brain was associated with successful memory in YAs, such relationship was absent in OAs. These observations converge with our previous findings in **Chapter 2**, suggesting the central role of MTL during memory retrieval in YAs and the impact of age on this system. In addition, schema congruency showed modulatory effects on the connectivity of two PFC sub-systems in OAs, indicating the presence of schema-related strategies. In contrast, no schema effect was found in YAs. Taken together, the results in **Chapter 4** and **Chapter 5** provide preliminary neural evidence that OAs may prefer schema-related processing during memory encoding and retrieval.

2. Age-related Compensatory Reconfiguration of PFC Functional Connectivity during Episodic Memory Retrieval[1]

2.1 Introduction

Despite substantial anatomical and functional decline, the aging brain retains a surprising degree of neural plasticity and functional flexibility (Cabeza, Albert, et al., 2018; D. C. Park & Reuter-Lorenz, 2009). In functional neuroimaging studies, for example, compared to YAs, OAs tend to exhibit increased neural activity in the PFC in a wide range of tasks (Turner & Spreng, 2012; Cabeza & Dennis, 2012; Lighthall, Huettel, & Cabeza, 2014; Spreng & Turner, 2019). This age-related increase in PFC activation is often attributed to *functional compensation*, which has been defined as a cognition-enhancing over-recruitment of neural resources in response to cognitive demands (Cabeza, Albert, et al., 2018). Most previous studies reporting compensation in OAs have focused on the activity of individual regions without addressing how those regions are interconnected with other brain areas. The human brain is, however, a large-scale complex network of interconnected and interdependent regions, and the transient, dynamic patterns of functional connections between them is essential for human

[1] The contents in this chapter are extracted from a coauthored publication on *Cerebral Cortex*: "Deng, L., Stanley, M. L., Monge, Z. A., Wing, E. A., Geib, B. R., Davis, S. W., & Cabeza, R. (2021). Age-Related Compensatory Reconfiguration of PFC Connections during Episodic Memory Retrieval. Cerebral Cortex (New York, NY: 1991), 31(2), 717-730". LD, SD, and RC were supported by grant NIH-MH114253-01. EW and RC were additionally supported by grants NIH-AG058574 and AG019731. ZM and BG were supported by grants F31AG060691 and F31MH114454, respectively. Copyright is granted by the Oxford University Press through the Copyright Clearance Center.

cognition (Bressler & Menon, 2010; Medaglia, Lynall, & Bassett, 2015; Cabeza, Stanley, et al., 2018; Stanley, Gessell, & De Brigard, 2019). For this reason, age-related compensation can only be successful if it involves not only changes in the activity of individual brain regions but also changes in functional connections between these regions and the rest of the brain. Thus, it is critical to show that the PFC regions over-recruited by OAs change their topological properties within the whole-brain network to facilitate functional compensation.

To investigate this issue, we assessed large-scale functional brain networks in YAs and OAs during episodic memory retrieval. We addressed three specific goals. The first goal was to investigate whether PFC regions become more integrated, or functionally interconnected, with the rest of the functional brain network in OAs relative to YAs, and whether this age-related increase in PFC-brain connectivity is associated with better cognitive performance. If a systematic shift in PFC functional connectivity (fCON) is associated with better cognitive performance in OAs, such result would meet the first of two essential criteria for identifying functional compensation (Cabeza, Albert, et al., 2018). Finding a positive association between network integration and cognitive performance is crucial for interpreting changes as compensatory – this is because network integration increases are not always advantageous. Some studies using task-related fMRI have linked increased network integration to better cognitive performance in YAs (Westphal, Wang, & Rissman, 2017; Geib, Stanley, Dennis, Woldorff, & Cabeza,

2017; Geib, Stanley, Wing, et al., 2017) and in OAs (Gallen et al., 2016; Crowell et al., 2020). However, resting-state fMRI studies have linked age-related increases in network integration to a loss of differentiation in the modular network structure (Chan, Park, Savalia, Petersen, & Wig, 2014; Chan, Alhazmi, Park, Savalia, & Wig, 2017) and a reduction in grey matter volume (Geerligs, Renken, Saliasi, Maurits, & Lorist, 2015). Thus, increased PFC integration is not necessarily beneficial for cognitive performance, and it could reflect a reduction in neural specificity. Therefore, a positive association with performance is essential for attributing this effect to functional compensation.

The second goal of the current study was to examine whether OAs, relative to YAs, are more likely to *reconfigure* their PFC connections to enhance memory performance. Whereas "integration" refers to mean increases in connectivity strength between discrete pairs of cortical nodes in different brain communities or modules (e.g., aging increases the average connectivity between Regions A, B, and C), "reconfiguration" refers to changes in the pattern of connections (e.g., aging increases connectivity between Region A and Region B but reduces connectivity between Region A and Region C, although the average connectivity between them may remain unchanged). That is to say, we focused on whether and to what extent the global connectivity patterns of PFC nodes in the high memory state display dissimilarity with the global connectivity patterns in the low memory state. Converging lines of evidence suggest that transient, dynamic changes in patterns of functional connectivity are crucial

for supporting cognitive functions across task domains and demands (Cole et al., 2013; Cole, Bassett, Power, Braver, & Petersen, 2014; Spielberg, Miller, Heller, & Banich, 2015; Gallen et al., 2016; Simony et al., 2016; Hearne et al., 2017; Geib, Stanley, Wing, et al., 2017; Geib, Stanley, Dennis, et al., 2017; Davis et al., 2018). The ability for PFC regions to flexibly reconfigure their functional connections is thought to subserve control-related functions (Cole et al., 2013), including those that play a role in facilitating successful memory retrieval (Monge, Stanley, Geib, Davis, & Cabeza, 2018). Therefore, the age-related compensatory role of PFC regions during episodic memory retrieval might be associated with greater reconfiguration of PFC connections.

Finally, the third goal of the study was to investigate whether increased age-related PFC functional reconfiguration is associated with any deficit in another task-related region, such as the MTL. The notion of functional compensation implies the existence of a deficit that is being "compensated for." Thus, it is essential to show that the age-related change in neural activity or connectivity attributed to compensation is associated with an insufficiency in some other neural event thought to support the cognitive function. Such a finding would fulfill the second essential criterion for identifying compensation (Cabeza, Albert, et al., 2018). In healthy YAs, recent research has indicated that increases in memory performance are associated with the reconfiguration of functional connections in the MTL, a region commonly implicated in successful episodic memory retrieval (Geib, Stanley, Dennis, et al., 2017; Geib, Stanley,

Wing, et al., 2017). In univariate activation studies, increased PFC activity in OAs has been linked to reduced MTL activity (Gutchess et al., 2005; St. Jacques, Dolcos, & Cabeza, 2009), suggesting that PFC over-recruitment might compensate for MTL deficits in episodic memory (Cabeza & Dennis, 2012). It remains unclear, however, whether increased reconfiguration of PFC functional connections is associated with a difficulty of MTL regions to reconfigure their functional connections.

In the current study, we first investigated whether the PFC and MTL systems can be delineated by the functional network structure in a data-driven approach. We then investigated, if in OAs, compared to YAs, (1) the PFC system become more integrated with the rest of the network as a function of successful performance (*1st compensation criterion*), (2) PFC show greater performance-related network reconfiguration, and (3) PFC reconfiguration is negatively correlated with MTL reconfiguration (*2nd compensation criterion*). During fMRI scanning, YA and OA participants encoded and then recalled visual scenes with different degrees of success (low vs. high recall). Functional whole-brain networks were constructed from recall trials, with separate *high* and *low* recall networks for each individual participant. Patterns of functional connections were then characterized for *high* and *low* recall networks using several complementary graph theoretic metrics.

2.2 Methods

2.2.1 Participants

A total of 22 YAs and 22 OAs participated in this study for monetary compensation. Participants did not exhibit significant health problems (including atherosclerosis, neurological and psychiatric disorders), and not taking medications known to affect cognitive function or cerebral blood flow (except antihypertensive agents), according to their self-report. The OAs were further screened with the Beck Depression Inventory (BDI) (Beck, Ward, Mendelson, Mock, & Erbaugh, 1961) and the modified Mini-Mental State Examination (Folstein, Folstein, & McHugh, 1975) (inclusion criterion ≥ 27, M = 29.2, SD = 0.7). All participants were right-handed, fluent English speakers, and had completed at least 12 years of education. One YA and one OA were excluded because of missing functional data from the first run caused by a technical error; one additional OA was excluded from analysis due to a poor quality T1 image, which prevented the participant's functional images from being properly normalized into MNI space. Consequently, these data were analyzed with the remaining 21 YAs (M_{age} = 23.5 years, SD = 3.0 years, age range = [18-30], 9 men, 12 women) and 20 OAs (M_{age} = 70.5 years, SD = 5.4 years, age range = [61-82], 11 men, 9 women). Results from the sample of YAs (but not the sample of OAs) were previously reported in two publications (Wing, Ritchey, & Cabeza, 2015; Geib, Stanley, Wing, et al., 2017). The Duke University

Institutional Review Board approved all experimental procedures, and participants provided informed consent prior to engaging in the experiment.

2.2.2 Experimental Paradigm

Participants completed three encoding runs followed by three retrieval runs **(Figure 1A)**. During the encoding runs, participants studied pictures of complex scenes (e.g., beach, barn). There were 32 pictures shown in each encoding run, and the order of presentation was randomized within each run across participants. In total, participants viewed 96 pictures of distinct scenes. During each encoding trial (4 sec), participants were presented with a single picture that included a descriptive label below the image (e.g., "tunnel" or "barn"). Participants rated, on a 4-pt scale, the representativeness of the image for the given label (1 = not representative, 4 = highly representative). This task was included to ensure that participants would remain focused and attend to the details of each picture. Each encoding trial was followed by an active baseline interval of 8 sec, during which participants were presented whole numbers ranging from 1 to 4. Participants were instructed to select the button corresponding to the presented number. The retrieval runs were identical in format to the encoding runs with the exception that only the descriptive labels of the encoded pictures were presented. Participants were instructed to recall the scene that previously accompanied the label with as much detail as possible, and to rate the amount of memory detail with which they could remember

for the specific picture on a 4-pt scale (1 = least amount of detail, 4 = highly detailed memory).

Immediately after the scanning session, participants completed a four-alternative forced-choice recognition test outside of the scanner. For each recognition trial, the target picture from the encoding run and three distractor pictures were presented on the computer screen. Participants selected the picture they believed they saw during encoding. Then, participants rated how confident they were in the preceding recognition decision using a 4-pt scale (1 = guess, 4 = very confident).

2.2.3 MRI Acquisition

MRI data were collected on a General Electric 3T MR750 whole-body 60 cm bore MRI scanner and an 8-channel head coil. The MRI session started with a localizer scan, in which 3-plane (straight axial/coronal/sagittal) localizer faster spin echo (FSE) images were collected. Then, the functional images were acquired using a SENSE spiral-in sequence (repetition time [TR] = 2000 ms, echo time = 30 ms, field of view [FOV] = 24 cm, 34 oblique slices with voxel dimensions of 3.75 x 3.75 x 3.8 mm). The functional images were collected over six runs – three encoding runs and three retrieval runs. There was also a functional resting-state run after the third encoding run, which is not reported here. Stimuli were projected onto a mirror at the back of the scanner bore, and responses were recorded using a four-button fiber-optic response box (Current Designs, Philadelphia, PA, USA). Following, a high-resolution anatomical image (96 axial slices

parallel to the AC-PC plane with voxel dimensions of 0.9 x 0.9 x 1.9 mm) was collected. Finally, diffusion-weighted images were collected, which are not reported here. Participants wore earplugs to reduce scanner noise, and foam pads were used to reduce head motion. When necessary, participants wore MRI-compatible lenses to correct vision.

2.2.4 fMRI Preprosessing

For each run, the first six functional images were discarded to allow for scanner equilibrium. All functional images were preprocessed in a SPM12 (London, United Kingdom; http://www.fil.ion.ucl.ac.uk/spm/) pipeline. The functional images were slice time corrected (reference slice = first slice), realigned to the first scan in the first session, and subsequently un-warped. To see whether head motion was different in the two groups, we calculated the RMS of realignment parameters (Power, Mitra, et al., 2014) in both groups. No statistically significant age difference in head motion was found ($t(39)=0.93$, $p=0.36$), although the average head motion RMS showed a higher trend in OAs (0.32 mm in OAs vs 0.23 mm in YAs). In addition, head motion did not confound the results in our network analyses (see **Appendix A**, subsection '**Considerations of Head Motion and Brain Measures**'). The functional images were then co-registered to the skull-stripped high-resolution anatomical image (skull-stripped by segmenting the high-resolution anatomical image and only including the gray matter, white matter, and cerebrospinal fluid segments). The functional images were normalized into MNI space

using DARTEL (Ashburner, 2007). The study specific high-resolution anatomical image was created using all of the study participants. The voxel size was maintained at 3.75 x 3.75 x 3.8 mm^3 and the normalized-functional images were not spatially smoothed. Lastly, the DRIFTER toolbox (Särkkä et al., 2012) was used to reduce the cardiac and respiratory signals in the functional images.

2.2.5 Network Construction

We created functional brain networks for each participant during retrieval using a beta time-series analysis (Rissman, Gazzaley, & D'Esposito, 2004; Geib, Stanley, Wing, et al., 2017; Geib, Stanley, Dennis, et al., 2017). The nodes in the network were defined by the 90 regions of interest (ROIs) in AAL atlas, excluding cerebellar regions (Tzourio-Mazoyer et al., 2002). The beta time-series of each node was obtained by averaging the beta-estimate of each trial within that ROI. To obtain the beta-estimates for each retrieval trial, we conducted a single-trial model analysis within a general linear model (Mumford, Turner, Ashby, & Poldrack, 2012). This approach estimates a first-level model in which one regressor models a specific trial of interest and another regressor models all the other trials. This single-trial modelling process was repeated for every unique trial, and the beta estimates of the trials of interest were gathered for further analysis. Each trial was modeled with a stick function at trial onset convolved with standard hemodynamic response function (HRF). The temporal and dispersion derivatives of the HRF were also modelled in order to control for potential age

difference in hemodynamics (Samanez-Larkin & D'Esposito, 2008; Wright & Wise, 2018). Each model also included the six raw motion regressors, a composite motion parameter (derived from the Artifact Detection Tools [ART][2]), outlier TRs (scan-to-scan motion > 2.0 mm or degrees, scan-to-scan global signal change > 9.0 z-score; derived from ART), the white matter time-series, and cerebrospinal fluid time-series. We also modeled the temporal and dispersion derivatives and implemented a 128 sec cutoff high-pass temporal filter.

Beta-values for each trial were then matched to the memory detail scores reported by participants during each trial on the 4-pt scale. Beta-values obtained during trials where participants reported high levels of detail during recollection (ratings of 3 and 4) were combined into a beta-series for constructing the functional brain networks in the *high* memory condition; beta-values obtained during trials where participants reported low levels of detail during recollection (ratings of 1 and 2) were combined into a beta-series for constructing the functional brain networks in the *low* memory condition. For each memory condition (i.e., *high* vs. *low* memory), a connectivity matrix was constructed for each participant by calculating the Pearson's correlation of the condition-specific beta-series between all possible pairs of regions.

[2] https://www.nitrc.org/projects/artifact_detect, developed by Shay Mozes and Susan Whitfield-Gabrieli based on a previous tool by Paul Mazaika, Susan Whitfield, and Jeffrey C. Cooper.

Because the *high* and *low* memory networks were often constructed with an unequal number of trials, a bootstrap process was employed to eliminate the potential confound that observed differences in network topology could be the product of unequal trial counts in functional network construction. For the condition (i.e., *high,* or *low* memory) with more trials, a subset of *N* trials was randomly sampled, where *N* equals the number of trials in the other condition. This process was repeated 500 times, creating 500 connectivity matrices for the bootstrapped condition. Finally, the 500 connectivity matrices were averaged into one representative matrix for the bootstrapped condition. For network analyses, the diagonal values of the obtained connectivity matrix were set to zero.

2.2.6 Network Analyses

Modularity. We started the network analysis by identifying functional sub-systems, or modules. In brief, a modularity analysis based on the Louvain algorithm (Blondel, Guillaume, Lambiotte, & Lefebvre, 2008; Rubinov & Sporns, 2010) was used to detect common modular structure of the retrieval network in order to allow comparison of network measures across groups and condition (i.e., memory performance). Extra steps were included in the analysis to ensure that the modules would not bias specific age group or condition, which are detailed as follows. In the first step, a *common representative network* was created in a two-step manner. We first averaged the connectivity matrices for each age group (YA/OA) in each memory condition

(High/Low) individually, and then we averaged these four age and condition-specific networks. No statistically significant difference in the average connectivity level was found between YAs and OAs ($t(39)= -0.73$, $p= 0.47$), suggesting that the common representative network did not seem to be biased by either age group. Then, in the second step, a mask of strong connections was created by obtaining a set of X% (X tested in a range between 5 and 30 with an increment of 1) strongest connections for each *age-specific representative network* (averaged across condition), and then performing union operation on these two sets of strong average connections. The mask was then used to threshold the *common representative network* (averaged across age and condition), setting the weak connections to zeros. Here, the rationale for using a thresholded, weighted network for module detection instead of a binary network or a fully weighted network (i.e., no threshold at all) is that it allows us to optimally utilize the information in strong connections and, at the same time, exclude weak or negative connections that are difficult to interpret or just noise. Finally, the thresholded, weighted common representative network was submitted to the Louvain algorithm using a default resolution parameter (gamma) of 1. The algorithm was run 1000 times on this network, and the optimal module assignment with the highest modularity Q value was elected as the optimal module assignment under the given sparsity.

The similarity between module assignments across different levels of sparsity was quantified using a partition-similarity algorithm based on mutual-information

(Meilă, 2007). Across the different sparsity levels, we consistently obtained a 6-module partition (see **Figure 2**) when the sparsity of age-specific network was between 5% and 16%, and when the sparsity was between 5% and 10%, the module assignments were almost identical **(Appendix A, Figure 18)**. We used the module assignment at 10% sparsity as the module definition in our following analysis, because (i) this partition is clearly comparable to existing research on memory networks in aging (Gallen et al., 2016; Monge et al., 2018), (ii) it has the highest average consensus with the partition results at other thresholds (**Appendix A, Figure 18**), and (iii) this sparsity level ensures that the network will not fracture, allowing us to appropriately investigate connectivity between different modules. In addition, we computed the similarity of common module definition to the individualized module partition for each participant and compared this similarity measure between the two groups. The module partitions in OAs and YAs showed no statistically significant difference in similarity to the common module definition ($t(39)=1.13$, $p=0.27$), suggesting that the common module assignment did not seem to be biased by one of the two age groups.

Module connectivity properties. To quantify the integrative properties of the obtained modules, we computed within- and between-module connectivity (Guimerà & Amaral, 2005). The within-module functional connectivity refers to the average functional connectivity between all pairs of regions contained within the same module; the between-module functional connectivity refers to the average of all functional

connections linking the given module to other modules. Finally, a composite measure of whole-brain integration for each module was defined as the ratio of between-module functional connectivity to within-module functional connectivity:

$$Integration(Module\ x) = \frac{fCON^{x}_{between}}{fCON^{x}_{within}}, \quad (1)$$

This metric reflects the tendency of a specific module to exhibit functional interactions with other modules in the larger network. For the convenience of illustration, in the Results section the above analyses are based on 10% network sparsity (age-specific network), which is consistent with the sparsity used in the modularity analysis. It is worth noting that the results remained highly consistent across different network sparsity levels. These results are presented in **Appendix A**, **Figures 19 & 20**.

Reconfiguration. We defined the reconfiguration of functional connections between *high* memory and *low* memory conditions as one minus the Spearman's correlation of one node's connectivity vectors in *high* and *low* memory conditions (see **Figure 5A**):

$$Reconfiguration(Node\ i) = 1 - corr(\ fCON^{i}_{HighMem}\ ,\ fCON^{i}_{LowMem}), \quad (2).$$

To fully characterize the connectivity pattern and equalize the vector length for all nodes, the input connectivity vectors are based on non-thresholded network, containing all connectivity values. In consistency with previous studies (Geib, Stanley, Wing, et al., 2017), the reconfiguration values within each participant were *z*-scored before submitting to statistical analyses to control for between-participant variability,

which also served the purpose of controlling for age-related confounding factors (Wright & Wise, 2018). To ensure that fCON reconfiguration was not simply induced by statistical noise, we performed a bootstrap analysis, where the memory ratings for all trials were randomly shuffled to create surrogate *high* and *low* memory conditions **(Figure 5B)**. Bootstrapped fCON reconfiguration was calculated from the surrogate *high* and low memory fCON matrices. This process was repeated 1000 times for each participant in order to approximate a comparable null distribution of fCON reconfiguration that was not related to memory condition.

Statistical testing was carried out using R and the statistical toolbox in MATLAB (The MathWorks, Inc.). Participants' behavioral data and fCON network metrics were analyzed with repeated measures ANOVAs. In occasions involving multiple comparisons, false discovery rate (FDR) corrections were performed using the Benjamini-Hochberg procedure (Benjamini & Hochberg, 1995), and the p-values were reported as adjusted values. The brain networks were illustrated with the BrainNet Viewer (http://www.nitrc.org/projects/bnv/; Xia, Wang, & He, 2013).

2.3 Results

2.3.1 Behavioral Results

During recall in the scanner, participants rated the quality of their memory of the images from 1 (least amount of detail) to 4 (highly detailed memory) **(Figure 1A**, middle**)**. Outside the scanner, they performed a memory recognition task in which they

attempted to identify the encoded scene among 3 similar distractor scenes, and then they rated their confidence (**Figure 1A**, right). To confirm the objective validity of subjective in-scanner ratings, we analyzed recognition performance outside the scanner as a function of in-scanner ratings. We performed separate 2 (age: YA vs. OA) x 4 (in-scanner recall rating: 1-4) ANOVAs for accuracy and confidence as separate outcome variables. In these ANOVAs, higher in-scanner recall ratings were associated with higher post-scan recognition accuracy (**Figure 1B**; $F(3,117)=13.17$, $p=1.8e-7$) and confidence (**Figure 1C**; $F(3,117)=64.62$, $p=2e-16$), showing that in-scanner memory rating reliably tracked memory performance. In the ANOVAs, there were also significant main effects of age on accuracy ($F(1,39)=14.73$, $p=4.4e-4$) and on confidence ($F(1,39)=14.99$, $p=4.0e-4$), consistent with age-related episodic memory decline. Neither ANOVA yielded reliable interactions. In summary, the behavioral results confirmed the validity of in-scanner recall ratings, which we used to split retrieval trials to create separate networks for High vs. Low Recall. The average number of high and low memory trials in YAs were 54.62 (±13.16, range 24~79) and 40.38 (±13.31, range 17~72), respectively. The average number of high and low memory trials in OAs were 51.00 (±16.51, range 18~82) and 42.30 (±15.89, range 13~69), respectively. Three participants (1 YA, 2 OAs) with less than 20 trials in either high or low memory condition were included in the network analysis, as we did not find any of their network measures of interest to be statistical outliers. No difference in trial number was found between the two age groups.

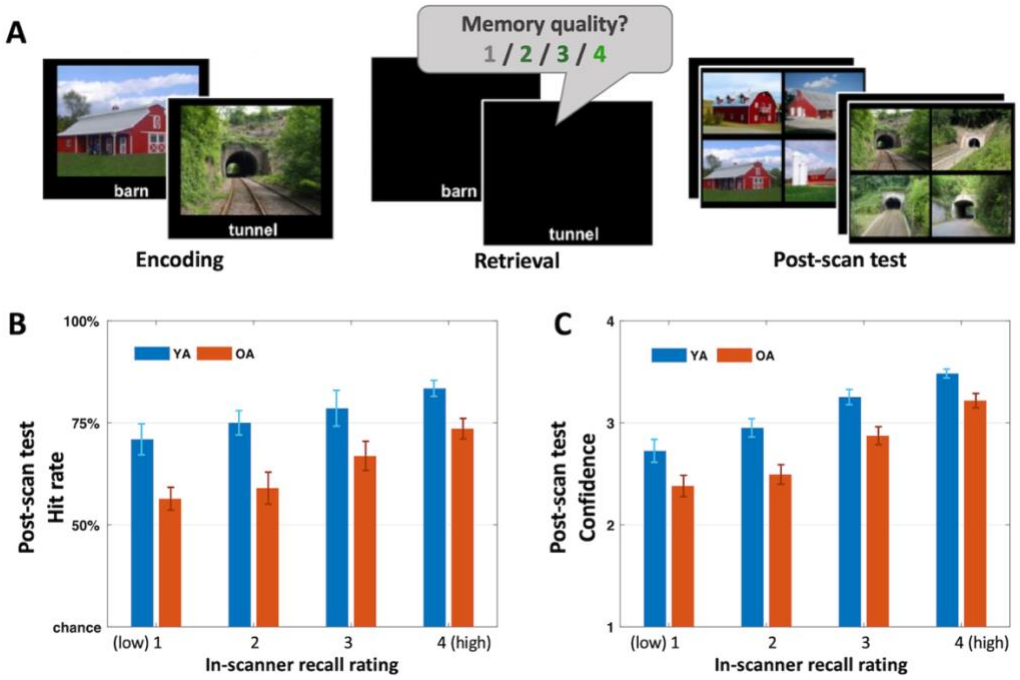

Figure 1: Experimental Paradigm and Behavioral Results. A) Experimental paradigm. B) Post-scan recognition hit rate as a function of in-scanner recall rating in YAs and OAs. C) Post-scan recognition confidence as a function of in-scanner recall rating in YAs and OAs. Error-bars indicate standard error of the mean (SEM).

2.3.2 Network Analyses

The following network analyses had three main goals: (1) investigate if PFC regions become more integrated with the rest of the brain in OAs than YAs, as a function of cognitive performance (first criterion of compensation); (2) examine if age-related changes in PFC recruitment involve a change in performance-related reconfiguration of connectivity patterns; and (3) investigate if PFC reconfiguration is associated with decreased MTL reconfiguration (second criterion of compensation). To start with, the modularity analysis on the combined YA-OA connectivity network yielded 6 modules

(**Figure 2**). Two modules, labelled as PFC+ and MTL+, visually characterized the PFC and MTL systems, respectively, suggesting the two brain systems of interest can be delineated in a data-driven manner. The PFC+ module consists of mainly PFC ROIs and a few strongly connected posterior regions (angular gyri and posterior cingulate cortices). The MTL+ module consists of core MTL structures (parahippocampal cortices, hippocampi, amygdala) and some surrounding regions (superior temporal poles, olfactory cortices). The ROIs in these two modules are listed in **Appendix A, Table 4**. To ensure that the additional areas did not drive the results reported, we performed supplementary analyses excluding them in **Appendix A**.

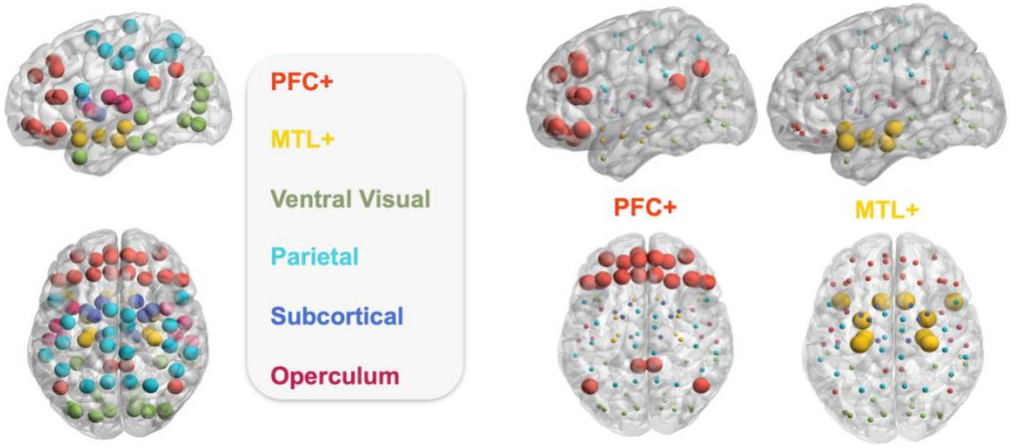

Figure 2: Modularity Assignment. Six modules are discovered by the modularity analysis in the common task network. The two modules of interest, PFC+ (red) and MTL+ (yellow), are shown on the right side. The PFC+ module consists of PFC ROIs but also bilateral angular gyri and posterior cingulate cortices. The MTL+ module consists of bilateral parahippocampal cortices, hippocampi, amygdala, superior temporal poles, and olfactory cortices.

2.3.2.1 Goal 1: PFC Integration and the Link to Cognitive Performance

PFC integration: Whole-brain integration (i.e., the ratio of between-module fCON to within-module fCON) was calculated for each module from each individual's fCON network (thresholded weighted network, including both high and low memory trials). Although the focus of our integration analyses was the PFC+ module, for sake of completeness we also investigated the effects on aging on all modules. An Age-by-Module repeated-measures ANOVA was performed, with module-specific whole-brain integration as the dependent variable. The mean and standard deviation values of integration can be found in **Table 5** in **Appendix A**. This analysis yielded a significant main effect of Module ($F(5,195)=17.11$, $p=5.13e-14$). As an exploratory analysis, we compared the whole-brain integration of two modules of interest (PFC+ and MTL+) with the average integration of the other 4 noninterest modules. PFC+ showed higher integration than the average integration in noninterest modules for both groups (YA: $t(20)=2.36$, $p=0.028$; OA: $t(19)=4.38$, $p=6.43e-4$), and MTL+ showed higher integration in YAs ($t(20)=5.52$, $p=4.14e-5$) but not in OAs (although with a marginal significance $t(19)=1.96$, $p=0.064$), presumably reflecting the contribution of these modules to integrative processing in the network. Importantly, the ANOVA yielded significant Age-by-Module interaction ($F(5,195)=13.08$, $p=5.52e-11$), indicating that aging had differential impact on whole-brain integration for different modules.

To further examine the age-related differences on the two modules of interest, we repeated our analysis on only the PFC+ and MTL+ module. Indeed, we again observed a significant Age-by-Module interaction (F(1,39)=13.44, p=7.32e-4) due to different age effect on integration for PFC+ and MTL+ modules (see **Figure 3**). In PFC+ module, integration with the rest of the brain network was significantly greater in OAs than YAs (t(39)=2.26, p=0.029), whereas in the MTL+ module there was a significant age difference in the opposite direction (t(39)=2.65, p=0.023). In sum, aging was associated with increased whole-brain integration in the PFC+ module and decreased whole-brain integration in the MTL+ module. This opposite effect of aging on PFC+ and MTL+ module organization is further examined below in reconfiguration analyses on differential effects of aging on PFC+ vs. MTL+ reconfiguration (*Goal 2*).

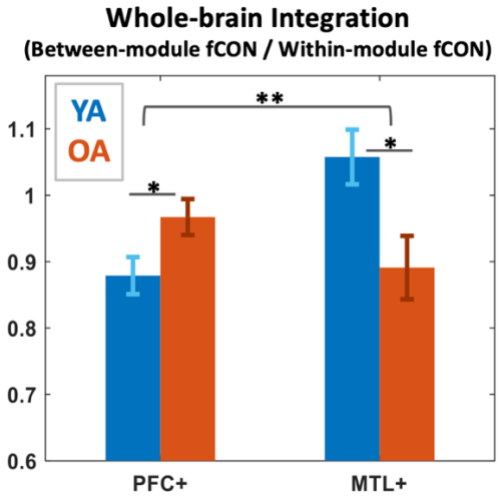

Figure 3: Network Integration of PFC+ and MTL+. Compared with YAs, OAs showed increased network integration in PFC regions. Horizontal bracket indicates Age x Module effect; horizontal line indicates two-sample t-test (: p<0.01; *: p<0.05). Error-bars indicate SEM.**

Link to cognitive performance: We then investigated whether age-related increase of PFC's role in the network contributes to cognitive performance in OAs. We split the data into high/low memory trials and examined if the integration measure of the PFC+ module varied with memory success; this analysis did not yield a reliable Memory effect ($F(1,39)=0.18$, $p=0.67$) or an Age-by-Memory effect ($F(1,39)=0.82$, $p=0.37$). Given that the integration is the ratio of between-module fCON to within-module fCON, we then investigated age-related difference in each of these two types of fCON. We performed 2 (Age group: YA vs. OA) x 2 (Memory: high vs. low) ANOVA on within-module and between-module connections separately. For within-module fCON (**Figure 4A**), the ANOVA yielded a significant main effect of Age ($F(1,39)=4.92$, $p=0.033$), but no reliable main effect of Memory ($F(1,39)=2.27$, $p=0.14$) or Age-by-Memory interaction ($F(1,39)=1.38$, $p=0.25$). In contrast, for between-module fCON, the ANOVA yielded no reliable main effect of Age or Memory, but there was a significant Age-by-Memory interaction ($F(1,39)=5.09$, $p=0.030$). As illustrated by **Figure 4B**, this interaction reflected the fact that fCON connecting PFC+ module to other systems in the brain was greater for high than low memory trials in OAs ($t(19)=2.52$, $p=0.042$) but not in YAs ($t(20)=-0.66$, $p=0.51$). This finding provides evidence for a significant link between increased PFC+ connectivity in OAs and successful memory performance (*1st compensation criterion*). Additionally, in a series of supplementary analyses, we found

that the above effect of Memory was only presented in PFC+ but absent in other modules **(Table 6)**, indicating a unique role of PFC+ connectivity.

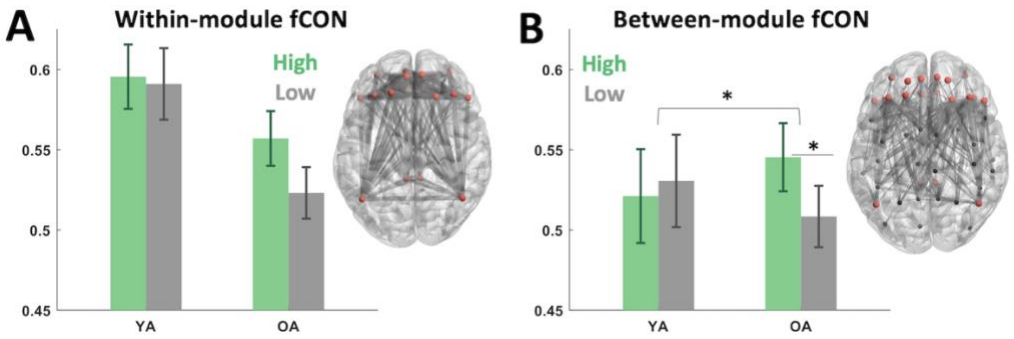

Figure 4: Functional Connectivity of PFC+. A) Average fCON within PFC+ module. B) Average fCON between PFC+ module and all other modules. Red nodes indicate brain regions in PFC+ module, while black nodes indicate regions belonging to other modules. Horizontal bracket indicated a significant Age x Module interaction; underscores indicated paired t-test (*: p<0.05). Error-bars indicate SEM.

2.3.2.2 Goal 2: Aging and Reconfiguration of PFC Connectivity

The second main goal of the study was to examine if age-related differences in PFC recruitment involve a change in network reconfiguration. The change of fCON between different memory states is multivariate in nature; thus, changes in fCON may not be fully observable by measurements such as average fCON strength. Therefore, the fCON reconfiguration between memory conditions was measured in each ROI for each participant **(Figure 5A)**. One premise is required for further analysis on connectivity reconfiguration: that this measure should reflect real memory-related change in connectivity patterns, rather than simply being driven by the instability of connectivity computation due to sub-sampling the total set of trials (i.e., drawing the high and low memory trials from the trial set and computing the connectivity based on each drawing).

Thus, we compared the actual reconfiguration values to random reconfiguration by subtracting the average bootstrap reconfiguration values from the actual reconfiguration values for each node in each participant. We then examined the actual-to-random difference as a function of the magnitude of the actual reconfiguration values **(Figure 5B)**. Indeed, at the highest quantile, actual reconfiguration values were significantly greater than the expected random reconfiguration ($t(40) = 14.58$, $p = 1.35e-17$), whereas lower actual reconfiguration values in the lowest two quantiles were significantly below the expected random reconfiguration (first quantile: $t(40) = -9.47$, $p = 9.00e-12$; second quantile: $t(40)=-11.90$, $p=1.03e-14$). Such a difference in distribution indicates that the reconfiguration measure captures memory-related, multivariate change in the fCON network that is substantially different from the statistical null distribution, therefore securing the validity of the following analyses into this measure.

As illustrated in **Figure 5C**, PFC+ reconfiguration from low to high memory was greater for OAs than YAs, which can be attributed to the difference in the value distribution between the two groups (**Figure 21A**). Importantly, at the group level, the age difference in PFC+ reconfiguration was driven by PFC+ ROIs in the highest reconfiguration quantile in OA group (i.e., ROIs in the 4th quantile of OA group-averaged reconfiguration, $p=0.017$, **Figure 21C**). This suggests that the effects of aging on PFC+ connectivity are not merely quantitative, as the pattern of PFC+ connectivity may reconfigure as a function of memory performance. In comparison, the ROIs in MTL+

were mostly in the highest reconfiguration quantile for YAs but, in contrast, mostly in the lowest reconfiguration quantile for OAs (**Figure 21B**), leading to significantly lower MTL+ reconfiguration (**Figure 5C**). This suggests an age-related reconfiguration deficit in the MTL system. Examining the relationship between PFC+ reconfiguration and MTL+ reconfiguration would help further interpret such age-related differences, to which we turn to in the following section.

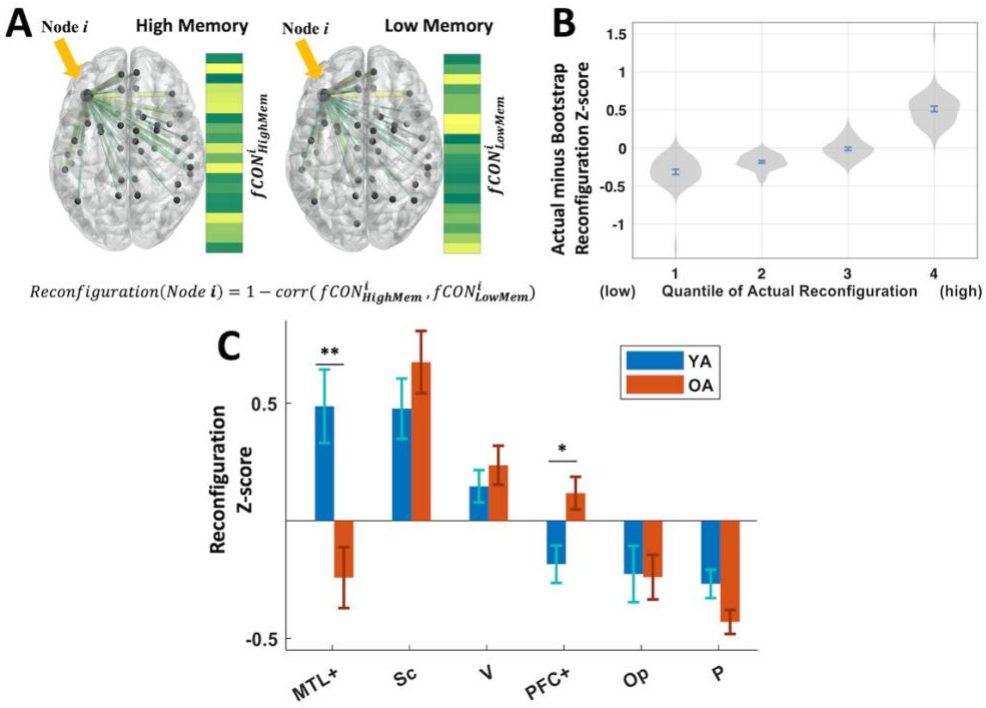

Figure 5: Memory-related Reconfiguration. A) An illustration of the computation of memory-related reconfiguration. B) The differences between actual and bootstrapped reconfiguration were binned into 4 equal-size samples for each subject according to the actual reconfiguration value. C) The value distribution of reconfiguration across all modules (V: Ventral Visual; Sc: Subcortical; Op: Operculum; P: Parietal). Error-bars indicate SEM. (: p<0.01)**

2.3.3.3 Goal 3: Relationship between PFC and MTL Reconfiguration

Our third goal was to investigate if PFC reconfiguration is negatively correlated with MTL reconfiguration. To examine this idea, we started by measuring reconfiguration in YAs and OAs in all six network modules **(Figure 5C)**. The mean and standard deviation values of reconfiguration can be found in **Table 5** in Appendix A. A 2 (Age group) x 6 (modules) ANOVA yielded a significant Age x Module interaction ($F(5,195)=5.59$, $p=7.7e-5$), and post-hoc tests showed that the only modules showing significant age-related differences in integration were PFC+ and MTL+ ($t_{PFC+}(39)= -2.85$, $p_{PFC+}= 0.021$; $t_{MTL+}(39)= 3.57$, $p_{MTL+}= 0.0057$, FDR corrected). Given that age-related differences in PFC+ and MTL+ modules were in opposite directions, we performed another ANOVA including just these two modules to investigate the interaction (**Figure 6A**). The ANOVA yielded a significant Age x Module interaction ($F(1,39)=14.71$, $p=4.5e-4$), because as the post-hoc t-test revealed, YAs showed stronger reconfiguration in MTL+ than PFC+ ($t_{YA}(20)=3.17$, $p_{YA}=0.0096$), while OAs displayed the opposite pattern ($t_{OA}(19)=2.22$, $p_{OA}=0.039$).

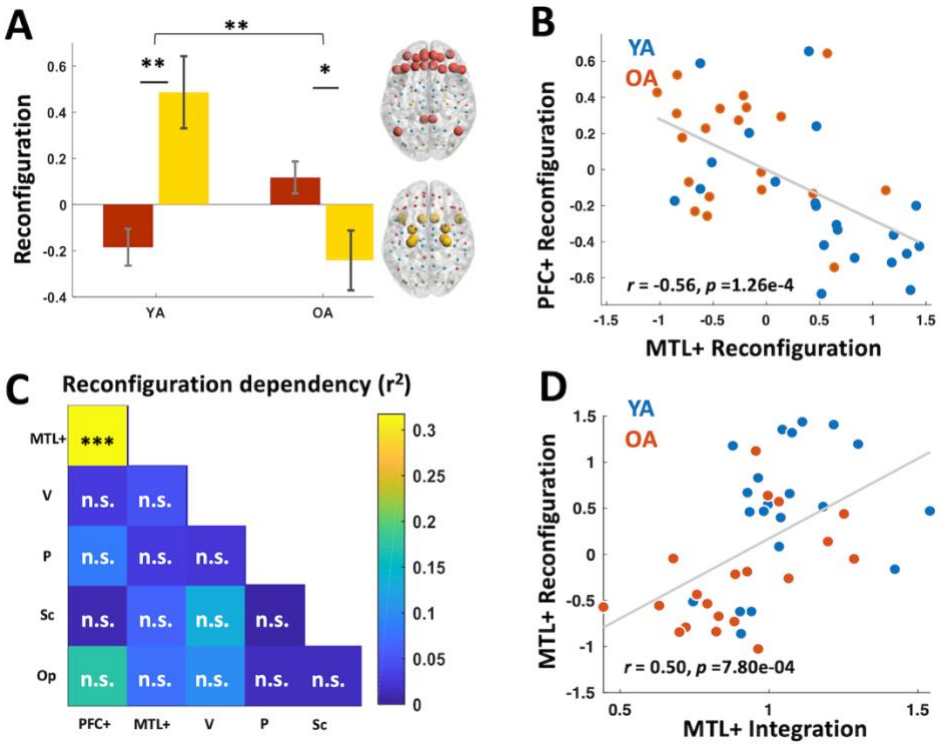

Figure 6: Reconfigurations of PFC+ and MTL+ Connectivity. A) The values of reconfiguration in PFC+ and MTL+ modules. Horizontal bracket indicated a significant Age x Module interaction; underscores indicated paired t-test (*: p<0.05; **: p<0.01). Error-bars indicate SEM. B) The dependency between reconfiguration in MTL+ and PFC+ modules across all subjects. C) The dependency (Pearson's r-square) of reconfiguration between all possible combination of modules (*: p<0.001; n.s.: not significant). D) The dependency between reconfiguration and integration in MTL across all subjects**

The results in **Figure 6A** suggest that PFC reconfiguration in OAs compensates for reconfiguration deficit in MTL (2nd criterion of compensation). To investigate this hypothesis, we correlated reconfiguration in these two brain regions. As illustrated by **Figure 6B**, consistent with compensation, we found a negative correlation between PFC+ and MTL+ reconfiguration across all participants (Pearson's r=-0.56, p=1.26e-4). Importantly, across all possible pairs of modules, this significant negative correlation

was present uniquely between MTL+ and PFC+ modules **(Figure 6C)**. This negative dependency between PFC+ and MTL+ reconfiguration remained in an additional partial correlation analysis, where age group was regressed out as the variable being controlled for (r=-0.45, p=0.0034).

Furthermore, if reduced MTL+ reconfiguration is indicative of a deficit, this should be convergently supported by other network measures. To explore this possibility, we conducted a post-hoc correlation analysis between MTL+ reconfiguration and integration **(Figure 6D)**. A significant positive correlation between integration and reconfiguration in MTL+ (Pearson's r=0.50, p=7.80e-4) was found across all participants. In addition, the reconfiguration-integration correlation was significant for the OA group (r=0.51, p=0.022) but not for the YA group (r=0.29, p=0.20). These results indicated that, in OAs, the reduced MTL+ reconfiguration is accompanied by a weakened MTL+ integration into the global brain network. This reconfiguration-integration relationship exists only in the MTL+ module after correcting for multiple comparisons. In summary, fulfilling the 2nd compensation criterion, we observed a negative association with increased PFC+ reconfiguration in OAs and reduced MTL+ reconfiguration.

2.4 Discussions

A fundamental goal in the cognitive neuroscience of aging is to understand the variability of age-related cognitive decline across individuals, especially when that decline negatively impacts their everyday lives (Salthouse, 2004; Habib, Nyberg, &

Nilsson, 2007; D. C. Park & Reuter-Lorenz, 2009; Cabeza, Albert, et al., 2018). The notion of *functional compensation* in aging offers not only a theoretical foundation to better understand differences in cognitive abilities across older adults, but also valuable information for developing possible interventions even after neural degeneration occurs. By leveraging recent advances in network neuroscience, our study investigates how certain brain regions, through their patterns of functional connections, play a different role within the large-scale brain networks of OAs (relative to YAs) to elicit cognition-enhancing effects attributable to functional compensation.

This study yielded three main findings. First, PFC regions became more functionally integrated with the rest of the brain network in OAs relative to YAs, and critically, the increased connectivity from PFC regions was associated with improved memory performance within OA individuals. Second, PFC regions tended to reconfigure their functional connections to support better memory performance in OAs. Third, the extent of functional reconfiguration of PFC connections in aging closely tracked the extent of reconfiguration deficits of MTL regions thought to play a critical role in successful memory retrieval. Taken together, our findings provide strong support for the age-related functional compensation of PFC regions during episodic memory retrieval. By satisfying these essential requirements for identifying cases of functional compensation (Cabeza, Albert, et al., 2018), our findings offer the first evidence for age-related functional compensation at the level of large-scale networks. We discuss each of the three main findings in more detail below.

2.4.1 Retrieval Performance in OA Supported by PFC Integration

Our first goal was to investigate whether PFC regions become more functionally interconnected with the rest of the functional brain network in OAs, and whether this is associated with better cognitive performance. Theorists have suggested that through increased activation of PFC regions, some OAs are able to maintain relatively high cognitive functioning during demanding tasks—including episodic memory tasks—when MTL or occipital cortical function is impaired (Grady et al., 1995; Davis et al., 2008; D. C. Park & Reuter-Lorenz, 2009; Cabeza & Dennis, 2012; although, see Morcom & Henson, 2018). These PFC regions are thought to serve control and monitoring functions that aid in the successful retrieval of information from memory (Cabeza & Dennis, 2012; Eichenbaum, 2017; Inman, James, Vytal, & Hamann, 2018).

While these previous studies have provided valuable information about *what* regions play compensatory roles in aging, recent developments in network neuroscience may bring further insights into *how* compensation is achieved. There has been growing consensus that although many cognitive functions can be attributed to specific 'core' brain regions, they are in fact carried out collaboratively by many different regions (Bressler & Menon, 2010; Sporns, 2014; Medaglia et al., 2015)S(Stanley et al., 2019). Episodic memory retrieval, for example, is associated with the activation of many disparate brain regions, which play different but complementary roles, such as storing and indexing memory traces, and evaluating the quality of retrieval (Cabeza & Nyberg,

2000; Wagner, Shannon, Kahn, & Buckner, 2005; Cabeza, 2008; Spaniol et al., 2009; Huijbers, Pennartz, Cabeza, & Daselaar, 2011; Rugg & Vilberg, 2013), and is also supported by increased connectivity across the network (Geib, Stanley, Wing, et al., 2017; Geib, Stanley, Dennis, et al., 2017). Our results are consistent with the heuristic that if the PFC regions do play a compensatory role in the memory retrieval process, then this role should be realized through network-level interactions.

To be compensatory, a brain region might exhibit increased direct and indirect communication with other task-related regions, leading to a highly integrative network architecture. Indeed, among resting-state fMRI studies, greater integration between disparate network modules during normal aging has been consistently observed (Betzel et al., 2014; Chan et al., 2014; Geerligs et al., 2015; Grady, Sarraf, Saverino, & Campbell, 2016). However, resting-state studies cannot fully disentangle the detrimental effect of aging and the brain's adaptive response to such effect. Specifically, a more integrated network structure in the aging brain may reflect the deleterious effects of aging on brain function, which would be associated with poorer cognitive performance, or they may reflect compensatory response to age-related decline, which would be associated with better cognitive performance. Here, by using task-related fMRI and comparing functional brain networks within-subjects as a function of cognitive performance, we were able to directly link the increase in network integration in some brain areas, such as the PFC, with age-specific cognition-enhancing effect. Our results are also consistent

with a recent study comparing working memory task networks in OAs and YAs, where the task-related regions in OAs integrate more into the whole brain network when the task demands increased (Crowell et al., 2020). Nonetheless, it is still unclear whether increased integration in OAs serves as a generalizable mechanism of compensation in aging for brain systems supporting other cognitive functions beyond memory. Also, given the more prevalent application of resting-state fMRI in neuroimaging studies, it remains an important question for future studies whether the age-related integration in task and resting state are mediated by shared or distinct underlying neural mechanisms.

2.4.2 Age-related Differences in Connectivity Reconfiguration

The second goal of the current study was to investigate whether OAs, relative to YAs, are more likely to reconfigure their patterns of PFC connections in a way that is associated with better memory performance. Accumulating evidence suggests that changes in functional connectivity are crucial for supporting cognitive functioning across varying task domains (Cole et al., 2013; Gallen et al., 2016) and demands (Hearne et al., 2017; Davis et al., 2018). Such changes imply selective recruitment and/or disengagement of regions with regard to the specific functional roles of the regions, the consequence of which would be a qualitative reconfiguration in the complex pattern of global connectivity (Hearne et al., 2017) rather than quantitative shifts (i.e., overall increase or decrease) of connectivity strength. Thus, in the current study, a correlation-based method was used to measure reconfiguration between high and low memory

conditions, as this measure is sensitive to qualitative changes in connectivity patterns while concomitantly remaining insensitive to changes in simple connectivity features such as scaling or baseline shifts.

Reconfiguration can be assessed at the levels of whole-brain network (Cole et al. 2014; Gallen et al. 2016; Hearne et al. 2017), task-related subnetwork (Davis et al., 2018), or individual regions (Geib, Stanley, Wing, et al., 2017). In the current study, examining reconfigurations at an ROI level gave us the best resolution to test our hypothesis regarding how the 'hot spots' of reconfiguration may shift in relation to age. As expected, OAs showed greater-than-average reconfiguration in PFC regions, further supporting the possibility that the PFC plays a critical role in OAs during successful memory retrieval. Our results accord with a previous study on cognitive control, in which participants performed 64 different tasks during fMRI scan (Cole et al., 2013). In this study, brain regions in the fronto-parietal network – regions key to the cognitive control functions – exhibited the highest reconfiguration of connectivity between different tasks, and the level of reconfiguration between two tasks was driven by the dissimilarity of the two tasks. Our study corroborates the idea that reconfiguration of functional connectivity could reveal the functional importance of a brain region in driving the brain from one cognitive state to another (in our case, the high vs. low memory state). Our results further indicate that the inter-subject variability of dynamic

functional network reconfiguration may possibly be mediated by many factors such as age, which is an area that remains largely unexplored.

2.4.3 PFC Compensates for MTL Deficit by Reconfiguration

Functional compensation implies a deficit for which the PFC is compensating. Here, an MTL deficit in OAs is suggested by low MTL reconfiguration **(Figure 6B)** accompanied by less MTL integration with the rest of the brain network **(Figures 3, 6C, 6D)**. These observations are in line with several previous studies, which have identified age-related reductions in MTL activity during memory retrieval (Daselaar et al., 2005; Dennis, Daselaar, et al., 2007; Dennis, Kim, & Cabeza, 2007; Davis et al., 2008; St. Jacques, Rubin, & Cabeza, 2012; Dew, Buchler, Dobbins, & Cabeza, 2012), pointing to an MTL deficit in healthy OAs. The presence of PFC compensation is indicated by the negative relationship between PFC and MTL connectivity reconfiguration **(Figures 6A, 6B)**, which is consistent with a previous study showing a negative relationship between PFC and MTL activation in a memory encoding task in OAs (Gutchess et al., 2005). Our results further extend these previous findings, showing an increased task-dependency of PFC connectivity profile when the capacity of MTL – the core regions of memory retrieval – is compromised by aging. These results may further the understanding of the way age-related compensation is systemically implemented in the brain.

It is worth noting that both OAs and YAs showed a negative correlation between memory-related PFC and MTL reconfiguration. This finding is not inconsistent with the

idea that PFC reconfiguration compensates for MTL reconfiguration because compensatory mechanisms in OAs often exist also in YAs. It is commonly assumed that during episodic memory retrieval, MTL regions mediate the recovery of stored memory representations, whereas PFC regions mediate control processes during retrieval (e.g., monitoring the retrieval output) (Moscovitch & Melo, 1997; Curran, Schacter, Norman, & Galluccio, 1997; Cabeza & Dennis, 2012). Thus, in general, when MTL-mediated recovery is low, PFC-mediated control demands tend to increase. For example, MTL activity is greater for high-relative to low-confidence hits (Daselaar, Fleck, & Cabeza, 2006; Kim & Cabeza, 2007), whereas PFC activity is greater for low-than high-confidence hits (Henson, Shallice, & Dolan, 1999; Fleck, Daselaar, Dobbins, & Cabeza, 2006) (Kim & Cabeza, 2007). This "seesaw" relationship between MTL and PFC is consistent with the negative correlation between memory-related reconfiguration in both YAs and OAs. Thus, rather than using a completely new mechanism, OAs are likely to be tapping a mechanism that also exists in YAs to compensate when the MTL output is low.

It is unclear which exact retrieval processes are driving PFC reconfiguration in OAs. In the retrieval task investigated, participants must process a name of a visual scene (e.g., harbor), generate the visual image of an encoded scene that matches the name, and rate the quality of the retrieved scene. Thus, age-related differences may involve one or more of the following three processes: (1) schema processing, (2) generation, and (3) post-retrieval monitoring. First, schema processing (e.g., how a

harbor looks like) has been strongly associated with PFC regions, especially ventromedial PFC (Van Kesteren, Rijpkema, Ruiter, & Fernández, 2010; Preston & Eichenbaum, 2013; Ghosh et al., 2014; Hebscher & Gilboa, 2016; Gilboa & Moscovitch, 2017), and there is evidence that OAs rely more on schematic knowledge relative to YAs (Mather et al., 1999). The fact that OAs tended to have higher reconfiguration in ventral PFC regions is consistent with such a possibility **(Figure 21C)**. Second, generation is essential for recall tests, which are more dependent on PFC regions (Cabeza et al., 1997) than generation-independent item recognition tests. Due to weaker MTL-mediated memory recovery, OAs may generate more alternative scenes from memory trying to match the verbal label. Finally, post-retrieval monitoring refers to assessing the validity of retrieved memory and is strongly linked with dorsolateral PFC regions (Henson et al., 1999; Fleck et al., 2006). In OAs, the reduction in memory quality may lead to increases in PFC-mediated 'quality control' (Jacoby, Shimizu, Velanova, & Rhodes, 2005; Jacoby, Shimizu, Daniels, & Rhodes, 2005; Dew et al., 2012). In short, the current study hints at potential interplay between aging, large-scale brain network dynamics, and shifts in cognitive strategies, which may be further investigated in the future.

2.4.4 Limitations

Considerable debate persists over the choice of atlas for defining nodes in network analyses (Stanley et al., 2013). The AAL atlas has been used in multiple different network analyses of task-related fMRI data that are directly relevant to our

current study (Stanley et al., 2015; Gallen et al., 2016; Geib, Stanley, Dennis, et al., 2017; Geib, Stanley, Wing, et al., 2017). Therefore, using the AAL atlas can facilitate more straight-forward comparison with relevant published works. The main methodological concern of the AAL atlas for defining nodes is that its larger ROIs may contain multiple functional regions, an issue that may be overcome by the use of recently-developed, high-resolution functionally defined atlases (Yeo et al., 2011; Gordon et al., 2014; Power, Schlaggar, & Petersen, 2014; Schaefer et al., 2018). However, most functionally-defined atlases are derived from younger adult samples, which could introduce an age bias in the current study. Taking these considerations together, in Appendix A, we described a series of supplementary analyses based on a fine-parcellated, anatomy-based Harvard-Oxford Atlas (HOA), which has been used in several recent studies (Davis, Luber, Murphy, Lisanby, & Cabeza, 2017; Monge et al., 2017; Davis et al., 2018; Beynel et al., 2020; Crowell et al., 2020). We found that results from these supplementary analyses were generally consistent with the results based on the AAL atlas.

Modularity analysis on a common network enabled us to directly examine compensation-related hypotheses for specific sub-systems of interests in the brain. In our study, extra efforts were made to control for potential age-related biases in the common module assignment, and a supplementary analysis further supports the presence of the two modules of interest (PFC & MTL) in both age groups (**Figure 18c**). Still, we acknowledge that age-related differences in community structure may exist, as

is indicated by recent studies (Geerligs et al., 2015; Gallen et al., 2016). It would be important to explore the influence of aging on the community structure of functional networks across different cognitive tasks. However, due to the limited sample size, it is beyond the scope of our current study to systematically characterize the age-related differences in the global network structure during memory retrieval, which remains an interesting question for future studies.

2.4.5 Summary

Developing a better understanding of how some OAs functionally compensate to preserve high cognitive functioning remains an important goal in the research of aging and cognition, as this information may lead to potential interventions aimed at slowing cognitive decline. Our results are largely consistent with the previous studies identifying PFC compensation in aging, and yet develop a more detailed picture of how network interactions in the PFC help subserve compensatory function in aging, and how these interactions are implemented through both an increase of functional communication with other brain systems and a dynamic reconfiguration of patterns of functional connections.

3. Age-related Dedifferentiation and Hyperdifferentiation of Perceptual and Mnemonic Representations[1]

3.1 Introduction

As we age, the anatomy and physiology of our brain declines, impairing cognitive abilities such as perception and memory (Grady, 2008; Grady, 2012). Most prior fMRI studies investigating the neural bases of these impairments have focused primarily on *processes* (operations performed on information) and only rarely examined age effects on *representations* (the nature of the information processed) (Cowell, Barense, & Sadil, 2019). In fMRI studies, differences in the mean activity level (univariate measure) of a group of voxels is assumed to reflect differences in processes, whereas differences in the spatial distribution (pattern) of activity (multivariate measure) within a group of voxels is assumed to reflect differences in representations (Haxby et al., 2001; Norman et al., 2006; Kriegeskorte, 2008). There has been accumulating evidence that activation patterns elicited by different types of visual stimuli (faces, places, etc.) are less distinct in OAs than in YAs (D. C. Park et al., 2004; Chee et al., 2006; Payer et al., 2006; Voss et al., 2008; Goh, Suzuki, & Park, 2010; Bowman, Chamberlain, & Dennis, 2019;

---

[1] The contents in this chapter are extracted from a coauthored publication on *Neurobiology of Aging*: "Deng, L., Davis, S. W., Monge, Z. A., Wing, E. A., Geib, B. R., Raghunandan, A., & Cabeza, R. (2021). Age-related dedifferentiation and hyperdifferentiation of perceptual and mnemonic representations. Neurobiology of Aging, 106, 55-67". Copyright is obtained from the publisher. An earlier version of this study was described in the dissertation by Z. A. Monge: "Monge, Zachary Adam (2020). Age-Related Differences in Mnemonic Neural Representations: Perceptual and Semantic Contributions. Dissertation, Duke University. Retrieved from https://hdl.handle.net/10161/20881". This work was supported by the National Institute on Aging (R01 AG019731 awarded to RC and F31 AG060691 awarded to ZAM) and National Institute of Mental Health (F31 MH114454 to BRG). We thank four anonymous reviewers for their valuable comments.

Koen et al., 2019; Koen & Rugg, 2019; Koen, Srokova, & Rugg, 2020). This phenomenon, known as *age-related neural dedifferentiation*, suggests that aging impairs the quality of representations during visual perception (*perceptual representations*). Yet, two fundamental questions remain unanswered: (1) what aspects of perceptual representations are impaired by aging? and (2) are age-related deficits in perceptual representations associated with deficits in visual memory traces (*mnemonic representations*)? The current study investigates these two critical questions.

1. *What aspects of the perceptual representations are impaired by aging?* This is a critical issue because perceptual representations consist of multiple features, which are processed in different brain regions and are affected differentially by aging. In particular, it is well established that sensory features of visual representations are processed primarily in early visual cortex and that these features form conjunctions of categorical and semantic features in more anterior ventral pathway regions, such as the anterior temporal lobe (ATL) (Bussey, Saksida, & Murray, 2005; Clarke & Tyler, 2014). The sensory-to-categorical feature distinction is relevant to aging because OAs tend to be impaired in perceptual processes (D. C. Park et al., 2004; Chee et al., 2006; Goh et al., 2010; Bowman et al., 2019; Koen et al., 2019; Koen & Rugg, 2019; Koen et al., 2020). However, their abilities to process categorical and conceptual information are relatively preserved (Owsley, 2011; Cherry et al., 2012; Mohanty, Naveh-Benjamin, & Ratneshwar, 2016; Monge & Madden, 2016), suggesting that age-related perceptual impairment could

be driven more by the deficit in processing lower-level visual/sensory information. Thus, we hypothesized that age-related visual dedifferentiation impairs sensory features of perceptual representations in early visual cortex but not categorical features in the ATL (*Hypothesis 1*). Given than some aspects of categorical-related processing are actually better in OAs than YAs (Laumann Long & Shaw, 2000; D. C. Park et al., 2002), an intriguing possibility is that categorical features in the ATL could be enhanced by aging.

We investigated Hypothesis 1 using representational similarity analyses (Kriegeskorte, 2008; Kriegeskorte & Kievit, 2013), in which the *sensory* and *categorical* similarities between stimuli are coded by two separate *stimuli models*. In the *sensory model*, pair-wise stimuli similarity is based on sensory visual features, such as shape (e.g., gun ≈ hair dryer), whereas in the *categorical model*, it is based on categorical features (e.g., gun ≈ sword). The pair-wise stimuli similarity coded by the model is then correlated with pair-wise similarity in fMRI activation patterns (representations) for the same set of stimuli. The resulting *model-brain fit* (2^{nd} order correlation) identifies brain regions that process and/or store representations emphasizing sensory and/or categorical visual features (**Figure 7A**). As stimuli models code the differences between images based upon a selective feature of interest (e.g., sensory, categorical), this model-brain fit may be operationalized as a measure of differentiation, where higher values in a brain region indicate greater neural differentiation.

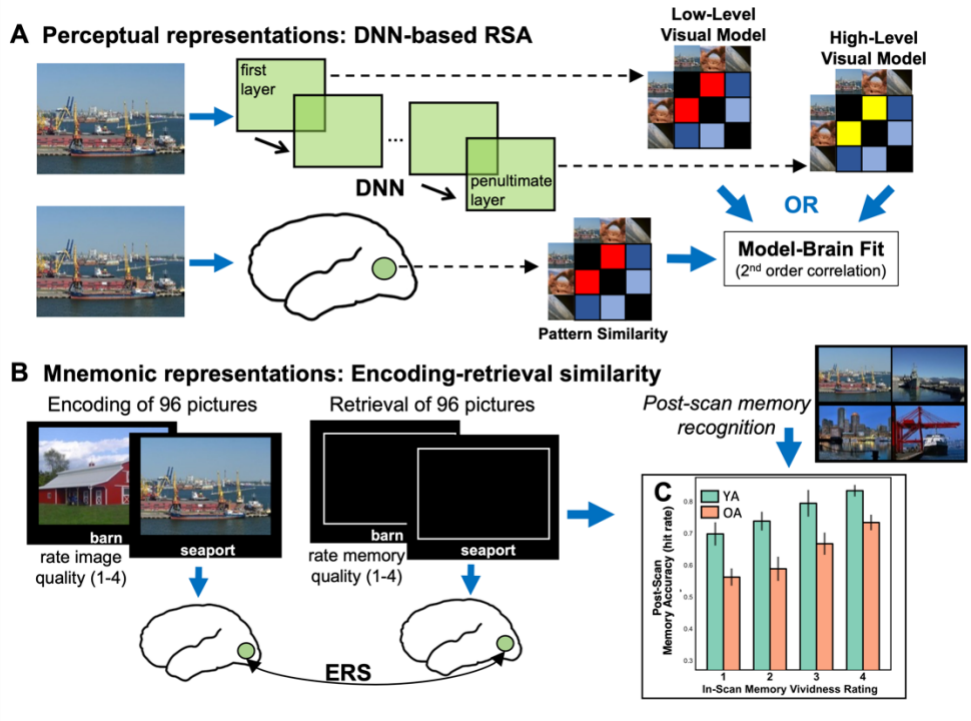

Figure 7: Analysis Approaches of Perceptual and Mnemonic Representations. A) A model of the analysis combining representational similarity analysis and DNN layers. To create models from DNN layers, the image stimuli are submitted to the pre-trained DNN and at each layer of interest, the "activation" values are extracted. Here, our layers of interest were the first and penultimate layers. For each image and layer of interest, the vectors of activation values are correlated with each other resulting in a stimuli model for each layer of interest. The stimuli models may then be used to predict brain activation patterns (model-brain fit) within 'searchlight' volumes (green circle). B) Study paradigm. Participants, while undergoing fMRI scanning, studied images (while rating the quality of the images) and later retrieved their memories of the scenes (while rating the vividness of their memories). We quantified the similarity of encoding to retrieval representations by calculating ERS. C) Post-scan memory accuracy (hit rate) as a function of in-scan vividness rating. Error bars represent the standard error of the mean.

In the current study, our stimuli models were derived from deep convolutional neural networks (DNNs) (Krizhevsky, Sutskever, & Hinton, 2017; Lecun, Bengio, & Hinton, 2015). DNNs consist of layers of convolutional filters and can be trained to

classify images into categories with a high level of accuracy. During training, DNNs "learn" convolutional filters in service of classification in the final layer, where filters from early layers predominately detect sensory features and while later layers organize items by their categorical features (Zeiler & Fergus, 2014). Previous work has demonstrated that progressive layers of typical DNNs (AlexNet, VGG16, etc.) may help to model visual representations along the ventral visual pathway, where early layers map brain activation patterns predominately in early visual cortex and late layers map brain activation patterns in more anterior ventral visual pathway regions (Leeds, Seibert, Pyles, & Tarr, 2013; Khaligh-Razavi & Kriegeskorte, 2014; Kriegeskorte, 2015; Güçlü & van Gerven, 2015; Wen et al., 2018; Davis et al., 2021). Thus, a major advantage of DNNs is that they afford the ability to model a continuum of low-level sensory features to more semantically meaningful categorical features. These models are especially helpful in addressing the complex visual arrays typical of most scenes (as opposed to single objects, Josephs & Konkle, 2019), especially with scenes where their categories are less clear. DNNs allow for this hierarchy to be investigated within a single framework. Furthermore, DNNs outperform traditional theoretical models of the ventral visual pathway, such as HMAX and object-based models (Cadieu et al., 2014; Groen et al., 2018) in their capacity to identify specific objects with the appropriate category- or basic-level label. Therefore, a DNN is an ideal model to investigate this sensory-to-categorical feature distinction. Here, we used a pre-trained 16-layer DNN, the VGG16 (Simonyan &

Zisserman, 2015), which was successfully trained to classify 1.8 million scenes into 365 categories (Zhou, Lapedriza, Khosla, Oliva, & Torralba, 2018). The first hidden layer generated a sensory model, since this model is derived from a layer that detects sensory features, and the penultimate layer, a categorical model, since this model is derived from the layer before the images are explicitly categorized into the trained categories (Bankson, Hebart, Groen, & Baker, 2018; Devereux, Clarke, & Tyler, 2018; Groen et al., 2018).

Given the posterior-anterior organization of the ventral visual pathway, we expected that the sensory model would correlate with activation patterns in early visual cortex, and the categorical model, with activation patterns in more anterior temporal regions such as the ATL. Based on Hypothesis 1, we predicted that, compared to YAs, (1) the correlation between brain activation patterns and the sensory model (i.e., model-brain fit) would be reduced in OAs, whereas (2) the correlation between brain activation patterns and the categorical model would be spared (or even enhanced) in OAs.

2. Are age-related deficits in perceptual representations associated with deficits in mnemonic representations? Age-related sensory and cognitive deficits are strongly related to each other (Lindenberger & Baltes, 1994; Baltes & Lindenberger, 1997), possibly because sensory deficits cascade through the cognitive system impairing downstream cognitive processes (Monge & Madden, 2016). Consistent with this idea, degrading stimuli (i.e., mimicking sensory impairment) by adding noise yields cognitive deficits in

YAs that resemble cognitive deficits in OAs (Pichora‐Fuller, Schneider, & Daneman, 1995; Murphy, Craik, Li, & Schneider, 2000; Gilmore, Spinks, & Thomas, 2006; Monge & Madden, 2016). In contrast, spared categorical processing in OAs may explain why age-related memory deficits are attenuated for semantically rich stimuli (Kausler, 1994; Naveh-Benjamin, 2000). Thus, the sensory to categorical dissociation we postulated for perceptual representations *(Hypothesis 1)* is likely to apply also to mnemonic representations.

We operationalize "perceptual representations" as the model-brain fit during the initial image presentation during the encoding phase of our study. Two types of perceptual representations are investigated, sensory representations and categorical representations. In contrast, we operationalize "mnemonic representations" in terms of the reactivation of the encoded activation during retrieval, as measured by the similarity between encoding and retrieval activation patterns or encoding-retrieval similarity (ERS) (**Figure 7B**). In the case of mnemonic representations, however, the age-related deficit is likely to affect not only visual cortex but also downstream memory-binding regions, such as the hippocampus. The hippocampus shows strong evidence of reactivation during retrieval (Danker & Anderson, 2010; Moscovitch, Cabeza, Winocur, & Nadel, 2016) and shows age-related deficits in activity and connectivity during retrieval (Daselaar et al., 2006; Trelle, Henson, & Simons, 2019; Deng, Stanley, et al., 2021). Thus, we hypothesized that aging is associated with impaired mnemonic

representations in early visual cortex and hippocampus but spared, or possibly even enhanced, mnemonic representations in the ATL (*Hypothesis 2*).

We investigated Hypothesis 2 using a reactivation fMRI paradigm (Danker & Anderson, 2010; Rugg & Vilberg, 2013). As illustrated by **Figure 7B**, during encoding scans, samples of YAs and OAs viewed 96 pictures of scenes paired with labels, and during retrieval scans, they recalled the scenes in response to the labels and rated the quality of their memories. These in-scan ratings were validated with a post-scan forced-choice memory recognition test, which showed that greater in-scan ratings were associated with better post-scan accuracy (**Figure 7C**; see the Materials and Methods for more details on participants and the experimental design). Previous reactivation fMRI studies with OAs compared broad categories of stimuli (T. H. Wang, Johnson, de Chastelaine, Donley, & Rugg, 2016; Abdulrahman, Fletcher, Bullmore, & Morcom, 2017; Johnson, Kuhl, Mitchell, Ankudowich, & Durbin, 2015; Thakral, Madore, & Schacter, 2017) or presented stimuli multiple times during encoding (St-Laurent, Abdi, Bondad, & Buchsbaum, 2014), precluding reactivation measures for individual events. In contrast, we measured the reactivation of individual events (each scene) by directly measuring ERS in activation patterns (Ritchey, Wing, LaBar, & Cabeza, 2013; Wing et al., 2015). On the bases of Hypothesis 2, we predicted that, compared to YAs, OAs would show reduced ERS in the early visual cortex but spared (or even enhanced) ERS in the ATL.

3.2 Materials and Methods

3.2.1 Participants

Our study sample included 22 YAs and 22 OAs. One YA and one OA were excluded from analysis because of functional data missing from the first fMRI run due to a technical error. Another OA was excluded from analysis due to a poor quality T1 image, not allowing the participant's functional images to be properly normalized into MNI space. This left a study sample of 21 YAs (12 women, age range = 18-30 years, M = 23.5 years, SD = 3.0 years) and 20 OAs (9 women, age range = 61-82 years, M = 70.5 years, SD = 5.4 years). Participants self-reported to be free of significant health problems (including atherosclerosis, neurological and psychiatric disorders), and not taking medications known to affect cognitive function or cerebral blood flow (except antihypertensive agents). Also, all participants were right-handed and completed at least 12 years of education. The OAs were additionally screened for dementia via the Mini-Mental State Examination (MMSE; inclusion criterion ≥ 27; M = 29.2, SD = 0.7; Folstein et al., 1975); no exclusions were necessary based upon this criterion. After study completion, participants were monetarily compensated for their time. Study results from the sample of YAs were previously reported in other manuscripts (Wing et al., 2015; Geib, Stanley, Wing, et al., 2017). The Duke University Institutional Review Board approved all experimental procedures, and participants provided informed consent prior to testing.

3.2.2 Experimental Paradigm

Participants completed three encoding runs followed by three retrieval runs. During the encoding runs, participants explicitly studied a total of 96 color pictures of complex scenes (32 images per run, order randomized within run). The 96 images were very similar to the ones used to train the DNN model we employed (VGG16), including many of the same images. During each encoding trial (4 sec), participants were presented a single picture with a unique descriptive label below the image (e.g., "tunnel" or "barn"). Within the trials, participants were asked to rate, on a four-point scale, the quality of the image (i.e., how well the image represents the label, 1 = low quality, 4 = high quality). This was to ensure participants would pay attention to the details of each image. Each encoding trial was followed by an active baseline interval of 8 sec, in which participants were presented digits from 1 to 4 and pushed the button corresponding to the presented numbers.

The retrieval runs were identical in format to the encoding runs, except the pictures of the scenes were not presented. During each retrieval trial, participants were presented the 96 descriptive scene labels previously presented along with the pictures of the scene, and participants were instructed to recall the corresponding image from encoding with as much detail as possible. Participants then rated, on a four-point scale, the amount of detail with which they could remember for the specific picture (1 = least amount of detail, 4 = highly detailed memory).

Immediately after the retrieval runs, participants completed a four-alternative forced-choice recognition test outside the scanner, in a testing room located adjacent to the MR scanner. For each recognition trial, the participants selected the picture they believed they saw during encoding among 4 pictures (1 target picture, 3 distractors) that were simultaneously presented for 5 sec (**Figure 7B**, right). Participants then reported their confidence in the recognition decision using a 4-pt scale (1 = guess, 4 = very confident) in each trial. The performance of post-scan memory recognition for each participant was measured as the hit rate (the number of correct trials over the number of total trials).

3.2.3 MRI Acquisition

MRI data were collected on a General Electric 3T MR750 whole-body 60 cm bore MRI scanner and an 8-channel head coil. The MRI session started with a localizer scan, in which 3-plane (straight axial/coronal/sagittal) localizer faster spin echo (FSE) images were collected. Following, using a SENSE spiral-in sequence (repetition time [TR] = 2000 msec, echo time = 30 msec, field of view [FOV] = 24 cm, 34 oblique slices with voxel dimensions of 3.75 x 3.75 x 3.8 mm3), the functional images were acquired. The functional images were collected over six runs – three encoding runs and three retrieval runs; there was also a functional resting-state run after the third encoding run, which is not reported here. Stimuli were projected onto a mirror at the back of the scanner bore, and responses were recorded using a four-button fiber-optic response box (Current

Designs, Philadelphia, PA, USA). Following, a high-resolution anatomical image (96 axial slices parallel to the AC-PC plane with voxel dimensions of 0.9 x 0.9 x 1.9 mm) was collected. Finally, diffusion-weighted images were collected, which are not reported here. Participants wore earplugs to reduce scanner noise, and foam pads were used to reduce head motion, and, when necessary, participants wore MRI-compatible lenses to correct vision.

3.2.4 fMRI Preprocessing

For each run, the first six functional images were discarded to allow for scanner equilibrium. All functional images were preprocessed in a SPM12 (London, United Kingdom; http://www.fil.ion.ucl.ac.uk/spm/) pipeline. Briefly, the functional images were slice timing corrected (reference slice = first slice), realigned to the first scan in the first session, and subsequently unwarped. Following, the functional images were co-registered to the skull-stripped high-resolution anatomical image (skull-stripped by segmenting the high-resolution anatomical image and only including the gray matter, white matter, and cerebrospinal fluid segments). The functional images were normalized into MNI space using DARTEL (Ashburner, 2007); the study specific high-resolution anatomical image was created using all of the study participants. The voxel size was maintained at 3.75 x 3.75 x 3.8 mm3 and the normalized-functional images were not spatially smoothed. Lastly, the DRIFTER toolbox (Särkkä et al., 2012) was used to denoise the functional images. We also calculated the temporal signal-to-noise ratio

(SNR), that is, the ratio between mean and the standard deviation of the time series in a given ROI (Welvaert & Rosseel, 2013).

3.2.5 fMRI Analysis

To obtain the beta estimates for each event, we conducted a single-trial model analysis within a general linear model. These beta estimates were calculated using a least squares-separate approach (Mumford et al., 2012). This approach estimates a first-level model in which one regressor models a specific event of interest and another regressor models all the other events (each run included a regressor modeling these other trials). Each event was modeled with a stick function placed at stimulus onset convolved with a standard hemodynamic response function with the temporal and dispersion derivative. Each model also included the six raw motion regressions, a composite motion parameter (derived from the Artifact Detection Tools [ART]), outlier volumes (scan-to-scan motion > 2.0 mm or degrees, scan-to-scan global signal change > 9.0 z score; derived from ART), the white matter timeseries, and cerebrospinal fluid timeseries. In each model we also modeled the temporal and dispersion derivatives and implemented a 128 sec cutoff high-pass temporal filter.

These beta-images were used for (1) the representational similarity analysis combined with DNNs and (2) ERS. These analyses were conducted using in-house MATLAB (Natick, MA, USA) scripts (https://github.com/brg015). For the ERS analyses,

we excluded trials in which participants responded (during retrieval) either not at all or in less than 250 msec.

3.2.5.1 Representational Similarity Analysis Combined with Convolutional Neural Networks

To examine our first goal, we performed representational similarity analysis (Kriegeskorte, 2008) based on stimuli models derived from DNNs (Leeds et al., 2013; Khaligh-Razavi & Kriegeskorte, 2014; Kriegeskorte, 2015; Wen et al., 2018) that captured the similarities between the stimuli in two different aspects (i.e., sensory vs. categorical aspects). The stimuli models (96 x 96 matrix) were correlated with the brain activation patterns similarity matrix (96 x 96 matrix) derived from searchlight volumes using Spearman's correlation (a.k.a. model-brain fit), and the level of such model-brain fit may indicate the extent the neural representation reflects the processing of features associated with the given model (Kriegeskorte, Goebel, & Bandettini, 2006).

For the searchlight analysis across brain regions, a 5 x 5 x 5 voxel cube (Wing et al., 2014) was placed around a voxel location and the activation values from this cube were extracted and vectorized for each beta image, representing the local activation pattern associated with each stimulus at this voxel location (**Figure 7A**). This procedure was conducted for each stimulus and the activation values from each stimulus were correlated (Fisher-transformed Pearson's *r*) with each other, representing the brain activation patterns. The brain activation patterns were then correlated (Spearman's correlation) with the DNN-stimuli models (model-brain fit), which was the value placed

in the voxel location. This procedure was repeated for every voxel in the brain and the output of this analysis was searchlight volumes representing brain activation pattern-DNN layer stimuli model similarity.

For the stimuli model, we used a popular DNN known as VGG16 (Simonyan & Zisserman, 2015), which is pre-trained on approximately 1.8 million images of scenes in service of categorizing the images into 365 scene categories (Zhou et al., 2018). The VGG16 consists of 13 convolutional layers and 3 fully connected layers. The first hidden DNN layer is a convolutional layer whose artificial neurons directly receive image inputs and have small spatial receptive fields. This layer is sensitive to low-level visual features, such as Gabor patches, boundaries, and blobs (Eickenberg, Gramfort, Varoquaux, & Thirion, 2017). In comparison, the penultimate layer is the last hidden layer with 4096 artificial neurons, whose collective activation pattern is sent to the output layer (a.k.a. Softmax layer) to produce evidence scores of each of the 365 scene categories. Thus, the penultimate layer contains a rich array of computational information that is not defined by one visual feature (e.g., horizontal lines) or a simple combination of a few features (e.g., red horizontal lines) but instead a high-dimensional feature matrix which may dissociate many object classes (here, 365 classes), based on complex spatial configurations of information associated with different objects (ships, house, etc.) and backgrounds (sea, farmland, etc.) that allow to distinguish one scene from another (e.g., seaport vs. barn). In other words, the representation in the VGG16

penultimate layer directly supports its categorical outputs, which are highly consistent with the categorical judgements from human.

Therefore, we created stimuli models from the first hidden DNN layer (reflecting sensory features) and penultimate DNN layer (reflecting categorical features). These stimuli models were constructed by feeding the study stimuli through the pretrained DNN and for each stimulus at each layer of interest (i.e., the first and penultimate layers), extracting the activation values. For each layer of interest, the activation values between stimuli were correlated (Pearson correlation) with each other. This yielded two 96x96 matrices (one for each layer of interest), which represent the similarity of the DNN activation values and are the image models (sensory and categorical image models). It should be noted that, although the first convolutional layer mimics low-level visual processing, and the penultimate layer, categorical judgement, the whole VGG16 should not be viewed as a model that emulates the entire ventral visual pathway.

After conducting the searchlight analysis examining model-brain fit, the searchlight volumes were spatially smoothed with a 5 mm Gaussian kernel (Clarke & Tyler, 2014; Clarke, Pell, Ranganath, & Tyler, 2016). Then, for each model, we extracted model-brain fit from *a priori* ROIs derived from the AAL atlas (Tzourio-Mazoyer et al., 2002), which consisted of early visual cortex (bilateral calcarine, cuneus, and lingual ROIs) and ATL (left dorsal temporal pole and ventral temporal pole). We chose to examine only the left ATL because of our interest in categorical representations and an

extensive literature demonstrating greater processing of categorical-related features (e.g., conceptual processing) in the left hemisphere (Warrington & McCarthy, 1983; Hodges, Patterson, Oxbury, & Funnell, 1992; Tyler et al., 2004). See the Introduction for an explanation of *a priori* ROI choice.

Two additional analyses were conducted to validate the VGG16 as a model of sensory to categorical representations in our study. (i) The VGG16 was already successfully trained to classify 1.8 million scenes into 365 categories (Zhou et al., 2018), but we wanted to confirm it could also classify the 96 images employed in our study. Given that some of the scene labels we used were different than the categories used to train the VGG16 but were nevertheless closely related terms (e.g., "seaport" in **Figure 7B**, versus "harbor" in the VGG16 output category), it is difficult to evaluate the performance of VGG16 directly. Therefore, we created a slightly modified VGG16 for binary indoor-outdoor scene classification. This was achieved by removing the last layer of the VGG16 and adding a layer with two outputs (with a Softmax activation function), corresponding to indoor and outdoor scenes. The revised VGG16 was then trained using three pictures from each image category (images from the post-scan recognition task besides the target images) and tested on the pictures presented within the scanner. After 30 epochs, the revised VGG16 was able to classify the images into indoor vs. outdoor domains with 94.8% accuracy, suggesting that the stimuli images were well-matched with the training images. It should be noted that the model with this binary indoor-

outdoor scene classification was only used to validate the use of the VGG16 within our study; the original pretrained VGG16 was used for stimuli model construction. (ii) We correlated the sensory and categorical stimuli models based on the original pretrained VGG16 and found that they were only moderately correlated with each other (r = 0.32, Figure S1), indicating that each model represents unique features. In comparison, the stimuli models constructed from adjacent layers are more closely correlated with each other (**Appendix B, Figure 23**).

3.2.5.2 Encoding-retrieval Similarity Analysis

To examine our second goal, we calculated ERS for each item using a searchlight procedure (Kriegeskorte et al., 2006). For each item (e.g., 'barn'), its corresponding encoding and retrieval activation patterns were extracted from searchlight spheres, forming an encoding-retrieval vector pair. A 5 x 5 x 5 voxel cube was placed around each voxel and the activation patterns were extracted and vectorized. For each item, the encoding and retrieval vectors were correlated and the correlation value (Fisher-transformed Pearson's r, which is ERS) was placed in the original center voxel location. Within each voxel location, the ERS value for each stimulus was averaged across all 96 encoding items. This procedure was repeated for every voxel within the brain. Afterwards, the searchlight volumes were spatially smoothed with a 5 mm Gaussian kernel (Clarke & Tyler, 2014; Clarke et al., 2016). We then extracted ERS from *a priori* ROIs derived from the AAL atlas, which consisted of early visual cortex (bilateral

calcarine, cuneus, and lingual ROIs), ATL (left dorsal temporal pole and ventral temporal pole), and the hippocampus (bilateral hippocampi). See the Introduction for an explanation of *a priori* ROI choice. In addition to item-level ERS, as a control analysis, we also calculated set-level ERS, which is ERS between an item and every other item within the stimuli set (Ritchey et al., 2013; Wing et al., 2015), reflecting the baseline level of recurring activation patterns that were non-specific to the retrieval of specific item. Thus, the value of dissociating item- and set-level ERS is that we are able to control for the amount of pattern similarity that would be seen between any pair of items, and describe a more specific re-instantiation of a neural pattern unique to the target item. The analysis contrasting item and set ERS was constrained to the items that were subsequently remembered on the post-scan memory task.

3.2.6 Statistical Analysis

Statistical analyses (unless otherwise stated) were conducted within StatsModels (Seabold & Perktold, 2010) ran in Python 3 (Python Software Foundation, https://www.python.org/). Repeated measures ANOVAs were used to assess omnibus effects. Two-sided linear mixed effects models, with participant specified as a random effect, were used as a substitute of t-test or correlation. This model allowed us to include SNR as a nuisance variable when needed, as ATL can be vulnerable to low SNR. The significance of effects was based on the z-scores associated with the parameter estimates.

Before entering the data into the linear mixed effects models, all values were *z*-transformed. All effect sizes reported in the manuscript were Cohen's *d*.

3.3 Results

3.3.1 Behavioral Results

We started by investigating the memory performance of the two age groups. In the post-scan recognition test, OAs showed lower number of hits comparing with YAs (YA: 75.10±10.98, OA: 61.00±8.26, t=4.63, p=4.02e-5), as well as lower recognition confidence (YA: 3.11±0.30, OA: 2.74±0.41, t=3.31, p=0.0022), suggesting age-related memory decline. In the retrieval scan, the two age groups showed comparable level of self-report recall vividness inside scanner (YA: 2.72±0.46, OA: 2.70±0.40, t=0.12, p=0.91). The post-scan memory accuracy (hit rate) was positively related to vividness rating during retrieval **(Figure 7C),** as is indicated by a significant effect of vividness (F(3,117)=13.17, p<2e-7). In addition, the confidence level of post-scan recognition was also significantly contributed by in-scan vividness (**Appendix B, Figure 24**; F(3,117)=64.62, p=2e-16). Memory performance for each stimulus can be found in **Appendix B**, **Table 8.**

3.3.2 Perceptual Representations: DNN-based Representational Similarity Analysis

Our first hypothesis was that age-related visual dedifferentiation impairs the differentiation of sensory features in early visual cortex but not categorical features in the ATL, which may even be enhanced in aging. Using DNN-based representational

similarity analysis, we tested this hypothesis by comparing age-related differences in model-brain fit for the sensory model based on the first VGG16 layer, and for the categorical model based on the penultimate VGG16 layer. We tested this hypothesis in two *a priori* ROIs – early visual cortex and ATL. For raw model-brain fit values (see **Appendix B, Figure 25a**), we performed an omnibus *Model_Type* (sensory/categorical) x *ROI* (early visual cortex/ATL) x *Age* (YA/OA) repeated measures ANOVA, and we found a significant main effect of *ROI* ($F(1,39)=15.37$, $p<0.001$) and a significant *Age x ROI* interaction ($F(1,39)=12.14$, $p<0.005$), while the main effect of *Model_Type* ($F(1,39)=0.34$, $p=0.57$), *Model_Type x Age* interaction ($F(1,39)=1.66$, $p=0.21$), *Model_Type x ROI* interaction ($F(1,39)=0.095$, $p=0.76$) and *Model_Type x ROI x Age* interaction were not significant ($F(1,39)=1.82$, $p=0.185$). In an ROI-level analysis, as illustrated in **Figure 8A**, which shows *z*-scored 2nd order correlations, the evidence was consistent with our first hypothesis: compared to the YAs, in early visual cortex, the sensory model-brain fit was reduced in the OAs ($\beta = -0.39$, $z = 19.86$, $p < .0001$, $d = 0.83$), whereas in the ATL, the categorical model-brain fit was enhanced in the OAs ($\beta = 0.26$, $z = 12.82$, $p < .0001$, $d = 0.53$). In other words, whereas early visual cortex showed age-related *de*differentiation, the ATL showed age-related *hyper*differentiation. As the ATL is particularly vulnerable to low signal-to-noise ratio (SNR), we repeated the analysis statistically controlling for SNR and still found that in the ATL that categorical model-brain fit was enhanced in the OAs compared to YAs ($\beta = 0.26$, $z = 15.61$, $p < .0001$). We did not find statistically

significant age-group differences of the sensory model-brain fit in the ATL (β = 0.17, z = 1.39, p = .17, d = 0.33), but we did find, compared to YAs, that the categorical model-brain fit in the early visual cortex was reduced in the OAs (β = -0.27, z = 3.25, p < .01, d = 0.54). In sum, this is, to our knowledge, the first evidence of age-related hyperdifferentiation of activation patterns in the ventral pathway or any brain region.

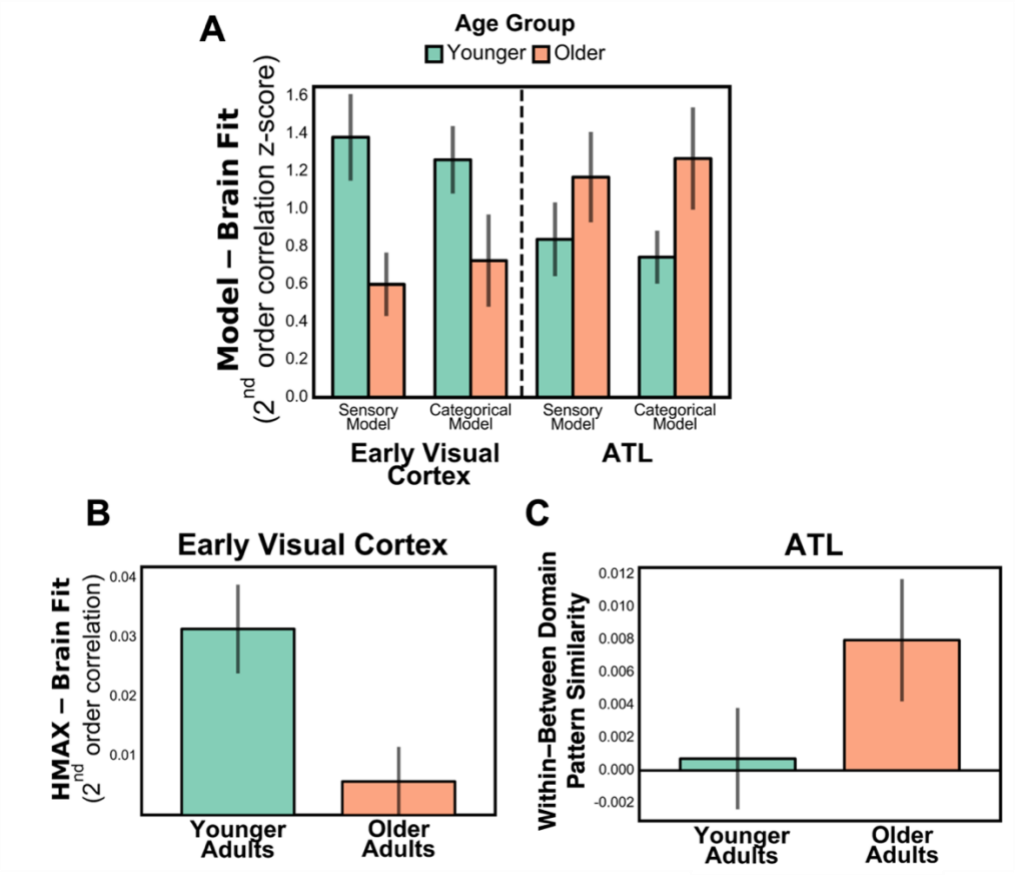

Figure 8: Age-related Neural Dedifferentiation and Hyperdifferentiation. A) The model (sensory and categorical)-brain fits in early visual cortex and ATL; the figure shows z-scored (mean set to one) 2nd order correlations. B) The HMAX C1 response model-brain fit in early visual cortex. C) The brain activation pattern similarity for within-domain minus between-domains (domains = indoor vs. outdoor scenes) in the ATL. Error bars represent the standard error of the mean. Error bars represent the standard error of the mean.

Although DNNs provide stronger models of visual representations in the ventral visual pathway than traditional theoretical models, DNNs are sometimes critiqued for being too complex and, therefore, less interpretable. We believe that this level of complexity is necessary to map representations within the brain (Kriegeskorte & Douglas, 2018), but the critique of interpretability is well received. Therefore, we examined if the age-related differences can also be observed using more traditional models. (i) For sensory representations, we used the C1 responses of the HMAX model (Clarke and Tyler, 2014), which was proposed to reflect properties of early visual cortex (Maximilian Riesenhuber & Tomaso Poggio, 1999; Serre, Wolf, Bileschi, Riesenhuber, & Poggio, 2007). Consistent with the DNN analysis, compared to the YAs, the OAs exhibited reduced HMAX-based model-brain fit in early visual cortex (**Figure 8B**; β = -0.39, z = 13.73, p < .0001, d = 0.82). In addition, the HMAX-based model-brain fit was strongly correlated with the early DNN-based model-brain fit across participants (r = 0.74, p < 0.001), suggesting good consistency of the two measurements. (ii) For categorical representations, we examined brain activation pattern similarity for within- compared to between-domains (indoor vs. outdoor scene trials), since images within the same domain likely share large amounts of objects and visual features, as demonstrated in our preliminary analysis using the VGG16 to classify indoor and outdoor scenes (see Preliminary analyses in the Results). We performed a *Model_Type* (HMAX C1/within-minus-between domains) x *ROI* (early visual cortex/ATL) x *Age* (YA/OA) ANOVA on

these two alternative model-brain fit measures. We found significant main effect of *ROI* ($F(1,39) = 5.23$, $p < 0.05$), *Age* x *ROI* interaction ($F(1,39) = 9.61$, $p < 0.005$), and *Model_Type* ($F(1,39) = 4.89$, $p < 0.05$). The *Model_Type* x *Age* interaction ($F(1,39) = 3.51$, $p < 0.1$), *Model_Type* x *ROI* interaction ($F(1,39) = 3.52$, $p < 0.1$) and *Model_Type* x *ROI* x *Age* interaction ($F(1,39) = 3.52$, $p < 0.1$) were non-significant, although noticeable to some extent. Consistent with the DNN analysis, compared to the YAs, the OAs exhibited enhanced activation pattern similarity for within- than between-domains in the ATL (**Figure 8C**; $\beta = 0.23$, $z = 3.36$, $p < .001$, $d = 0.46$; see **Appendix B, Figure 25b** for pattern similarity values within- and between-domains). These findings supported the robustness of DNN-based analysis on perceptual representation, providing further evidence for age-related dedifferentiation of sensory features in early visual cortex and hyperdifferentiation of categorical features in ATL.

As an exploratory analysis, we further investigated the links between encoding representations and memory (**Appendix B, Table 9**). In YAs, we found a significant positive correlation between post-scan memory accuracy and sensory model-brain fits in early visual cortex (DNN Layer 1 model-brain fit: $r = 0.45$, $p < 0.05$; HMAX C1 model-brain fit: $r = 0.51$, $p < 0.05$), suggesting the sensory representation in visual cortex supported later memory retrieval. In comparison, in OAs, such a correlation between memory and sensory model-brain fits was absent (DNN Layer 1 model-brain fit: $r = 0.04$, $p > 0.5$; HMAX C1 model-brain fit: $r = -0.03$, $p > 0.5$), although there were no significant

differences between the correlations of the two age groups. Collapsing across all participants (YAs & OAs), the association between early sensory model-brain fits for early layer models (DNN Layer 1, HMAX C1) and memory accuracy was significant (DNN Layer 1 model-brain fit: $r = 0.46$, $p < 0.005$; HMAX C1 model-brain fit: $r = 0.47$, $p < 0.005$); when corrected for age effect, such behavioral correlate was still significant for the HMAX C1 model (partial correlation, $r=0.32$, $p=0.042$) and almost reaching significant for the DNN Layer 1 model (partial correlation, $r=0.31$, $p=0.051$). We did not find significant correlation between memory and categorical model-brain fits in ATL in either YAs ($r=0.14$, $p=0.54$) or OAs ($r=0.053$, $p=0.83$).

Although the *a priori* ROI analysis was used to test our hypothesis, as an exploratory analysis, we conducted the whole-brain searchlight analysis. Within both age groups, the first layer of the VGG16 was primarily associated with early visual regions, and the penultimate layer was additionally linked to anterior temporal, parietal, and frontal regions (**Figure 9**; see **Appendix B, Table 7** for cluster coordinates). This is consistent with previous research that early DNN layers identified posterior brain regions mediating sensory representations, and later layers, anterior brain regions mediating categorical representations (Leeds et al., 2013; Khaligh-Razavi & Kriegeskorte, 2014; Kriegeskorte, 2015; Güçlü & van Gerven, 2015; Wen et al., 2018). With respect to age-related differences, YAs showed stronger sensory model-brain fit in the early visual regions, whereas OAs showed stronger categorical model-brain fit in anterior

parahippocampal gyrus and some frontal regions (**Appendix B, Table 7**). In sum, the whole-brain searchlight analysis largely mirrors the *a priori* ROI analysis.

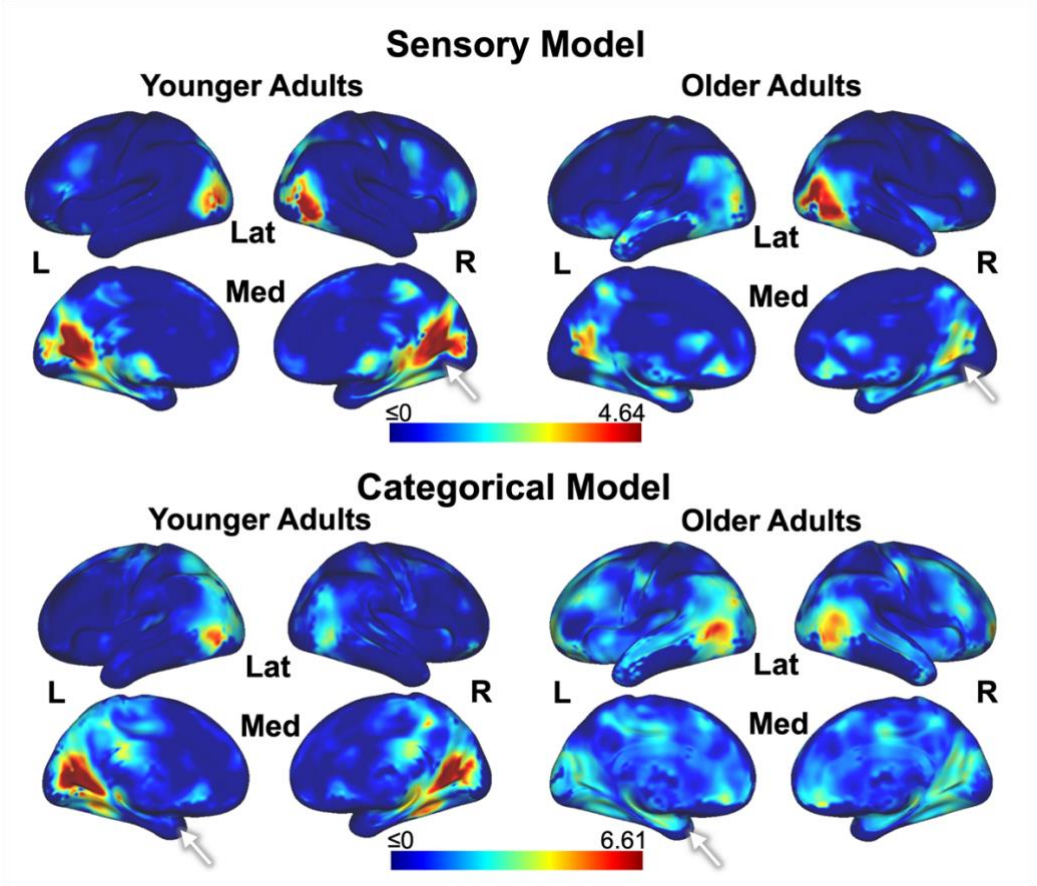

Figure 9: Whole-brain Searchlight Analysis. The figure shows the whole-brain searchlight analysis of the stimuli model (sensory and categorical)-brain fit. Within both the YAs and OAs, we found that the sensory model (based upon the first DNN layer) correlated predominately with brain activation patterns in the visual cortices and the categorical model (based upon the penultimate DNN layer) additionally correlated with brain activation patterns in anterior temporal, parietal, and frontal regions. Qualitatively, in these maps it can be seen that that the sensory model is more strongly associated with earlier visual cortex region activation patterns in YAs than OAs, whereas the categorical model is more strongly associated with more anterior ventral visual pathway region, such as the ATL, activation patterns in OAs than YAs (see white arrows). L = left; R = right; Lat = lateral; Med = medial.

3.3.3 Mnemonic Representations: Encoding-retrieval Similarity

Our second hypothesis was that aging impairs mnemonic representations for sensory features in early visual cortex and hippocampus but not for categorical features in the ATL. To test this hypothesis, we calculated encoding-retrieval similarity (ERS; Ritchey et al., 2013; Wing et al., 2014). We tested this hypothesis using the same *a priori* ROIs used to test our first hypothesis with the addition of the hippocampus because of the second hypothesis's relation to memory (see the Methods for more details). Consistent with Hypothesis 2, as shown within **Figure 10A**, we found that, compared to YAs, OAs exhibited reduced ERS in the early visual cortex (β = -0.35, z = 14.34, p < .0001, d = 0.74) and hippocampus (β = -0.45, z = 3.37, p < .001, d = 0.97), but increased ERS in the ATL (β = 0.20, z = 3.62, p < .001, d = 0.39; see **Appendix B, Figure 25c** for raw ERS values). As the ATL is particularly vulnerable to low SNR, we repeated the analysis statistically controlling for SNR and still found the same effect within the ATL (β = 0.24, z = 2.98, p < .01). In sum, these results indicated age-related decrease in mnemonic representations within regions associated with sensory features, as well as age-related increase in mnemonic representations within regions associated with categorical features.

In order to determine whether the dedifferentiation of sensory representations observed in early visual cortex were associated with a deficit in mnemonic representations, we examined the correlation between the sensory-model brain fit during encoding and ERS in early visual cortex. We found a significant positive

correlation (all participants, age-controlled partial correlation: r = 0.39, p = 0.01; YA: r = 0.36, p = 0.11; OA: r = 0.46, p = 0.042). This finding supports the assumption that age-related perceptual dedifferentiation is associated with a deficit in mnemonic representations.

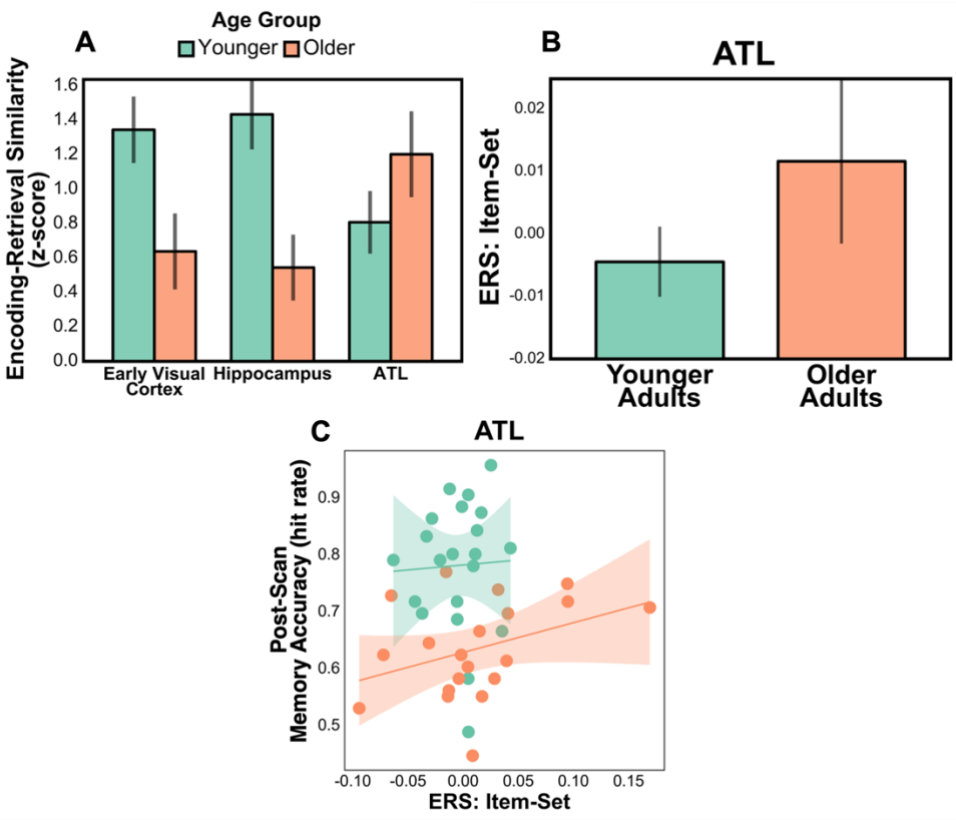

Figure 10: Age-related Differences in Mnemonic Representations. A) Age-related differences in ERS. The figure shows z-scored (mean set to one) ERS; error bars represent the standard error of the mean. B) Item-specific ERS (item-minus-set level ERS) in the ATL for trials that were subsequently remembered on the post-scan memory recognition task. Error bars represent the standard error of the mean. C) The relationship between item-specific ERS in the ATL (limited to the trials that were subsequently remembered) and accuracy of the post-scan memory recognition task. In the OAs, increased item-specific ERS in the ATL was associated with better accuracy of the post-scan memory recognition task; translucent bars around the regression lines represent the 95% confidence intervals.

Within the previous analysis we examined ERS for individual items (i.e., the similarity between pairs of encoding and retrieval activation patterns of the same scenes; item-level ERS). However, in order to make the claim that such retrieval reactivation is related to the specific memory items during encoding, it is necessary to also compare item-level ERS with set-level ERS, that is, average encoding-retrieval pattern similarity between one scene and all other scenes in the stimuli set, which reflects baseline neural reactivation (Wing et al., 2015). Furthermore, in order to strengthen our claim that ERS here reflects memory, it is necessary to repeat the analysis only on items that were subsequently remembered on the post-scan memory recognition task. Therefore, we repeated the analysis subtracting set-level ERS from item-level ERS and only including trials that were subsequently remembered on the post-scan memory task. The only region that still exhibited the same age group difference pattern was the ATL, in which, compared to YAs, OAs exhibited enhanced ERS in the ATL (**Figure 10B**; $\beta = 0.016$, $z = 2.59$, $p = .01$, $d = 0.37$; see **Appendix B, Figure 25d** for raw ERS values). The age-related increase in item-specific ERS in the ATL suggests that this region contributes to memory to a greater extent in OAs than YAs. To investigate this idea, we examined the relation between item-specific ERS (item-minus-set ERS) in the ATL and performance on the post-scan memory recognition task. As illustrated in **Figure 10C**, greater ATL item-specific ERS was associated with better accuracy of the post-scan memory recognition

task in the OAs (β = 0.51, z = 2.17, p < .05) but not YAs (β = 0.082, z = 0.092, p = .93); it should be noted, however, that the age group by ERS interaction was not statistically significant (β = 0.40, z = 0.42, p = .68). As a control analysis, the item-specific ERS of subsequently forgotten items was not associated with better post-scan recognition accuracy in YAs (β = -0.10, z = -1.55, p = .12) or OAs (β = 0.44, z = 1.34, p = .18). Meanwhile, since such association with behavior was across participant, we further performed an Age (YA/OA) x Memory (Hits/Misses) repeated measures ANOVA on item-specific ERS in ATL. We did not find a higher ERS associated with hit items ($F(1,39) = 0.02$, $p = 0.90$) or a significant Age x Memory interaction ($F(1,39) = 1.74$, $p = 0.19$).

In sum, consistent with our second hypothesis, we found that OAs exhibited reduced ERS in the visual cortex and hippocampus but increased ERS in the ATL. The latter effect was found to be item-specific and related to better memory accuracy across OA participants.

3.4 Discussions

The overarching goal of the study was to examine age-related differences in the quality of perceptual and mnemonic representations. We had two main findings. First, in early visual cortex, activation patterns associated with sensory features showed dedifferentiation in OAs, replicating previous age-related dedifferentiation findings, whereas in the ATL, activation patterns associated with categorical features showed *hyper*differentiation in OAs. This is, to our knowledge, the first report of age-related

hyperdifferentiation. Second, for mnemonic representations, we found that increased age was associated with impaired mnemonic representations (i.e., decreased ERS) in the early visual cortex and hippocampus but enhanced mnemonic representations (i.e, increased ERS) in the ATL. The enhanced mnemonic representations in the ATL was associated with better memory in OAs. These findings are discussed in greater detail below.

3.4.1 Age-related Neural Dedifferentiation

Previous studies have brought accumulating evidence for age-related neural dedifferentiation (Chee et al., 2006; Payer et al., 2006; Voss et al., 2008; Goh et al., 2010; Carp, Park, Polk, & Park, 2011; Zheng et al., 2018; Trelle et al., 2019; Bowman et al., 2019; Koen et al., 2019). Age-related dedifferentiation has been often operationalized as reduced specificity of neural responses towards different stimuli sets (e.g., faces vs. places, living vs. non-living), which are heterogeneous domains with considerable within-domain variation. The current approach expands the utility of the research concept of dedifferentiation by considering how specific aspects of visual perception representations may be impaired in the visual system in older adults. Here, we compared age-related differences in the cortical differentiation of sensory vs. categorical features using a novel DNN-based representational similarity analysis approach (Leeds et al., 2013; Khaligh-Razavi & Kriegeskorte, 2014; Kriegeskorte, 2015; Güçlü & van Gerven, 2015; Wen et al., 2018). Consistent with our hypothesis, within early visual

cortex, we found evidence for age-related neural dedifferentiation of sensory features, where, compared to the YAs, brain activation patterns in early visual cortex exhibited a worse fit with the sensory model in the OAs (**Figures 8A, 8B**). It is well known that increased age is associated with a robust decline in visual performance (Owsley, 2011; Monge & Madden, 2016). Our finding suggests that this decline may reflect not only a decline in perceptual operations (*processes*) performed on sensory information coming from earlier regions in the ventral stream, but also a deficit in the quality of visual information itself (*representations*) (Carp, Park, Polk, et al., 2011).

The dedifferentiation observed in early visual cortex may have downstream influences on subsequent encoding-retrieval pattern matching, as indicated by the significant positive correlation between sensory model-brain fit and ERS within early visual cortex (all participants, age-controlled partial correlation: $r = 0.39$, $p = 0.01$; YA: $r = 0.36$, $p = 0.11$; OA: $r = 0.46$, $p = 0.042$), suggesting that the quality of perceptual representations at encoding will affect later mnemonic reinstatement. Interestingly, no correlation between sensory model-brain fit in early visual cortex and categorical model brain fit in ATL was found (all participants, age-controlled partial correlation: $r = 0.017$, $p = 0.92$; YA: $r = -0.15$, $p = 0.52$; OA: $r = 0.15$, $p = 0.53$), suggesting that the downstream hyperdifferentiation was not driven by dedifferentiation in visual cortex.

We used a straightforward recognition test to evaluate for successful retrieval, but future studies may wish to examine what influence this representational shift has for

age-related changes in strategic retrieval operations mediated by more anterior PFC networks. Although the current analysis did not include multivariate measures of connectivity between regions, such an analysis would provide for a fruitful means of determining how OA networks adapt to declining differentiation of neural signals in primary visual regions.

3.4.2 Age-related Neural Hyperdifferentiation

In contrast to sensory features in early visual cortex, we found that categorical features in the ATL were not just spared but actually enhanced within OAs. Within the ATL, compared to YAs, activation patterns had a better fit with the categorical model in the OAs (**Figure 8A**). Thus, in contrast to age-related dedifferentiation in early visual cortex, in the ATL, we found age-related hyperdifferentiation. Regarding the regions that exhibited age-related hyperdifferentiation, the ATL is hypothesized to store prior knowledge (Ralph, Jefferies, Patterson, & Rogers, 2016; Zhao et al., 2017). Given that OAs have a stronger knowledge network than YAs (Laumann Long & Shaw, 2000; D. C. Park et al., 2002), likely from more years of knowledge accruement, it is possible that certain processes, such as object recognition, are more reliant on categorical features. Perhaps the enhanced categorical model-brain fit in the ATL within the OAs reflects OAs utilizing enhanced semantic knowledge in service of perception.

Given that we operationalized dedifferentiation using RSA, as a reduction in the fit between activity patterns and a model of the stimuli (visual or categorical),

hyperdifferentiation was conversely operationalized as an increase in this fit. We believe that the hyperdifferentiation finding reflects age-related differences in the strategies used during encoding. Representations are not necessarily 'hard-wired' into the brain and the representational space can be warped in response to task demands (Çukur, Nishimoto, Huth, & Gallant, 2013; W. C. Wang, Brashier, Wing, Marsh, & Cabeza, 2018; Martin, Douglas, Newsome, Man, & Barense, 2018). During encoding, participants rate the representativeness of its picture for its label; we speculate that YAs paid more attention to visual features (e.g., *dark* forest, *shiny* bathroom, *tall* cathedral), whereas OAs paid more attention to scene-level conceptual features (e.g., *jungle-like* forest, *master* bathroom, *Gothic* cathedral). The latter strategy is consistent with a greater age-related reliance on gist-level representations of scenes (Gutchess et al., 2005), and would tend to enhance the fit of activation patterns with late DNN layers (i.e., close to the scene label), which is what we mean by hyperdifferentiation of categorical representation in the current study.

Furthermore, this age-related shift in encoding strategies is likely to emerge slowly over the lifespan; we found no correlation between the strength of corresponding sensory—early visual cortex and categorical—ATL representations ($r = -0.08$, $p = 0.59$), suggesting that it may not be feasible to observe this shift in a cross-sectional cohort. In order to confirm our interpretation of the results, a study manipulating participants' use of sensory and categorical representations is necessary. It would be also important to

investigate the phenomenon of hyperdifferentiation of conceptual information using models of stimulus semantics based on validated feature norms, rather than inferring category selectivity via DNNs. For example, in a recent RSA study (Davis et al., 2021) using object pictures instead of scenes, we decomposed semantic features into Observed ("is round"), Taxonomic ("is a fruit"), and Encyclopedic ("is sweet") sub-categories based on an independently collected set of conceptual feature norms and a validated organization of feature categories (McRae, Cree, Seidenberg, & McNorgan, 2005). This type of analyses could build on the current DNN-based results by providing more information about the nature of the conceptual representations underlying the current age-related hyperdifferentiation finding, revealing perhaps the type of semantic information that is most relevant reliable memory formation in younger or older adults.

3.4.3 Age-related Differences in Mnemonic Representations

Our second question examined age-related differences in mnemonic representations. To examine this question, we examined the *reactivation* of mnemonic representations, which was assessed as the similarity between activation patterns during encoding and retrieval (ERS). Consistent with previous studies (St-Laurent et al., 2014; Johnson et al., 2015), compared to YAs, in OAs ERS was weaker in the early visual cortex (**Figure 10A**). Given that we also found age-related dedifferentiation of sensory representations in this region, the age-related attenuation of ERS in early visual cortex likely reflects a negative impact of degraded sensory features on visual memories. It

should be noted that even though there are studies that have also demonstrated age-related reductions in reactivation within visual cortex (St-Laurent et al., 2014; Johnson et al., 2015), some previous studies did not find this pattern (T. H. Wang et al., 2016; Abdulrahman et al., 2017; Thakral, Wang, & Rugg, 2019). The latter used multi-voxel pattern analysis (MVPA) to identify the reactivation of *classes of stimuli* (e.g., words vs. objects), whereas we used ERS to detect the reactivation of individual items of the same class. Thus, it is possible that MVPA is less sensitive than ERS in detecting age-related reactivation deficits. We also found an age-related ERS reduction in the hippocampus (**Figure 10A**). This finding is consistent with evidence of impaired hippocampal activity in OAs (Kennedy et al., 2015; Nyberg, 2017), and it extends this evidence to multivariate activation patterns. Besides normal aging, the use of ERS to investigate hippocampal memory representations could be useful for investigating Alzheimer's disease, in which the hippocampus structure and function are known to be particularly compromised (L. Wang et al., 2006; Dickerson & Sperling, 2008; Frisoni, Fox, Jack, Scheltens, & Thompson, 2010; Rathore, Habes, Iftikhar, Shacklett, & Davatzikos, 2017).

Finally, we found that, compared to YAs, OAs exhibited enhanced ERS in the ATL (**Figure 10A**). As the ATL has been associated with abstract semantic representations (Ralph et al., 2016; Zhao et al., 2017), enhanced ATL ERS in OAs may reflect a greater reliance on semantic knowledge in service of memory. This idea is consistent with our finding of age-related hyperdifferentiation for categorical features in

this region (**Figure 8A**). The accumulation of knowledge during the lifespan is likely to lead to more distinct and detailed semantic representations, which could partially counteract the degraded quality of sensory information flowing through the visual system (Monge & Madden, 2016).

3.4.4 Limitations and Further Considerations

For our analysis on the perceptual representation, the significant ROI x Age interaction points to an age-related shift in the recruitment of different brain regions for information processing, such that model fits in anterior temporal regions were greater for older adults. However, the nature of the information processed by these regions needs to be confirmed with further investigation. Assuming the validity of our RSA models, the lack of a significant Model_type by ROI interaction indicates that sensory cortex and ATL do not differ strongly in the processing of sensory vs. categorical representations. Likewise, the lack of a Model_Type x ROI x Age interaction suggest that age-related differences in the role of sensory cortex and ATL in processing sensory and categorical information should not be overemphasized. There may be several explanations to such lack of model specificity. Firstly, the DNN may not fully characterize the region-specific processing of perceptual information, which may be addressed by using improved models in future studies. Secondly, the sensory and categorical aspects of the stimuli may not be completely independent. Note that, the DNN-based sensory and the categorical models were moderately correlated (see

Appendix B, **Figure 23**), and it is common that scenes within a category may share similar low-level visual features (e.g., city skyline scenes may all have horizontal and vertical straight lines and sharp angles; rollercoaster scenes may all contain smooth spiral curvatures). Such overlap between sensory and categorical information may also explain the fact that YAs also showed stronger categorical model-brain fit in early visual cortex (**Figure 8A**; **Appendix B, Table 7**). In comparison, the analyses on alternative models (HMAX C1 for sensory versus indoor-outdoor for categorycal) showed improved Model_Type x ROI effect and Model_Type x ROI x Age effect (both $p < 0.1$), probably due to the fact that scenes within the same broad domain (indoor or outdoor) were more heterogeneous in their low-level visual features, leading to better model specificity in different brain regions. Despite these limitations, our study points to the application of these computational models in quantifying sensory and categorical information, which could help future studies better control for the dependency between different feature similarities across stimuli items before carrying out the experiments.

We found that in OAs, increased item-specific ERS in the ATL was associated with better accuracy of the post-scan memory recognition task (**Figure 10C**), supporting the importance of ATL representational quality for memory in aging. This across-subject correlation suggests that individual differences in memory performance may be at least partially mediated by neural representational quality. However, it is important to note that such association with behavior was across participant, whereas, within individuals,

we did not find a higher ERS associated with hit items ($F(1,39) = 0.02$, $p = 0.90$) or a significant Age x Memory interaction ($F(1,39) = 1.74$, $p = 0.19$). Therefore, based on current evidence, caution is needed to interpret enhanced ERS in ATL as a compensatory mechanism in OAs. In addition, the post-scan memory test is a largely visual memory task that may not rely on the type of semantic processing we show to be centered in the left ATL. Therefore, future research may further elucidate the functional consequences of such age-related shift to ATL engagement by adopting a more diverse array of post-scan memory tests tapping both perceptual and conceptual memory.

Lastly, while the age-related shift in the location of representations may reflect changes in *what kind* of scene or object information is brought to mind during encoding (i.e., relying on semantic details instead of perceptual details), it could also reflect changes in *how* visual concepts are processed. For example, the fact that OA showed higher within- than between-domain similarity in ATL may indicate a greater reliance on generalizing representations within a stimulus category–so called gist-related processing (Dennis, Kim, & Cabeza, 2008; Dennis, Hayes, et al., 2008; Webb, Turney, & Dennis, 2016). While the hippocampus and other medial temporal lobe structures have often been the focus of such an age-related shift from detail-oriented memory processing to a more familiarity-based strategy (Dennis, Kim, et al., 2008), lateral and anterior temporal regions coding for specific stimulus features may also drive this effect. It is

worth investigating in the future if the representations in ATL reflect mainly complex, meaningful categorical information that may support encoding rather than simple gist.

3.4.5 Summary

The traditional idea that aging is associated with a generalized decline in cognitive abilities and their underlying neural mechanisms has been challenged by evidence that although some cognitive and brain mechanisms are impaired by aging, others are not only spared but even enhanced by aging (Laumann Long & Shaw, 2000; D. C. Park et al., 2002). One aspect of cognition that is spared by aging are processes that rely on categorical features, such as conceptual and semantic processing, but the neural mechanisms of these spared functions are largely unknown. The results of the present study suggest that one factor contributing to the preservation of these processes in old age is the enhanced quality of categorical representations in the ATL. These spared categorical representations may contribute not only to perceptual but also to mnemonic aspects of cognition. Lastly, these findings have implications not only for understanding normal aging but also the effects of pathological aging (e.g., Alzheimer's disease) on memory representations, which, to our knowledge, has yet to be examined.

4. Age-invariant and Age-specific Effects of Schema on object Representation in Occipital Temporal Cortices[1]

4.1 Introduction

In the previous two chapters, we revealed remarkable age-related differences in the brain during episodic memory. These differences manifested in multiple brain systems in the forms of neural representation and functional connectivity, implying qualitative differences in cognitive processes between the two age groups. However, such possibility was unexplored in the previous chapters due to a limitation in the task design. To examine the similarities and differences between age groups in representation and connectivity, paradigms that explicitly manipulate the accessibility of the cognitive process in investigation will be necessary.

As age is known to be associated with the accumulation of crystalized knowledge, one possible strategy that OAs may employ is the increased reliance on semantic processing and schema (D. C. Park et al., 2002). Preexisting knowledge has been known to support the formation of new memories (Spalding, Jones, Duff, Tranel, & Warren, 2015; A. Greve, Cooper, Tibon, & Henson, 2019). A growing body of neuroimaging studies points to the interplay of multiple brain systems during schema-congruent learning and memory involving mPFC (van Kesteren et al., 2010; van Kesteren et al., 2013), which is assumed to facilitate the integration of new information

[1] This work was supported by the National Institute on Aging (1RF1AG066901-01A1).

into pre-existing neocortical associations, complementing the function of hippocampus during encoding and retrieval when schema is present (Van Kesteren, Ruiter, Fernández, & Henson, 2012). However, existing neuroimaging research on the role of schema in memory has been mostly focused on young adults, and the interaction between age and schema is unclear.

We leveraged representational similarity analysis (RSA; Kriegeskorte, 2008) to explore the effects of schema on information processing in different age groups. It has been well-established that brain activation patterns in ventral visual regions during object perception is associated with low-level visual as well as categorical features of the objects, reflecting the storage of visual and semantic representations (Khaligh-Razavi & Kriegeskorte, 2014; Clarke & Tyler, 2014; Davis et al., 2021; Deng, Davis, et al., 2021; Naspi, Stensholt, Karlsson, Monge, & Cabeza, 2022). Several recent studies have found an age-related reduction in the quality of visual representations but also an age-related increase in the quality of semantic representations (Deng, Davis, et al., 2021; Naspi et al., 2022). This finding supports the idea that healthy older adults may rely more than younger adults on semantic and schematic knowledge to compensate for perceptual deficits. Meanwhile, recent studies have shown the neural representations are not 'hard-wired' and may be modulated by task design, such as participants' attention to certain features (Nastase et al., 2017; Martin et al., 2018; W. C. Wang et al., 2018), and artificial knowledge acquired in a laboratory setting (Schlichting, Mumford, & Preston, 2015;

Clarke et al., 2016). The latter observation suggests that schemas in real life may have influence on the neural representations of visual and semantic features in naturalistic objects. This influence is particularly worth considering with regard to aging, as realistic stimuli such as scenes and objects are closely related to schematic knowledge accumulated over time, and this accumulated schematic store may serve as a cognitive resource for older adults.

In this study, young and older adults viewed sequentially presented scene-object pairs with a broad range of schematic congruency, and then rated the likelihood of finding the object in the scene. Their recognition memory for visual and semantic properties of these objects was then tested in the following day. The strength of visual and semantic representations of the objects were quantified using RSA, and the scope of analysis was focused on ROIs located in occipital and/or temporal cortices (OTC). These ROIs included the early visual cortex (EVC) and anterior temporal lobe (ATL) that were investigated in Deng et al. (2021), as well as the lateral occipital cortex (LOC), fusiform gyrus (FG), and inferior temporal gyrus (ITG) (Naspi et al., 2022).

The investigations in this study aimed to achieve two goals. The first goal was to quantitatively depict the landscape of visual and semantic representations in OTC in the two age groups. Within this goal, we sought to replicate the conclusions of previous studies regarding the regional differentiation of visual and semantic processing in OTC (Davis et al., 2021; Naspi, Hoffman, Devereux, & Morcom, 2021; Naspi et al., 2022), as

well as the age-related decline of visual information processing in EVC (Deng, Davis, et al., 2021; Naspi et al., 2022). The second goal was to investigate the effect of schema on object representation in OTC. Given the functional specialization of OTC, we predicted that, instead of showing a uniform effect across all regions, schema congruency will affect certain type of representation in certain ROIs. While we expected that the effect of schema in some ROIs may be common for both age groups, interaction between age and schema, if observed, may help elucidate the cognitive relevance of age-related increase in semantic representation in previous studies (Deng, Davis, et al., 2021; Naspi et al., 2022).

4.2 Materials and Methods

4.2.1 Experimental Paradigm

The study consisted of three visits on separate days with MRI scans (**Figure 11**). In the first visit (referred to as the 'baseline session'), participants viewed, in total, 114 pictures of objects with descriptive labels (e.g., tractor, football, etc.) and responded how well the labels describe the objects. Each object image was presented for 4s, with jittered inter-trial interval lasting 4s on average. Data from this session was not analyzed in the current chapter.

The second visit was conducted at a minimum of 7 days after Session 1, in which participants viewed pictures of scenes and objects. In each trial, a scene depicting a well-known scene schema was presented for 3s, followed by a jittered blank screen (3s

average duration) and then an object for 4s. Scenes and objects were evenly divided into three subsets that were unknown to the participants, each containing 38 scenes and 38 objects. Within each subset, scenes and objects were manually paired at three congruency levels. During the task, the stimuli from three subsets are presented at different congruency levels, such that one third of the scenes were followed by objects that are congruent to the schemata of the scenes (e.g., farm -> tractor; pier -> sea gull), one third by incongruent objects (e.g., bakery -> football; prison -> poker table), and one third by neutral objects (not typical but not unlikely in the scene, e.g., desert -> cricket; woods -> railroad); congruency levels of the three subsets were counterbalanced between participants. When an object appeared, the participant responded how likely it is to find the object in the scene (1 = very unlikely to 4 = very likely). This session is referred to as the 'encoding session', with respect to Session 3 ('retrieval session') described below.

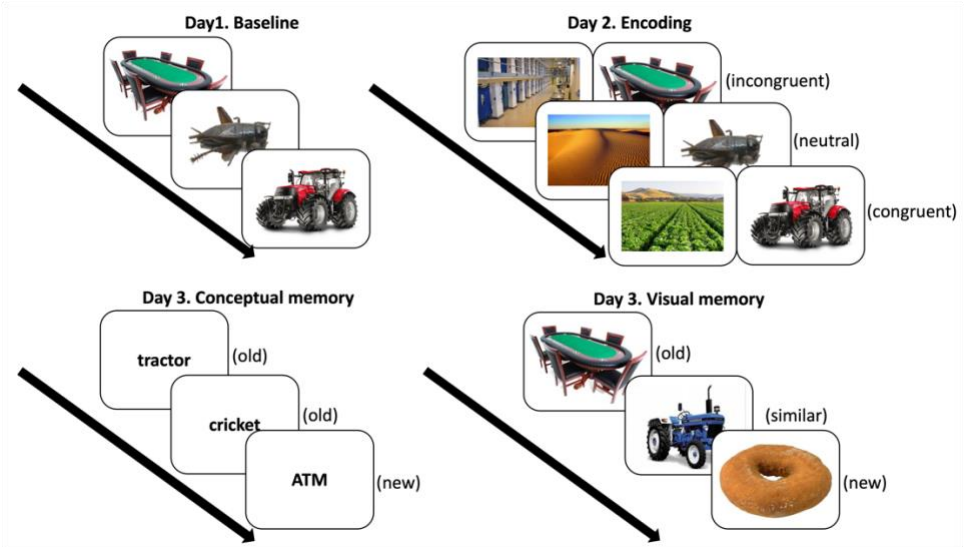

Figure 11: Experimental Design. Top left: session 1, 'baseline' visit. Top right: encoding task in session 2. Bottom left: conceptual memory task in session 3. Bottom right: visual memory task in session 3

The third 'retrieval' session was conducted approximately 24 hours later, in which participants were tested two forms of memory of the objects encoded in the previous day. A) In the *conceptual memory task*, 144 words in total were presented to the participants, among which 114 words represented objects that had been shown previously, and 30 distractor words that were not presented before. Participants responded whether the word represented an old object or a new object (1 = definitely new, 2 = probably new, 3 = probably old, 4 = definitely old). B) In the following *visual memory task*, 124 images in total were presented to the participants, in which 96 images were identical object images that have been shown before (32 per congruency level), 18 images were different exemplar of the objects shown in Sessions 1 and 2 (6 per each

congruency level), and 12 images were new objects. Participants responded whether the image is identical (3), similar (2), or new (1).

4.2.2 Participants

A total of 37 YAs and 19 OAs have participated in this study. Participants were free of significant neurological or psychiatric conditions, and not taking medications known to affect cognitive function or cerebral blood flow (except antihypertensive agents), according to their self-report. OAs were further screened with Montreal Cognitive Assessment (MoCA, Nasreddine et al., 2005, inclusion criteria > 23). All participants were fluent English speakers and had completed at least 12 years of education. Three YAs and one OA did not complete the full study due to sickness, potential SARS-CoV-2 exposure, and injury. Two YAs withdrew from the study after the first visit. One YA has incomplete MRI data in visit 3 due to technical issue. We also excluded one YA who reported falling asleep during visit 2. Consequently, for the investigation of encoding, the data were analyzed with 33 YAs (11 men, 22 women) and 19 OAs (7 men, 12 women).

4.2.3 MRI Acquisition

MRI data were collected on a General Electric 3T MR750 whole-body 60 cm bore MRI scanner and an 8-channel head coil. Each MRI session started with a localizer scan, in which 3-plane (straight axial/coronal/sagittal) localizer faster spin echo (FSE) images were collected. A high-resolution anatomical image (96 axial slices parallel to the AC-PC

plane with voxel dimensions of 0.9 x 0.9 x 1.9 mm) was collected. Then, the functional images were acquired using the GE EPI sequence (repetition time [TR] = 2000 ms, echo time = 30 ms, field of view [FOV] = 19.2 cm, 36 oblique slices with voxel dimensions of 3 x 3 x 3 mm). For each type of task, the functional images were collected over three runs. Stimuli were projected onto a mirror at the back of the scanner bore, and responses were recorded using a four-button fiber-optic response box (Current Designs, Philadelphia, PA, USA). Functional resting-state images and diffusion-weighted images were also collected, which are not reported here. Participants wore earplugs to reduce scanner noise, and foam pads were used to reduce head motion. When necessary, participants wore MRI-compatible lenses to correct vision.

4.2.4 fMRI Preprocessing[2]

Results included in this manuscript come from preprocessing performed using fMRIPrep 20.2.0 (Esteban, Markiewicz, et al., 2019; Esteban, Blair, et al., 2019) (RRID:SCR_016216), which is based on Nipype 1.5.1 (Gorgolewski et al., 2011; Gorgolewski et al., 2018) (RRID:SCR_002502).

Anatomical data preprocessing. A total of 1 T1-weighted (T1w) images were found within the input BIDS dataset. The T1-weighted (T1w) image was corrected for

[2] Copyright information: the text in this section was automatically generated by fMRIPrep and released under CC0 license, with the express instruction that users should copy and paste this text into the manuscript unchanged.

intensity non-uniformity (INU) with N4BiasFieldCorrection (Tustison et al., 2010), distributed with ANTs 2.3.3 (Avants, Epstein, Grossman, & Gee, 2008, RRID:SCR_004757), and used as T1w-reference throughout the workflow. The T1w-reference was then skull-stripped with a Nipype implementation of the antsBrainExtraction.sh workflow (from ANTs), using OASIS30ANTs as target template. Brain tissue segmentation of cerebrospinal fluid (CSF), white-matter (WM) and gray-matter (GM) was performed on the brain-extracted T1w using fast (FSL 5.0.9, RRID:SCR_002823, Zhang, Brady, & Smith, 2001). Brain surfaces were reconstructed using recon-all (FreeSurfer 6.0.1, RRID:SCR_001847, Dale, Fischl, & Sereno, 1999), and the brain mask estimated previously was refined with a custom variation of the method to reconcile ANTs-derived and FreeSurfer-derived segmentations of the cortical gray-matter of Mindboggle (RRID:SCR_002438, Klein et al., 2017). Volume-based spatial normalization to one standard space (MNI152NLin2009cAsym) was performed through nonlinear registration with antsRegistration (ANTs 2.3.3), using brain-extracted versions of both T1w reference and the T1w template. The following template was selected for spatial normalization: ICBM 152 Nonlinear Asymmetrical template version 2009c (Fonov, Evans, McKinstry, Almli, & Collins, 2009, RRID:SCR_008796; TemplateFlow ID: MNI152NLin2009cAsym).

Functional data preprocessing. For each of the 6 BOLD runs found per subject (across all tasks and sessions), the following preprocessing was performed. First, a

reference volume and its skull-stripped version were generated using a custom methodology of fMRIPrep. Susceptibility distortion correction (SDC) was omitted. The BOLD reference was then co-registered to the T1w reference using bbregister (FreeSurfer) which implements boundary-based registration (D. N. Greve & Fischl, 2009). Co-registration was configured with six degrees of freedom. Head-motion parameters with respect to the BOLD reference (transformation matrices, and six corresponding rotation and translation parameters) are estimated before any spatiotemporal filtering using mcflirt (FSL 5.0.9, Jenkinson, Bannister, Brady, & Smith, 2002). BOLD runs were slice-time corrected using 3dTshift from AFNI 20160207 (Cox & Hyde, 1997, RRID:SCR_005927). The BOLD time-series (including slice-timing correction when applied) were resampled onto their original, native space by applying the transforms to correct for head-motion. These resampled BOLD time-series will be referred to as preprocessed BOLD in original space, or just preprocessed BOLD. The BOLD time-series were resampled into standard space, generating a preprocessed BOLD run in MNI152NLin2009cAsym space. First, a reference volume and its skull-stripped version were generated using a custom methodology of fMRIPrep. Several confounding time-series were calculated based on the preprocessed BOLD: framewise displacement (FD), DVARS and three region-wise global signals. FD was computed using two formulations following Power (absolute sum of relative motions, Power, Mitra, et al., 2014) and Jenkinson (relative root mean square displacement between affines, Jenkinson

et al., 2002). FD and DVARS are calculated for each functional run, both using their implementations in Nipype (following the definitions by Power Mitra, et al. 2014). The three global signals are extracted within the CSF, the WM, and the whole-brain masks. Additionally, a set of physiological regressors were extracted to allow for component-based noise correction (CompCor, Behzadi, Restom, Liau, & Liu, 2007). Principal components are estimated after high-pass filtering the preprocessed BOLD time-series (using a discrete cosine filter with 128s cut-off) for the two CompCor variants: temporal (tCompCor) and anatomical (aCompCor). tCompCor components are then calculated from the top 2% variable voxels within the brain mask. For aCompCor, three probabilistic masks (CSF, WM and combined CSF+WM) are generated in anatomical space. The implementation differs from that of Behzadi et al. in that instead of eroding the masks by 2 pixels on BOLD space, the aCompCor masks are subtracted a mask of pixels that likely contain a volume fraction of GM. This mask is obtained by dilating a GM mask extracted from the FreeSurfer's aseg segmentation, and it ensures components are not extracted from voxels containing a minimal fraction of GM. Finally, these masks are resampled into BOLD space and binarized by thresholding at 0.99 (as in the original implementation). Components are also calculated separately within the WM and CSF masks. For each CompCor decomposition, the k components with the largest singular values are retained, such that the retained components' time series are sufficient to explain 50 percent of variance across the nuisance mask (CSF, WM, combined, or

temporal). The remaining components are dropped from consideration. The head-motion estimates calculated in the correction step were also placed within the corresponding confounds file. The confound time series derived from head motion estimates and global signals were expanded with the inclusion of temporal derivatives and quadratic terms for each (Satterthwaite et al., 2013). Frames that exceeded a threshold of 0.5 mm FD or 1.5 standardised DVARS were annotated as motion outliers. All resamplings can be performed with a single interpolation step by composing all the pertinent transformations (i.e. head-motion transform matrices, susceptibility distortion correction when available, and co-registrations to anatomical and output spaces). Gridded (volumetric) resamplings were performed using antsApplyTransforms (ANTs), configured with Lanczos interpolation to minimize the smoothing effects of other kernels (Lanczos, 1964). Non-gridded (surface) resamplings were performed using mri_vol2surf (FreeSurfer).

Many internal operations of fMRIPrep use Nilearn 0.6.2 (Abraham et al., 2014, RRID:SCR_001362), mostly within the functional processing workflow. For more details of the pipeline, see the section corresponding to workflows in fMRIPrep's documentation.

4.2.5 Single-trial Analysis

The functional activity for each trial served as the basis for the subsequent network and representational analyses. To estimate the activity for each trial, we

conducted a single-trial model analysis within a general linear model (Mumford et al., 2012). This approach estimates a first-level model in which one regressor models a specific trial of interest and another regressor models all the other trials. This single-trial modelling process was repeated for every unique trial, and the beta estimates of the trials of interest were gathered for further analysis. Each trial was modeled with a stick function at trial onset convolved with standard hemodynamic response function (HRF). The temporal and dispersion derivatives of the HRF were also modelled in order to control for potential age difference in hemodynamics (Samanez-Larkin & D'Esposito, 2008; Wright & Wise, 2018). Each model also included the six raw motion regressors, a composite motion parameter, the white matter time-series, and cerebrospinal fluid time-series. We also modeled the temporal and dispersion derivatives and implemented a 128 sec cutoff high-pass temporal filter.

4.2.6 Representational Similarity Analysis

To measure the degree to which visual and semantic features of the stimuli account for brain activation pattern, we conducted representational similarity analysis based on the fits between brain and two computational models (a.k.a. model-brain fit), which captured the visual and semantic features of the stimuli, respectively. To briefly describe, the computational model generates a similarity matrix ('feature similarity matrix') that characterizes the feature similarity between all pairs of object stimuli. Meanwhile, for every brain region, we also computed the neural similarity matrix that

characterizes the similarity structure of brain activation patterns across all objects. Finally, the model-brain fit was obtained by correlating the feature similarity matrix with the neural similarity matrix using Spearman's correlation. Since we are interested in the effects of schema on visual and semantic representations, we created the feature and the neural similarity matrices for the objects in incongruent, neutral, and congruent conditions separately, and the model-brain fits for visual and semantic features were calculated in respect to these three congruency levels.

To construct neural similarity matrices, we first obtained the brain activity patterns for all stimuli in different ROIs. We used the Brainnetome atlas (BNA) (Fan et al., 2016) that consists of 246 regions to extract activation pattern at different brain regions. The neural similarity matrix for a brain region was computed as the cross-correlation matrix of brain activation patterns for different objects. For the visual similarity matrix, we used a widely-used deep neural network model called VGG16 (Simonyan & Zisserman, 2015), which is pre-trained on a dataset of over 1.3 million object images. The first convolutional layer of VGG16, whose artificial neurons directly respond to image inputs, is known to be sensitive to low-level visual features (Eickenberg et al., 2017). Thus, the visual similarity matrix was defined as the cross-correlation matrix of the activation patterns in the first convolutional layer responding to different objects. For the semantic similarity matrix, we used a popular computational model for natural language processing called Word2vec (Mikolov, Chen, Corrado, &

Dean, 2013). This model is trained on a large corpus of text, and it converts words into vectors such that words that are semantically similar are located in proximity in the vector space. The semantic similarity matrix was then defined as the cross-correlation matrix of the word vectors.

4.2.7 Regions of Interests (ROIs)

We focused our analysis on OTC regions, in which neural representations have been shown to track visual and semantic features and also revealed age-related differences (Clarke & Tyler, 2014; Clarke et al., 2016; Davis et al., 2021; Deng, Davis, et al., 2021; Naspi et al., 2021; Naspi et al., 2022). We examined five ROIs in the OTC that spans the posterior and anterior visual stream (see **Figure 13A**), namely, (1) the early visual cortex (EVC) consisting of BNA regions 189-198, (2) the lateral occipital cortex (LOC) consisting of BNA regions 199-206, (3) the fusiform gyrus (FG) consisting of BNA regions 103:108, the inferior temporal gyrus (ITG) consisting of BNA regions 89-92 and 95-102, and (5) the anterior temporal gyrus (ATL) consisting of BNA regions 69, 70, 77, 78, 79, 80, 83, 84, 93, 94.

4.3 Results

4.3.1 Behavioral Results

To examine whether participants' ratings of scene-object likelihood matched the assigned congruency condition, and whether there is age difference in the likelihood judgement, we conducted a Congruency-by-Age repeated measures ANOVA with the

likelihood rating as the dependent variable. A significant effect of Congruency was observed ($F_{2,100} = 3084.31$, $p < 10^{-15}$). Consistent with the intended manipulation, participants rated the probability of the object occurring on the scene as very likely in the incongruent condition and very unlikely in congruent condition, with the neutral condition in between (**Figure 12A**). The likelihood rating was not associated with Age ($F_{1,50} = 0.68$, $p = 0.41$) or Age-Congruency interaction ($F_{2,100} = 0.38$, $p = 0.69$), indicating that the stimuli had similar relationships with schema congruency in both groups.

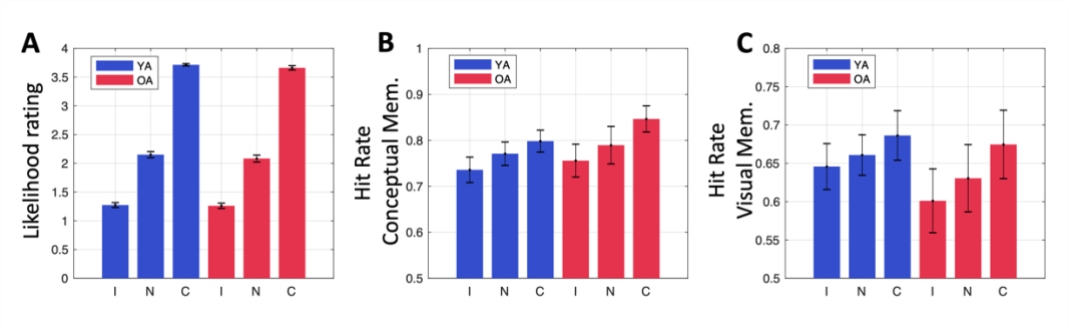

Figure 12: Behavioral Results. A) Encoding likelihood rating. B) Conceptual memory hit rate. C) Visual memory hit rate. I = incongruent; N = neutral, C = congruent. Error bars indicate standard error of the mean.

We then investigated whether conceptual and visual memory performances varied as a function of age group or schema congruency (**Figures 12B, 12C**). Two separate ANOVAs were conducted for two memory tasks, with the hit rates of the respective tasks as dependent variables. For conceptual memory, we observed a significant effect of Congruency ($F_{2,90} = 14.52$, $p < 10^{-5}$), but no effect of Age ($F_{1,45} = 0.93$, $p = 0.34$) or Age-by-Congruency interaction ($F_{2,90} = 0.12$, $p = 0.89$). Similarly, for visual memory, we observed a significant effect of Congruency ($F_{2,90} = 5.76$, $p < 0.005$), but no

effect of Age ($F_{1,45} = 0.2$, $p = 0.66$) or Age-by-Congruency interaction ($F_{2,90} = 0.41$, $p = 0.67$). Taken together, memory performance was modulated by semantic schemas in both groups. The lack of age and age-congruency interactions in memory performance is an advantage at the time of interpreting age and age-congruency interactions in fMRI results, as it indicates that the latter are not confounded by behavioral differences.

4.3.2 Visual and Semantic Representations in Ventral Visual Stream during Encoding

To investigate whether visual and semantic information were represented differentially in ventral visual stream ROIs, and whether the two types of information were preferentially processed by the two age groups, we conducted an omnibus RepresentationType-by-ROI-by-Age-by-Congruency ANOVA. As indicated by a significant effect of ROI ($F_{4,200} = 3.07$, $p = 0.017$) and a RepresentationType-by-ROI interaction ($F_{4,200} = 4.27$, $p = 0.0025$), visual and semantic model-brain fits were spatially non-uniform and showed different spatial distributions (**Figures 13B, 13C**, values were averaged across congruency for simplicity). To further investigate the anatomical relevance of the visual and semantic representations, for each type of representation, a series of two-tailed one-sample t-tests were conducted to explore if the model-brain fit is significantly greater than zero in any of the ROIs. Visual model-brain fit was found to be significant in EVC ($t_{51} = 3.52$, $p<0.001$, uncorrected) and LOC ($t_{51} = 2.15$, $p = 0.036$, uncorrected). In comparison, semantic model-brain fit was found to be significant in LOC ($t_{51} = 3.18$, $p = 0.0025$, uncorrected), FG ($t_{51} = 3.26$, $p = 0.0019$, uncorrected), and ATL

(t_{51} = 2.4, p = 0.019, uncorrected). These findings are consistent with previous studies (Naspi et al., 2022) that visual and semantic information are processed by different sub-regions in the ventral visual area.

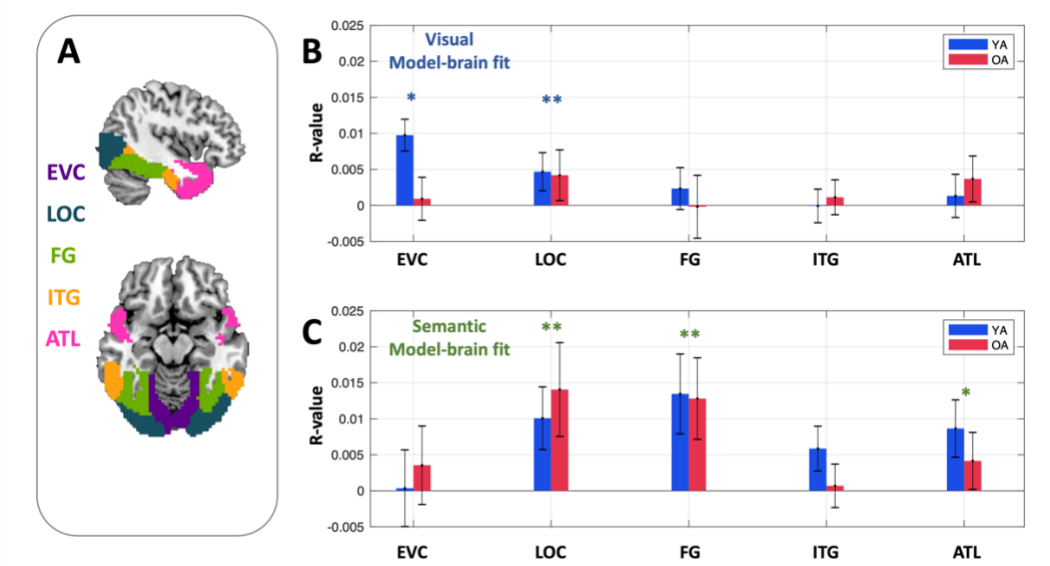

Figure 13: Visual and Semantic Representations in OTC regions. A) ROI definition. B) Visual representation. C) Semantic representation. Model-brain fit values were averaged across congruency for simplicity. Error bars indicate standard error of the mean. Asterisks indicate the significance of one-sample t-tests on whether a model-brain fit value is different from 0 (with the two age groups combined; blue = visual; green = semantic; *: p<0.05; **: p<0.01).

4.3.3 Effects of Schema on OTC Neural Representations

In addition to the significant effects of ROI and RepresentationType-by-ROI interaction (**Figure 13**), in the foregoing ANOVA we also observed a significant effect of Congruency ($F_{2,100}$ = 5.95, p = 0.0036), which we analyzed in separated regions. For this analysis, we focused on the regions that processed either visual or semantic representation, that is, regions with model-brain fits that were significantly above zero.

For each brain-model fit under investigation (i.e., visual representation in EVC and LOC, semantic representation in LOC, FG, and ATL), a Congruency-by-Age ANOVA was performed, and the results are summarized in **Table 1** and illustrated in **Figure 14**.

Table 1: Effects of Age and Congruency on Visual and Semantic Representations in OTC

Type	**Region**	**Effects – F-stat (p-val)**		
		Age	Congruency	Age x Congruency
Visual	EVC	**5.74(0.02)**	1.68(0.19)	0.66(0.52)
	LOC	0.012(0.91)	**3.61(0.031)**	0.44(0.65)
Semantic	LOC	0.28(0.60)	0.31(0.74)	0.87(0.42)
	FG	0.006(0.94)	**4.89(0.0094)**	1.57(0.21)
	ATL	0.39(0.53)	1.18(0.31)	**4.22(0.017)**

In EVC, a significant effect of Age was observed for the visual model-brain fit (**Figure 14A**, left), suggesting an age-related reduction in the processing of visual information that is consistent with our previous study (Deng, Davis, et al., 2021). In LOC, both visual and semantic model-brain fit were significantly above zero, suggesting processing of both types of information in this brain region. However, schema congruency only modulated the strength of visual representation, in which the schema-neutral condition showed highest visual model-brain fit (**Figure 14A**, right).

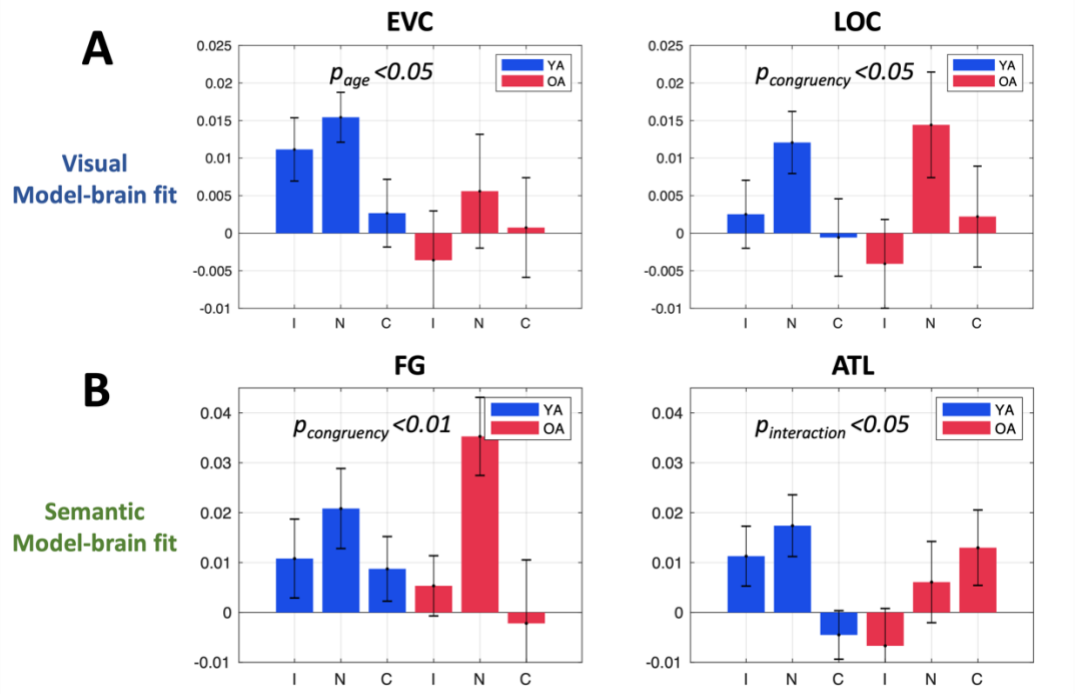

Figure 14: Effects of Age and Congruency on Visual and Semantic Representations. A) Visual representation. B) Semantic representation. I = incongruent, N = neutral, C = congruent. Error bars indicate standard error of the mean.

As for the semantic representation, schema congruency resulted in a significant effect in FG ($F_{2,90} = 4.89$, $p = 0.0094$), in which the semantic model-brain fit peaked at the schema-neutral condition for both age groups (**Figure 14B**, left). While the effects of schema in LOC and FG were age-invariant, the semantic representation in ATL showed a unique Age-by-Congruency interaction (**Figure** 14B, right; $F_{2,90} = 4.22$, $p = 0.017$). OAs showed highest model-brain fit in the congruent condition, while the YAs showed lowest model-brain fit in the same experimental condition.

Taken together, the above analyses replicated our previous finding of reduced visual representation in EVC in OAs. It also revealed evidence of modulatory effect of

schema on the processing of both visual and semantic information. Importantly, ATL showed different effects of schema on semantic representation in YAs and OAs, suggesting that this region might serve different function in the two age groups.

4.4 Discussions

In this study, we examined the quality of visual and semantic representations in young and older adults with respect to schema congruency. Our results showed an age-related reduction in visual representation in EVC, which is consistent with previous studies (Deng, Davis, et al., 2021; Naspi et al., 2022) and suggests a deficit in the processing of visual information in OAs. As for the effect of schema, both age groups showed enhanced memory for schema-congruent condition, suggesting that schema may influence the formation of cortical memory traces during encoding. Indeed, we observed a wide-spread schema effect on visual and semantic representation across OTC. In LOC, the visual representation was enhanced in the schema-neutral condition, and the same pattern was also observed for the semantic representation in FG. In comparison, in ATL, we observed an interaction between congruency and age, where the schema-congruent condition reduced semantic representation in YAs but enhanced the same type of representation in OAs. In sum, these results suggest support for the idea that older adults engage in a shift in both what kinds of information are represented, as well as in how that information is integrated with existing schemas. We outline these effects below.

4.4.1 Age-related Deficit in EVC Visual Processing

The current study adds to the existing evidence of the age-related decline in perceptual processing in OTC (Chee et al., 2006; Goh et al., 2010; Carp, Park, Polk, et al., 2011; Bowman et al., 2019; Koen et al., 2019; Trelle et al., 2019), commonly referred as neural dedifferentiation. As discussed in **Chapter 1**, age-related dedifferentiation has often been operationalized as the reduction of neural response specificity to different stimulus types or categories, and it is often quantified using cross-category and within-category neural pattern similarity. However, in the above-mentioned investigations based on categorical similarity, it is not fully clear the dedifferentiation is due to a deficit in visual or semantic processing, as stimuli items within the same category often share similar visual features as well as semantic meanings. The current study together with a few recent RSA-based studies (Deng, Davis, et al., 2021; Naspi et al., 2022) goes beyond the conventional category-based approach, and quantifies visual and semantic information separately. Convergent with Deng et al. (2021) and Naspi et al. (2022), in the current study, we only observed age-related decline in visual representation, while the semantic representation was largely preserved in OAs, suggesting that the well-documented OTC neural dedifferentiation could be due to the failure in processing purely visual information.

4.4.2 The Effects of Schema Congruency on Encoding Representation and Subsequent Memory

Our results revealed that naturalistic schema has broad behavioral and neural effects on object perception and memory. We found that the objects that were congruent with the scene-related schemas were better remembered for both age groups. This congruency benefit is convergent with empirical findings (van Kesteren et al., 2013; Gronau & Shachar, 2015; Spalding et al., 2015), supporting the idea that schema facilitates the integration of relevant information, such as visual objects that fit with a scene context (Morris, 2006; Van Kesteren et al., 2012). Interestingly, while we speculated that OAs might preferentially use schema-related processing, the memory performance in OAs did not show a stronger schema benefit than YAs. Future investigation may further elucidate the lack of Age-by-Congruency difference in memory performance.

The effect of schema on subsequent memory performance is likely linked to cortical neural coding that forms memory traces, which motivates the investigation of the association between encoding congruency and neural representation in OTC. Indeed, we observed main effect of schema in LOC and FG, convergent with growing evidence that neural representation is not hard-wired and may be shaped by factors such as attention (Martin et al., 2018) and knowledge (Clarke et al., 2016). The presence of schema affect both semantic representation and visual representation. Interestingly, while memory performance peaked at the congruent condition, the RSA results in LOC and FG showed enhanced representation for the neutral condition rather than a linear

relationship with congruency. We believe such trend may be contributed by both a top-down attention effect (Martin et al., 2018; W. C. Wang et al., 2018) and a congruency advantage effect. In the neutral condition, the relationship between scenes and objects is likely the most ambiguous, which makes this condition more challenging and results in the shift of top-down attention to the visual and semantic features of the objects. In contrast, when the scene-object combination is clearly congruent or incongruent, schema may facilitate the fast decision to integrate or suppress the information of the object, leading to less efforts and reduced need for processing visual and semantic information. Meanwhile, the relatively low level of visual and semantic representations in the congruent condition is also in line with the notion that schema improves the efficiency of learning of new information (Van Kesteren et al., 2012), as it lessens the need for information processing.

4.4.3 Age-specific Effect of Schema in ATL

An important finding of the current study is the Age-by-Congruency interaction effect in ATL, where the semantic representation increased with congruency in OAs but decreased in YAs in the congruent condition (**Figure 14B**). This finding indicates that ATL may play different roles in schema-related processing in the two age groups. In OAs, semantic representation of an object was preferentially enhanced in the presence of a congruent context. This observation offers a possible account for the finding in Deng & Davis et al. (2021) regarding the age-related increase of semantic representation in ATL,

implying a possibility that the ATL semantic representation could signal schema activation in OAs. In comparison, in our current study, YAs showed higher semantic representation in the less congruent conditions, which suggests a possibility that YAs may preferentially process semantic meaning when incoming information conflicts with a schema, perhaps due to a search for possible schematic relationships between object and scene. Given the two age groups showed very similar behavioral results, this finding further underscores the necessity of investigating the neural representation of information in future aging studies.

4.4.4 Further Considerations

The data in the current study was not fully consistent with the age-related increase of semantic representation in ATL as reported in **Chapter 3** (Deng, Davis, et al., 2021). Although the reason for such inconsistency is not fully clear, the lack of a main effect of age in the current study may be due to the difference in task design. The encoding task in the current study requires a deeper level of semantic processing, which could lead to ATL semantic representation in both age group. In contrast, in Deng & Davis et al. (2021) where the participants gave relatively simple representativeness rating, the age-related difference in semantic representation may reflect OAs' higher baseline propensity towards semantic information.

4.4.5 Summary

Neural representation of information is not hard-coded and will be co-determined by different factors, such as age and task. Consistent with a growing body of literature, we found reduced visual information in OAs in EVC, which is convergent with the notion of perceptual deficit in aging. While age-invariant schema effect was observed in LOC and FG, the semantic representation in ATL exhibited a unique interplay between age and schema congruency, which highlights the unique role of ATL in OAs during object perception.

.

5. Dissociable Effects of Memory Success and Encoding Schema Congruency: Functional Connectivity Network during Memory Retrieval in Young and Older Adults[1]

5.1 Introduction

Brain is a complex network of interdependent regions, of which the topological characteristics are constantly changing across brief and extended time scales, from transient shifts in cognitive demands (Cole et al., 2013; Spielberg et al., 2015; Simony et al., 2016), to development and aging (Tomasi & Volkow, 2012; Chan et al., 2014; Oldham & Fornito, 2019). Recent studies have shifted from resting-state networks to brain networks during task performances, such as memory retrieval in healthy YAs and OAs (Geib, Stanley, Wing, et al., 2017; Geib, Stanley, Dennis, et al., 2017; Deng, Stanley, et al., 2021). These studies characterized the pivotal role of MTL system in supporting successful memory through the reconfiguration of functional connectivity (fCON), as well as significant age differences involving this region.

Of note, older adults' MTL is less engaged in the global functional network and exhibits reduced reconfiguration between successful and unsuccessful memory retrieval (Deng, Stanley, et al., 2021) – a finding extending the well-documented age-related MTL decline in episodic memory reported by previous studies using univariate activation analysis (Dennis, Daselaar, et al., 2007; Dennis, Kim, et al., 2007; Davis et al., 2008; St.

[1] This work was supported by the National Institute on Aging (1RF1AG066901-01A1).

Jacques et al., 2012; Reagh, Delarazan, Garber, & Ranganath, 2020). Meanwhile, the engagement of PFC in successful memory retrieval is generally increased in OAs (Deng, Stanley, et al., 2021), suggesting a compensatory role of PFC for MTL deficits. The 'seesaw' relationship between MTL and PFC is consistent with the notion of 'compensation by selection' (Cabeza, Albert, et al., 2018), that is, under the same task condition (i.e., retrieval of scene images), OAs may recruit neural resources (i.e., PFC) associated with certain cognitive processes that are available to but not adopted by YAs. However, the exact cognitive mechanism was not explicitly examined.

As discussed in the previous chapters, aging is associated with the accumulation of crystalized knowledge (D. C. Park et al., 2002), and there is evidence that OAs tend to rely on schematic knowledge compared to YAs (Mather et al., 1999). A growing body of neuroimaging studies points to the orchestration of multiple brain systems during schema-congruent learning and memory (van Kesteren et al., 2010; van Kesteren et al., 2013; Masís-Obando, Norman, & Baldassano, 2022; Guo & Yang, 2022). In particular, medial PFC (mPFC) activity has been shown to increase with schema congruency during encoding, with hippocampus activity showing the opposite trend (van Kesteren et al., 2013; Bonasia et al., 2018). It is therefore theorized that mPFC augments the function of MTL when schema is presented during encoding by activating the cortical representation of relevant schema, facilitating the integration of new information into pre-existing cortical associations of schematic knowledge (Van Kesteren et al., 2012).

Given the complementary function of MTL and mPFC in schema processing, it would be worth investigating whether the compensatory role of PFC for MTL deficit reported in Deng & Stanley et al. (2021) can be attributed to similar cognitive mechanisms. However, it remains unknown whether age-related increases in schematization and age-related increases in prefrontal activation are somehow linked. This is unsurprising since it also remains unclear how global network functioning during memory retrieval is shaped by encoding schema, let alone across the lifespan. Therefore, in this chapter, we set to investigate age-related differences in functional brain network during retrieval, with regard to the effects of memory success and schema congruency of the items during encoding. Specifically, we advance the hypothesis that schema may have a stronger modulatory effect in OAs.

This investigation is built on the experimental paradigm and dataset described the previous chapter. In brief, younger and older participants viewed naturalistic scenes and objects that were paired together in varying schema congruency. Participants were instructed to judge the likelihood that the object appears in the scene. Memory for the concepts of the objects was tested on the following day inside scanner using an old-new recognition memory paradigm, in which participants judged whether the word on the screen was an old item that had been shown in the day before. The concurrent task fMRI data during retrieval scan was used to construct functional networks, and a data-driven modularity analysis was employed to discover brain regions belonging to PFC and

MTL, the two sub-networks of interest. Our first goal is to investigate if the fCON in PFC and MTL contributed differently to memory success in YAs and OAs. The second goal is to investigate if the retrieval functional network is modulated by schema congruency during encoding, and if such congruency effect is age-specific.

5.2 Materials and Methods

In this chapter, the experimental design and fMRI acquisition and preprocessing are identical with those in **Chapter 4**, and will be omitted in this section for simplicity.

5.2.1 Participants

A total of 37 YAs and 19 OAs participated in this study. The inclusion and exclusion criteria are described above in **Chapter 4**. Three YAs and one OA did not complete the full study due to sickness, potential SARS-CoV-2 exposure, and injury; two YAs withdrew from the study after the first visit; one YA has incomplete MRI data in visit 3 (retrieval scan) due to technical issue. These participants were not excluded in the Results section due to the lack of retrieval fMRI data. In addition, we also excluded one YA who reported falling asleep during visit 2 (encoding scan), and three YAs with poor conceptual memory performance at chance level (correct recognition, i.e., hit rate minus false alarm rate = -0.0017, -0.024, -0.33). Consequently, for current investigation concerning retrieval, the data were analyzed with 27 YAs (10 men, 17 women) and 18 OAs (7 men, 11 women).

5.2.2 Network Analysis

We obtained trial-level beta estimates of activation using the method described in Mumford et al. (2014), and then created functional brain networks using a beta time-series analysis (Rissman et al., 2004; Geib, Stanley, Wing, et al., 2017; Geib, Stanley, Dennis, et al., 2017). The nodes in the network were defined by the 246 regions of interest (ROIs) in Brainnetome atlas (Fan et al., 2016). The beta estimate value of a trial within an ROI was averaged across voxels to represent a timepoint in the beta time-series of this ROI. Trials belonging to the same condition were grouped into a condition-specific beta series, and a separate connectivity matrix was constructed for each condition and each participant by computing the Pearson's correlation across all pairs of ROIs. For our first goal that investigates the effect of memory success, we computed separate networks for remembered and forgotten items. For our second goal that investigates the effect of schema congruency, we grouped all trials that were subsequently remembered by their congruency level during encoding and computed three networks (incongruent, neutral, congruent) for each participant.

The functional sub-systems, or modules, were identified using a data-driven approach similar to Deng & Stanley et al. (2021). To begin with, a representative network was created in a two-step procedure. The connectivity matrices of all old item trials were averaged within each age group, and the resulting two connectivity matrices were further averaged into the final representative network. This ensures that this

representative network is not biased by the imbalanced numbers of participants in the two age groups. Then, the representative network was converted into a binary network, in which the connections were marked as 1 if they were among the top 10% strongest connections and 0 otherwise. Finally, this binary network was submitted to a modularity detection algorithm implemented in the Brain Connectivity Toolbox (Rubinov & Sporns, 2010) that divides the network into non-overlapping modules (Newman, 2006; Reichardt & Bornholdt, 2006). In the following analyses, the binary network also served as a mask to exclude weak or negative connections that are difficult to interpret.

Within-module connectivity and between-module connectivity (Guimerà & Amaral, 2005) were computed for the modules of interests for further investigation. The within-module fCON is defined as the average functional connectivity across all regions within the same module; the between-module fCON is defined as the average functional connectivity between a specific module and other modules. In consistency with Deng et al. (2021), we then defined a composite measure of whole-brain integration for each module as the ratio of between-module fCON to within-module fCON, which quantifies the tendency of a specific module to establish functional interactions with other modules in the larger network:

$$Integration(Module\ x) = \frac{fCON^{x}_{between}}{fCON^{x}_{within}}, \quad (1)$$

The memory-related reconfiguration was defined as the change of functional connection pattern between remembered and forgotten conditions, computed as one

minus the Spearman's correlation of connectivity vectors of an ROI in remembered and forgotten conditions:

$$Reconfiguration(Node\ i) = 1 - corr(\ fCON^{i}_{Remembered}\ ,\ fCON^{i}_{Forgotten}), \quad (2).$$

Consistent with previous studies in our group (Geib, Stanley, Wing, et al., 2017; Deng & Stanley et al., 2021), the reconfiguration values within each participant were transformed into *z*-score – a practice that serves to control for between-participant variability and reveals the relative strength of reconfiguration of an ROI in relation to other ROIs.

5.3 Results

5.3.1 Behavioral Results

We first investigated whether conceptual memory performance varied between age groups and across schema congruency. An Age-by-Congruency ANOVA was conducted, with the hit rates of the conceptual memory task as dependent variable. We observed a significant effect of Congruency ($F_{2,90} = 14.52$, $p < 10^{-5}$), but no effect of Age ($F_{1,45} = 0.93$, $p = 0.34$) or Age-Congruency interaction ($F_{2,90} = 0.12$, $p = 0.89$), suggesting the memory performance in both age groups benefited from congruent schema associated with the items.

5.3.2 Modularity Analysis

We began the analysis of functional brain network with the data-driven modularity analysis on the combined YA–OA connectivity network, which yielded six

modules that closely resembled the modules in the previous Deng & Stanley et al. (2021) study. Specifically, the analysis delineated the PFC and MTL systems (**Figure 15,** upper left; labeled also as PFC+ and MTL+ for consistency), indicating a global network topology during memory retrieval that is relatively stable across specific task paradigms. The scope of the following analyses will be focused on these two modules.

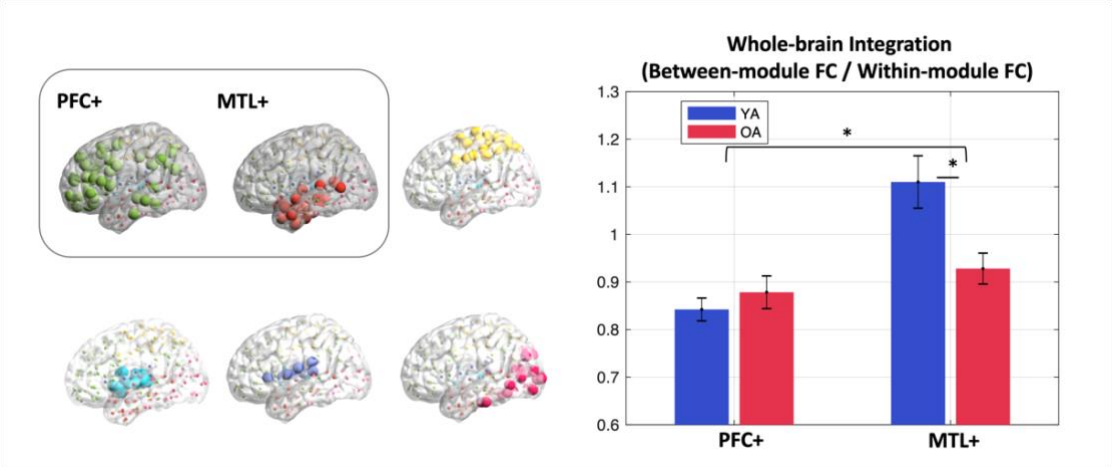

Figure 15: The PFC+ and MTL+ Modules, and Their Levels of Integration with the Global Brain Network. Error bars indicate standard error of the mean. Asterisks indicate p<0.05. Horizontal bracket indicates Age-by-Module interaction. Horizontal line indicates two-sample t-test between YAs and OAs.

To examine the age-related differences on the two modules of interest, an Age (YA/OA)-by-Module (MTL+/PFC+) ANOVA was conducted for the integration (i.e., the ratio between between-module fCON and within-module fCON) in the PFC+ and MTL+ modules. We observed a significant Age-Module interaction ($F_{1,43} = 6.20$, $p = 0.017$) driven by the MTL+ module, in which a significant age difference ($t_{43} = 2.51$, $p = 0.016$) showed a declined integration in OAs (**Figure 15,** right). For comparison, in the PFC+ module,

integration did not differ significantly between the two age groups ($t_{43} = -0.89$, $p = 0.38$), although OAs showed a slightly higher group average. These results partially replicated the findings in the previous study by Deng & Stanley et al. (2021), in which we found both an age-related decrease of integration in MTL+, as well as an age-related increase of integration in PFC+.

5.3.3 Memory-related fCON Changes in MTL+

The distinctive effects of aging on PFC+ and MTL+ module integration indicated that the two age groups may rely on different brain systems during memory retrieval, which motivated further investigation into these two modules linking fCON to memory performance. Therefore, we computed the brain network of remembered trials and the brain network of forgotten trials for each participant. Reconfiguration of connectivity between remembered and forgotten condition was computed for the PFC+ and MTL+ modules, and an Age(YA/OA)-by-Module(MTL+/PFC+) ANOVA was subsequently conducted. We observed a significant Age-Module interaction (**Figure 16A**, $F_{1,43} = 6.20$, $p = 0.017$), which is explained by a significant age difference in MTL+ reconfiguration ($t_{43} = 2.80$, $p = 0.0077$) and a lack of age difference in PFC+ reconfiguration ($t_{43} = -1.04$, $p = 0.31$).

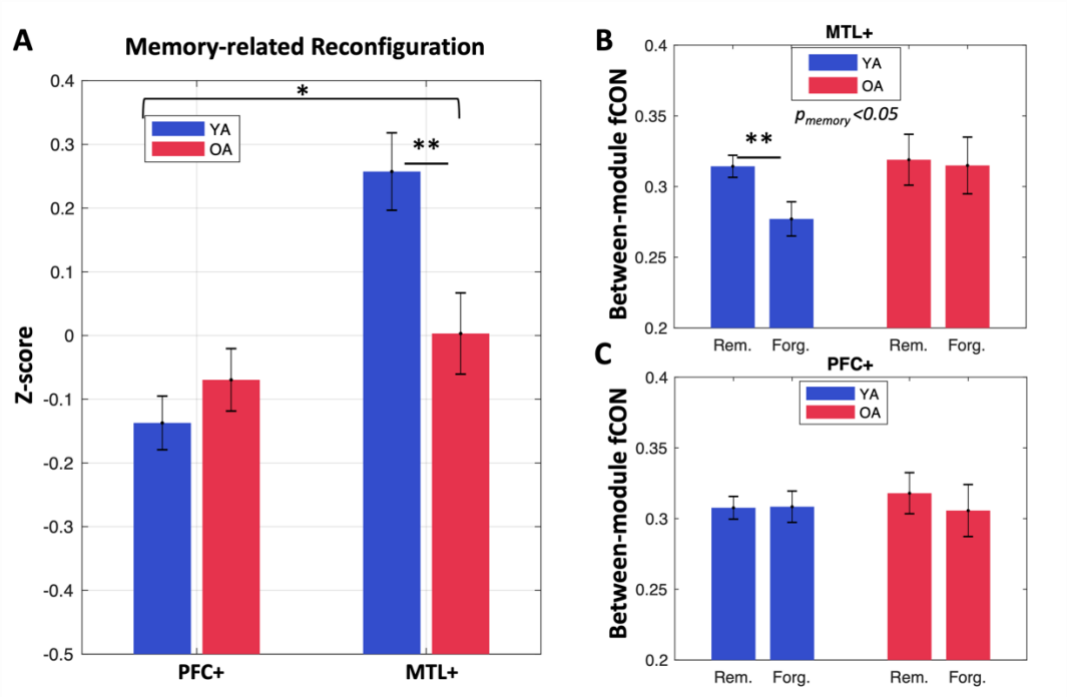

Figure 16: Memory-related Changes in MTL+ and PFC+ Connectivity. A) Memory-related reconfiguration of fCON pattern. B) Between-module fCON of MTL+ module for the remembered vs. forgotten trials. C) Between-module fCON of PFC+ module for the remembered (Rem.) vs. forgotten (Forg.) trials. Horizontal bracket indicates Age-by-Module interaction. Horizontal line indicates t-test between age groups or memory levels. Error bars indicate standard error of the mean. *: p<0.05; **: p<0.01

The fact that YAs showed both higher integration and memory-related reconfiguration in MTL+ suggested that the memory performance of YAs may benefit from the functional communication between MTL+ and other brain systems. To confirm this possibility, we then conducted an Age (YA/OA)-by-Memory (remembered/forgotten) ANOVA on the between-module fCON of the MTL+ module. This analysis yielded a significant effect of Memory (**Figure 16B**, $F_{1,43} = 6.13$, $p = 0.017$), driven by higher between-module fCON in remembered vs. forgotten condition for the

YA group ($t_{43} = 2.86$, $p = 0.0082$). In contrast, the between-module fCON for the OA group did not show significant memory-related difference ($t_{43} = 0.28$, $p = 0.78$), although the Age-Memory interaction effect just fell short of significance ($F_{1,43} = 2.82$, $p = 0.10$). Finally, we also conducted the same analysis on the between-module fCON of the PFC+ module (**Figure 16C**), which yielded non-significant effects of Age ($F_{1,43} = 0.053$, $p = 0.82$), Memory ($F_{1,43} = 0.43$, $p = 0.52$), and Age-Memory interaction ($F_{1,43} = 0.87$, $p = 0.36$). Taken together, these results suggested the role of MTL fCON in supporting memory retrieval is diminished in aging.

5.3.4 Effects of Schema on PFC+ Sub-systems

The second goal of the current inquiry is to examine whether schema congruency during encoding would later affect fCON during retrieval in the two modules of interest. Since schema congruency during encoding showed a supportive effect in memory success, it is of particular interest to investigate if fCON during successful memory trials is directly associated with encoding schema congruency, as it helps to dissociate the effect of schema and the effect of memory on fCON. Therefore, we computed fCON networks for the successful trials at each congruency level. As an exploratory analysis, we conducted Age-by-Congruency ANOVAs on the between-module connectivity and within-module connectivity for the two modules of interest. As shown in **Table 2**, we did not observe significant Congruency or Age-Congruency interaction effects for the listed connectivity measures. Importantly, the between-module

connectivity in MTL+ was associated with memory success (see previous analysis, **Figure 16B**) but not with schema congruency, suggesting that the effect of encoding schema on subsequent memory is unlikely mediated through MTL function during retrieval.

Table 2: Summary of Statistical Results for PFC+ and MTL+

Type	**Module**	**Effects – F-stat (p-val)**		
		Age	Congruency	Age x Congruency
Between-module	PFC+	0.39 (0.54)	0.78 (0.46)	1.86 (0.16)
fCON	MTL+	0.001 (0.97)	0.52 (0.59)	0.13 (0.88)
Within-module	PFC+	0.42 (0.52)	1.78 (0.18)	1.99 (0.14)
fCON	MTL+	**6.24 (0.016)**	0.54 (0.58)	1.03 (0.36)

Since the PFC+ module is comprised of a large set of ROIs that can be functionally heterogenous and may respond differently to schema congruency, sub-modules within PFC+ was further investigated. A secondary modularity analysis was performed on the sub-network within PFC+ module and revealed two sub-modules, namely, the default-mode network (DMN) sub-module and the frontoparietal network (FPN) (**Figure 17A**). Age-by-Congruency ANOVAs on the between-module connectivity and within-module connectivity were again conducted on these two sub-modules.

As shown in **Table 3**, we observed, in DMN, a significant main effect of Congruency ($F_{2,86} = 3.42$, $p = 0.037$) on within-module fCON (**Figure 17B**). The effect of Congruency was further tested on each age group using post-hoc one-way ANOVAs, and we found a significant Congruency effect in OAs ($F_{2,34} = 3.37$, $p = 0.046$, uncorrected) but not in YAs ($F_{2,52} = 0.78$, $p = 0.46$). In FPN, we observed a significant interaction effect between Age and Congruency on between-module fCON (**Figure 17C**). One-way ANOVAs were also carried out for each age group, and we found a significant Congruency effect in OAs ($F_{2,34} = 3.34$, $p = 0.048$, uncorrected), expressed as a congruency-related enhancement; such effect was absent in YAs ($F_{2,52} = 1.49$, $p = 0.24$).

Table 3: Summary of Statistical Results for FPN and DMN, the two sub-modules of PFC+.

Type	**Module**	**Effects – F-stat (p-val)**		
		Age	Congruency	Age x Congruency
Between-module fCON	FPN	0.16(0.69)	1.77(0.18)	**3.54(0.033)**
	DMN	0.88(0.35)	1.92(0.15)	1.49(0.23)
Within-module fCON	FPN	0.18(0.67)	0.49(0.62)	1.38(0.26)
	DMN	0.026(0.87)	**3.42(0.037)**	0.59(0.56)

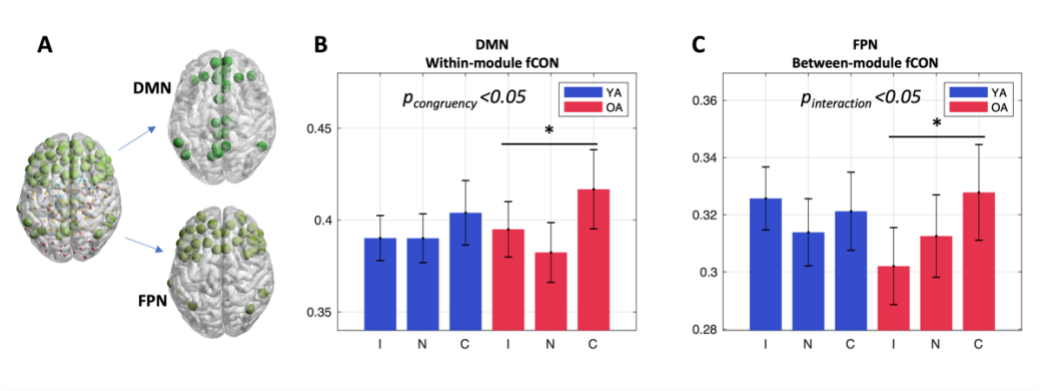

Figure 17: Effects of Schema Congruency in the fCON of Sub-modules of PFC+. A) Secondary modularity analysis on PFC+ yielded the DMN and the FPN sub-modules. B) Within-module connectivity of DMN for the Incongruent (I), Neutral (N), and Congruent (C) condition. C) Between-module connectivity of FPN for the Incongruent (I), Neutral (N), and Congruent (C) condition. Horizontal lines and asterisks indicate significant Congruency effects in one-way ANOVA. Error bars indicate standard error of the mean.

5.4 Discussions

Under the same objective task condition, young and older adults may recruit different neural resources (Cabeza, 2002; Davis et al., 2008). While this phenomenon is well-documented, possible processes that may contribute to such differential neural recruitments are less understood. In this study, we focused on MTL and PFC, two systems that have previously shown differential contribution to memory in YAs and OAs (Deng & Stanley et al. 2021). We investigated the functional connectivity of these two systems with respect to memory performance and schema congruency in encoding. Despite comparable memory performances, the two age groups showed qualitative difference in MTL and PFC connectivity. YAs, but not OAs, showed increased fCON between MTL and the rest of the brain network in successful memory trials, consistent

with the accumulating evidence of reduced reliance on MTL in OAs. The fCON level in MTL for successful memory trials was not explained by schema congruency during encoding, although schema congruency was linked to better memory performance. In comparison, we observed significant effects of schema in the fCON of DMN and FPN, the two sub-modules of PFC, and such effects were only observed in OAs but not in YAs. These findings suggest different roles MTL and PFC play during retrieval in the two age groups, indicating processes that are possibly mediated by PFC and related to schema in OAs.

5.4.1 Memory-related Changes and Age Differences in fCON

MTL is well-known for being the core structure of episodic memory, and the hippocampal-cortical interaction plays a critical role in forming and reactivating memory traces (Rolls, 2000; Ranganath, Heller, Cohen, Brozinsky, & Rissman, 2005; Ritchey et al., 2013; Wing et al., 2015; Geib, Stanley, Wing, et al., 2017). MTL is a brain structure that is particularly vulnerable to aging (Driscoll et al., 2003; Driscoll & Sutherland, 2005; Leal & Yassa, 2015), as functional neuroimaging studies in MTL during memory retrieval have revealed age-related reduction in activity (Dennis, Daselaar, et al., 2007; Dennis, Daselaar, et al., 2007; Davis et al., 2008; St. Jacques et al., 2012) and, more recently, functional connectivity (Monge et al., 2018; Deng, Stanley, et al., 2021). In line with these previous studies, we found that the MTL+ module in OAs displayed reduced functional integration with the global brain network. In addition,

reconfiguration of MTL connectivity due to memory success also showed significant age-related reduction. Specifically, in line with the hippocampal-cortical interaction account, YAs exhibited stronger between-module fCON during successful trials, while this relationship with memory was absent in OAs. Taken together, our results recapitulate the central role of MTL in functional network during episodic memory retrieval and its age-related deficit.

We found age invariance in PFC+ engagement during retrieval, as the two age groups showed comparable network integration and memory-related reconfiguration in PFC+. This null finding was not fully consistent with the previous finding of enhanced PFC connectivity in successful versus unsuccessful memory (Deng, Stanley, et al., 2021)., and may be attributed to the difference in the memory task in these two studies. In the current study, participants' memory was tested within a recognition memory paradigm consisted with targets and lures. The memory performance of OAs was not inferior to YAs, suggesting that the current paradigm may not be challenging enough for OAs to recruit extra compensatory neural resources in PFC. In comparison, in Deng & Stanley et al. (2021), participants were instructed to recall as much details as possible from previously encoded scenes with high visual complexity. The paradigm in Deng & Stanley et al. (2021) is arguably more challenging for OAs, as aging is associated with more impairment in recollection (Prull, Dawes, Martin, Rosenberg, & Light, 2006) and contextual memory (Spencer & Raz, 1995). Alternatively, the current paradigm

emphasized explicit semantic encoding strategies (i.e., “are these two images related?”), while the previous study did not. As such, this semantic elaboration may have given older adults a boost in their encoding, given the evidence for a semantic support effect in aging (REF). In addition, recollection process is more PFC-dependent (Cabeza et al., 1997; Wing, Marsh, & Cabeza, 2013), possibly leading to higher PFC engagement in OAs.

5.4.2 Schema Effects in MTL and PFC Sub-systems

A behavioral effect of congruency benefit was observed in this study, such that objects encoded in the schema-congruent condition in the previous day showed better subsequent memory in both groups. Theoretical frameworks and empirical findings have suggested the role of schema in supporting memory can happen in both the encoding and the retrieval stages (van Kesteren et al., 2010; van Kesteren et al., 2013; Robin & Moscovitch, 2017; Masís-Obando et al., 2022). While the current study employed direct manipulation of schema at the encoding stage, existence of schema-related strategy during retrieval cannot be ruled out. Therefore, we examine the functional connectivity in the PFC and MTL systems for the successfully remembered objects, with regard to their schema congruency during encoding.

Our first finding is the absence of the schema congruency effect in MTL+ fCON. Despite being a null finding, this observation is note-worthy, given higher between-module fCON in MTL+ has been shown to support successful memory trials in YAs

(**Figure 16B**). Had a schema-related process been involved in YAs, the central role of MTL would have been bypassed, leading to a reduced between-module fCON of MTL+ in schema-congruent condition (Van Kesteren et al., 2012)– a hypothetical scenario that is inconsistent with the current data. Therefore, this result suggests that the increase in MTL+ between-module fCON in YAs for successful memory reflects a hippocampus-centered, schema-independent process. In addition, schema congruency effect was also absent in PFC+ and its two sub-modules in YAs, further implying that, for YAs, the congruency benefit for memory is more likely mediated by the initial integration of schema-congruent information during encoding. For OAs, as their MTL+ fCON was unrelated to memory success, the absence of schema congruency effect in MTL+ is less indicative of an absence of schema-related processes.

Our second finding is the effects of schema congruency in OAs in the two sub-modules of PFC+, namely, the DMN and the FPN. Midline regions in DMN, such as mPFC and posterior cingulate cortex (PCC), have been well-documented to contribute to numerous schema-related processes (see review: Stawarczyk, Bezdek, & Zacks, 2021), such as self-referential processing (Gusnard, Akbudak, Shulman, & Raichle, 2001), conceptual semantic processing (Binder et al., 1999), and storing and processing of event schema (Masís-Obando et al., 2022). Therefore, the use of schema in OAs can serve as a reasonable interpretation of the increase in within-DMN fCON in schema-congruent condition (**Figure 17B**). Meanwhile, the increase in between-module fCON in FPN

(**Figure 17C**) may be a sign of increased cognitive effort to maintain or elaborate task-relevant information, that is, the representation of schema (Zacks, Speer, Swallow, Braver, & Reynolds, 2007), especially for the schema-congruent in which such information is most available. Taken together, these results indicate that OAs may utilize schema-related strategies in achieving successful retrieval at the level of their younger adult counterparts. However, further evidence is needed to uncover the exact strategy used by OAs.

5.4.3 Summary

Aging impairs some cognitive and neural resources but spares (and even enhances) others (Laumann Long & Shaw, 2000; D. C. Park et al., 2002). In this study, we examined whether schema shows a preferential effect in the functional brain networks of OAs. We observed a YA-specific effect of memory success in MTL, which is in line with existing literature on age-related decline in this core memory network. We found that, while schema-congruency effect was absent in YAs, it significantly modulated the functional connectivity in DMN and FPN in OAs. These findings suggest that, while neural resources in MTL may be depleting, OAs may be more in favor of frontal schema-related strategies during memory retrieval.

.

6. Conclusions

Brain is a distributed, network-like system: different regions execute distinct and relatively simple processing tasks, and these simple processing components are integrated together to meet more complex cognitive goals (Cabeza, Stanley, et al., 2018). This view is essential to the research in cognitive neuroscience of memory and aging. The detrimental effects of aging and the brain's adaptive responses to them often coexist and are expressed systematically, as univariate analyses in fMRI have shed light on the systematic differences in the recruitments of brain regions in OAs and YAs (Cabeza, 2002; Davis et al., 2008; Li et al., 2015). Nevertheless, a lack of thorough understanding still exists regarding to 1) *what information* is processed by the regions recruited by the two age groups, and 2) *how* these regions communicate to fulfill their roles. This dissertation attempts to approach to these questions with four studies, in which we surveyed the age differences in the neural representations of stimuli information and functional communications during memory encoding and retrieval. We revisit and discuss the key findings in the follow sections.

6.1 Network-level Compensation of PFC in OAs during Retrieval

There has been a growing body of literature on the substantial age differences in resting-state functional network (Tomasi & Volkow, 2012; Cao et al., 2014; Chan et al., 2014; Sala-Llonch, Bartrés-Faz, & Junque, 2015; Spreng, Stevens, Viviano, & Schacter, 2016; Chan et al., 2017). By linking the functional brain network with simultaneous

memory retrieval performance, our studies build on and extend these earlier investigations. In specific, the link between functional connectivity and performance allowed us to differentiate between the detrimental effects of aging and the potential compensatory mechanisms in OAs. In **Chapter 2** and **Chapter 5**, we observed a strong and consistent effect of aging on MTL fCON, the core system mediating memory retrieval. The reduction of functional interaction of MTL with the global brain network, along with its reduced reconfiguration of functional connectivity with memory, suggested a reduced importance of MTL for supporting memory success in OAs. These findings are consistent with numerous previous studies based on univariate analysis that support the age-related deficit of MTL function in OAs (Daselaar et al., 2005; Dennis, Daselaar, et al., 2007; Dennis, Kim, et al., 2007; Davis et al., 2008; St. Jacques et al., 2012; Dew et al., 2012). Our studies further extend their conclusions and suggest a mechanistic interpretation of such MTL deficit, that is, a reduction in functional communication with other neocortical brain regions that store memory traces or regulate MTL function. Meanwhile, in **Chapter 2**, the age-related reduction of memory-related reconfiguration in MTL is accompanied by an increase of reconfiguration in PFC, indicating a compensatory role of PFC that converges with earlier studies showing elevated PFC univariate activity in OAs (Gutchess et al., 2005; Davis et al. 2008).

6.2 Differential Effects of Aging on Visual and Semantic Representations

While network analysis sheds light on communication across brain regions, representational analysis allows the investigation of information processed within the brain region. Early studies have consistently revealed age-related reductions of task-related information in OTC regions, suggesting dedifferentiation of the processing of visual stimuli (D. C. Park et al., 2004; Chee et al., 2006; Goh et al., 2010; Carp, Park, Polk, et al., 2011; Bowman et al., 2019; Koen et al., 2019; Koen & Rugg, 2019; Koen et al., 2020). Using representational similarity analysis, we are able to disentangle, for the first time to our knowledge, the visual and semantic information carried by the naturalistic stimuli using state-of-the-art computational models. In two separate studies described in **Chapter 3** and **Chapter 4**, we found strong evidence that the neural representation of pure visual information in the early visual cortex is reduced in OAs, confirming the age-related dedifferentiation findings in earlier research. Importantly, aging does not seem to affect the processing of semantic information in higher visual regions in the occipital and temporal cortices (**Chapter 4**), and it is even enhanced in ATL (**Chapter 3**). These findings shed light on the neural basis of the OAs' well-known tendency of using semantic-related strategies (Mather et al., 1999; Spreng & Turner, 2019), and imply that the preserved ability to process semantic information in old age may serve as a cognitive reserve that can compensate for the reduced quality of sensory information.

6.3 The Effects of Schema on Functional Connectivity and Neural Representations

Chapter 2 and **Chapter 3** have demonstrated that network and representational analyses can be powerful instruments in the research of aging and episodic memory. The findings of OA-specific recruitments of brain regions, such as PFC and ATL, call for further research probing the latent differences on cognitive processes. Thus, in **Chapter 4** and **Chapter 5**, we carried out investigations on how the influence of schematic knowledge during episodic memory would be expressed at the network and representation levels.

Widespread effects of schema have been observed in the brain systems previously investigated in **Chapter 2** and **Chapter 3**. Some of these schema effects are age-invariant. For example, during encoding, the visual representation in LOC and the semantic representation in FG were strongest in the schema-neutral condition. This finding suggests that 1) although schema is essentially semantic, it is able to affect the processing of both visual and semantic information in OTC; 2) the relatively low representation in schema-congruent and schema-incongruent conditions may reflect reduced need of top-down attention to the visual and semantic information (Martin et al., 2018) – arguably an evidence that schema facilitated the performance of the task.

Notably, the effects of schema were expressed differently in the two age groups in ATL and PFC. (1) During encoding, OAs showed highest semantic representation in the schema-congruent condition in ATL, while YAs showed lowest semantic

representation in the same region. This observation offers a possible account for the age-related increase of semantic representation in ATL in **Chapter 3**. (2) During retrieval, although memory performance was linked to schema congruency in encoding for both YAs and OAs, the functional connectivity in PFC was only dependent on encoding congruency only in OAs but not in YAs. This suggests that OAs may engage in a schema-related strategy in a voluntary manner during the retrieval stage, whereas YAs may possibly benefit from congruent schema in the initial encoding stage. Taken together, our findings on representation and network hinted at the engagement of schematic knowledge in episodic memory among older populations. Lastly, it is worth noting that, while the scopes of investigation in **Chapter 4** and **Chapter 5** extended that of **Chapters 2 and 3**, the effects of aging and schema remain unexplored for *encoding functional network* and *retrieval neural representation*. Future investigations on these two aspects can provide a more holistic view of the role of schema in episodic memory formation and retrieval in OAs.

6.4 Further Considerations

Our studies may have other implications beyond the scope of aging and episodic memory. For example, network or representational analyses could guide the design of cognitive training and/or neural modulation paradigm that boost the compensatory neural resources and cognitive processes in OAs. On a more general note, network and representational analyses can be used to understand the nature of reorganizations in the

brain across long time scale, and aging is just one specific scenario. These recent analytical advances may bring promising discoveries in other research domains in cognitive neuroscience that bear similarity with the study of aging, such as neurodegenerative diseases and cognitive development.

6.5 Summary

To conclude, we employed functional network analysis and representational similarity analysis on a series of studies that investigate the age-related differences during memory encoding and retrieval. The findings in these studies are highly coherent with previous studies on aging and episodic memory that were based on univariate analysis, recapturing their key observations such as MTL and EVC deficits, and over-recruitment of PFC. In addition to knowing what regions are being recruited, we further contributed to the existing knowledge in this area by revealing the age differences in how brain regions communicate and process information. We also showed preliminary evidence that schematic knowledge may affect functional communication and information processing differently for OAs and YAs, which suggests that schema-related strategies may be preferentially selected by OAs. We hope that these findings will contribute to better understanding of the impairment and resilience in memory performance in aging populations.

Appendix A: Supplementary Information of Chapter 2

Supplementary Tables and Figures

The tables and figures below serve as supplementary information for some of the analyses in **Chapter 2**.

Table 4: Labels of AAL ROIs in PFC+ and MTL+ Modules.

Modules	**PFC+**		**MTL+**
ROIs	Frontal_Sup_L/R	Frontal_Sup_Orb_L/R	Olfactory_L/R
	Frontal_Mid_L/R	Frontal_Mid_Orb_L/R	Hippocampus_L/R
	Frontal_Inf_Tri_L/R	Frontal_Inf_Orb_L/R	ParaHippocampal_L/R
	Frontal_Sup_Medial_L/R	Frontal_Med_Orb_L/R	Amygdala_L/R
	Rectus_L/R	Cingulum_Ant_L/R	Temporal_Pole_Sup_L/R
	Cingulum_Post_L/R	Angular_L/R	

Table 5: Integration and Reconfiguration Values (mean ± SD) in All Brain Modules.

Modules	**Integration**		**Reconfiguration**	
	YAs	OAs	YAs	OAs
PFC+	0.88±0.13	0.97±0.12	-0.18±0.36	0.12±0.31
MTL+	1.06±0.19	0.89±0.21	0.49±0.71	-0.24±0.58
VentralVisual	0.83±0.10	0.82±0.11	0.15±0.31	0.24±0.37
Parietal	1.03±0.11	0.82±0.09	-0.27±0.28	-0.43±0.23
Subcortical	0.68±0.31	0.93±0.19	0.48±0.59	0.67±0.59
Operculum	0.75±0.14	0.68±0.17	-0.23±0.55	-0.24±0.42

Table 6: Null Effects of Memory on Integration and Between-module fCON in Non-PFC Modules

Modules	**Integration**		**Between-module fCON**	
	YAs	OAs	YAs	OAs
MTL+	p=0.86	p=0.66	p=0.46	p=0.50
VentralVisual	p=0.42	p=0.98	p=0.31	p=0.68
Parietal	p=0.03	p=0.38	p=0.50	p=0.12
Subcortical	p=0.39	p=0.30	p=0.34	p=0.49
Operculum	p=0.36	p=0.34	p=0.79	p=0.86

Note: Results reported as the raw p-values of High versus Low Memory paired t-tests. These control analyses guarantee that the effect of memory performance is uniquely associated with PFC+ in OAs. Although YAs showed lower Parietal integration in High Memory ($t(20)=-2.33$, $p=0.03$), the significance did not survive FDR correction.

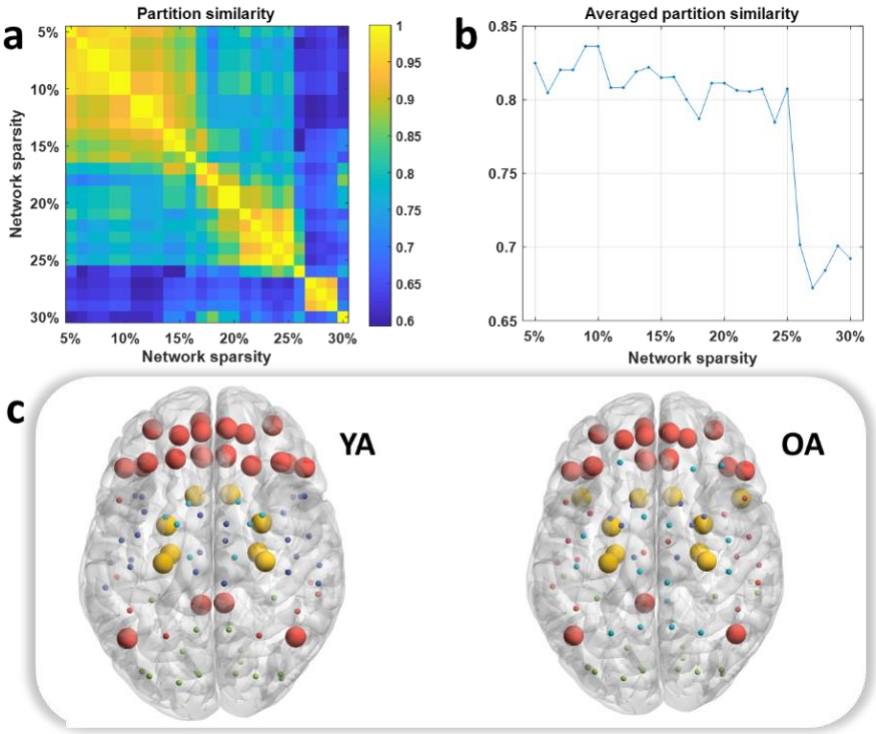

Figure 18: Reliability Analysis of the Module Assignment.a) The partition similarity of module assignment between different sparsity levels. b) The average partition similarity between module assignment at sparsity X and module assignment at sparsity Y (X≠Y), as a function of sparsity X. c) The module assignments of average networks for each age group. Nodes in the modules of interest (PFC+ and MTL+) are enlarged if they also belong to PFC+ or MTL+ in common module assignment in Figure 2 in the main text in Chapter 2.

The following two figures illustrate that the findings with regard to our Goal 1 in **Chapter 2** are robust across multiple network sparsity levels.

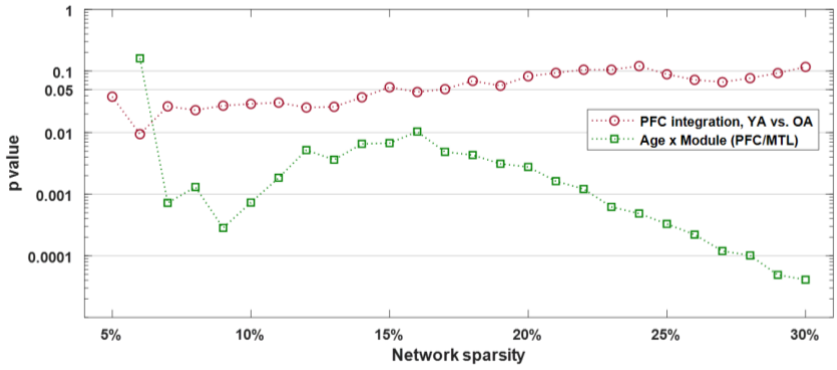

Figure 19: The P Values of the Statistical Analysis in Figure 3 as a Function of Alternative Network Sparsity.

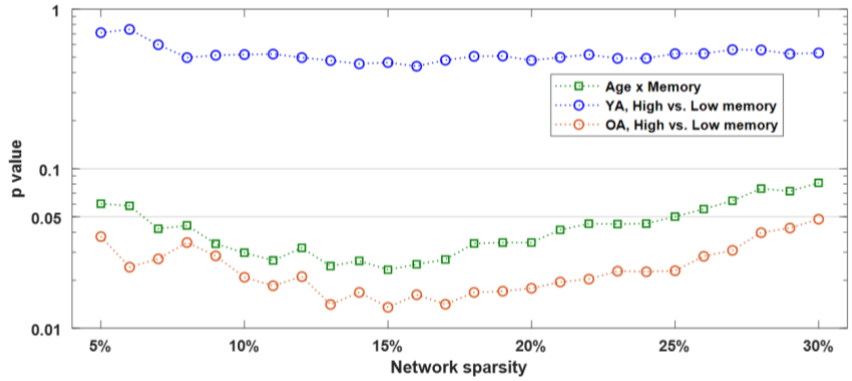

Figure 20: The P Values of the Statistical Analysis in Figure 4B as a Function of Alternative Network Sparsity.

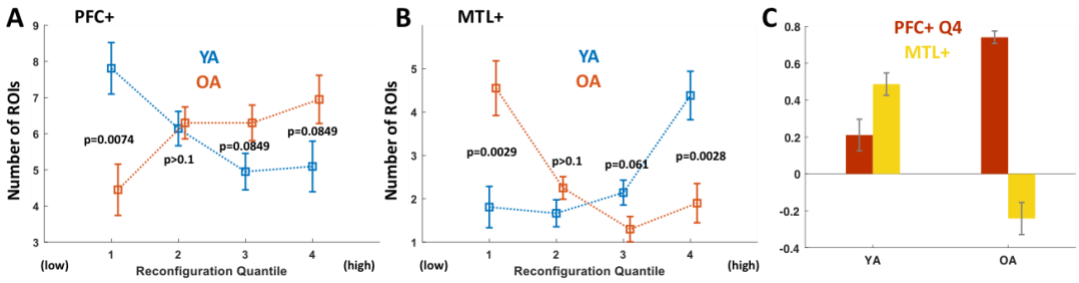

Figure 21: The Distribution of ROIs in PFC+ and MTL+ with Regard to their Reconfiguration Levels. A) and B) The counts of ROIs falling into the four reconfiguration quantiles for the PFC+ and MTL+ modules, respectively. The p-values show the FDR-corrected significance level for YA-OA comparison in each quantile. C) Reconfiguration in PFC+ ROIs that reconfigure strongly in OAs versus reconfiguration in MTL+. The high-reconfiguration PFC+ ROIs (red, marked as 'PFC+ Q4') are in the 4th quantile of averaged reconfiguration for the OA group, including the bilateral superior orbitofrontal gyri, middle orbitofrontal gyri, medial orbitofrontal gyri, and rectus gyri. In YAs, although these ROIs reconfigure less, they still have high reconfiguration among PFC+ ROIs. There is a significant interaction between Age (YA vs OA) and 'Modules' (PFC+ ROIs in quantile 4 vs MTL+ ROIs) ($F(1,39)=14.61$, $p=4.6e-4$). Importantly, this interaction is both driven by the age difference in MTL+ as we presented in the main text, as well as the fact that OAs reconfigure these subset of PFC+ ROIs more strongly than YAs ($t(39)=2.78$, $p_{FDR}=0.017$).

Considerations of Head Motion and Brain Measures

Although no reliable age difference in head motion was observed, we performed the following analyses to further ensure that our interpretations of the results were not confounded by head motion.

Firstly, head motion was not reliably correlated with brain measures. For the reconfiguration measure, we did not observe reliable correlation with motion RMS in any modules (maximum $|r|=0.22$). For the integration measure, no significant

correlation with motion RMS was found in any brain modules after FDR correction. Without FDR, motion RMS showed correlation with integration in PFC (r=0.39, p=0.012), MTL (r=0.32, p=0.044), and operculum network (r=0.37, p=0.019), but it was not correlated with integration in ventral visual (r=-0.18, p=0.27), parietal (r=-0.11 p=0.48), and subcortical (r=0.24, p=0.13) networks. We believe that motion is unlikely to cause artifacts in integration measures, as artifacts would have global effects on the measures across all modules.

Secondly, to further rule out any potential impact of head motion, we performed the following supplementary statistical analyses with motion RMS being added to the GLM as a covariate. The key statistical conclusions remain the same. **(i)** We found a significant Age-by-Module effects on integration ($F(1,37)=13.18$, $p=8.5e-4$), with higher MTL+ integration in YAs ($F(1,37)=8.06$, $p=0.015$) and higher PFC+ integration in OAs ($F(1,37)=5.94$, $p=0.020$). **(ii)** Age-by-Memory effect on PFC+ between-module fCON was also significant ($F(1,37)=5.24$, $p=0.028$), where OAs showed increased PFC+ between-module fCON in High Memory trials ($F(1,18)=6.25$, $p=0.045$). **(iii)** We also found a significant Age-by-Module interaction in reconfiguration ($F(1,37)=14.07$, $p=6.0e-4$), with higher MTL+ reconfiguration in YAs ($F(1,37)=12.42$, $p=0.0023$) and higher PFC+ reconfiguration in OAs ($F(1,37)=7.77$, $p=0.0083$).

Analyses Based on Subsets of ROIs in the PFC+ and MTL+ Modules

In order to investigate whether the observations related to PFC+ module were due to the frontal ROIs of the module, we performed additional analyses on a PFC sub-module without angular gyri and PCC. Similarly, to confirm whether the observations related to MTL+ module were due to the temporal ROIs of the module, we performed additional analyses on an MTL sub-module, where the bilateral olfactory cortices in the frontal lobe are excluded.

The additional analyses yielded results consistent with the findings in the main text. First, for the integration measure in PFC and MTL, we find a similar pattern of Age-by-Module interaction ($F(1,39)=6.77$, $p=0.013$), although no significant age difference was found in the two modules separately. For the between-module connectivity in PFC module, we also found a significant Age-by-Memory interaction ($F(1,39)=4.30$, $p=0.045$), and greater connectivity was found in high-memory trials in OAs ($t(19)=2.29$, $p=0.033$). Secondly, for the network reconfiguration measure, we found a similar pattern of Age-by-Module interaction for the two modules ($F(1,39)=12.27$, $p=0.0012$), where YAs showed higher reconfiguration in MTL than in PFC ($t(20)=2.61$, $p=0.017$), and OAs showed higher reconfiguration in PFC than in MTL ($t(19)=2.41$, $p=0.026$). Importantly, the PFC reconfiguration is negatively correlated with the MTL reconfiguration ($r=-0.57$, $p=1.07e-4$), and this relationship also existed when controlling for the age difference ($r=-0.47$, $p=0.0020$).

Analyses Based on High-resolution Atlas

We describe here a supplementary analysis based on a sub-parcellated HOA atlas with 471 ROIs used in several recent studies (Davis et al., 2017; Monge et al., 2017; Davis et al., 2018; Crowell et al., 2020; Beynel et al., 2020). The rationale of choosing this anatomy-based atlas is that, as mentioned in the discussion, most functional based parcellations are based on YAs and may thus introduce some bias to the OA group. We found the results from the two parcellations to be consistent in general, and we summarize the new results in the following.

Modularity: The network results were based on 362 ROIs in the cerebral cortex and subcortical structures with good spatial coverage with the mean EPI image in every participant. Using the same data-driven method in the main text, the network was first decomposed into 5 modules, including the PFC+ module shown in red below. We applied the modularity algorithm again to a large MTL-visual module, which dissociated into an MTL+ module (shown in yellow) and a ventral visual module. The six modules were highly consistent to the modules based on the AAL atlas in terms of spatial overlaps (Szymkiewicz–Simpson overlap coefficients for the six modules: PFC+ 82%, MTL+ 73%, Ventral Visual 97%, Parietal 88%, Subcortical 99%, Operculum 98%).

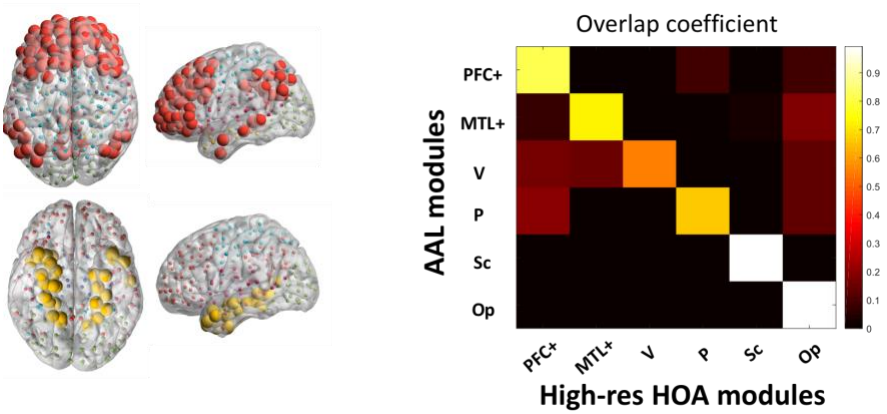

Figure 22: The Consistency of Modularity Analyses between Different Atlases

Integration: For the integration measure in PFC+ and MTL+, we find a similar pattern of Age-by-Module interaction in this atlas ($F(1,39)=23.49$, $p=2.03e-5$). Comparing with YAs, OAs show a higher integration in PFC+ ($t(39)=2.94$, $p=0.0056$), while YAs show an insignificant trend of higher integration in MTL+ ($t(39)=1.96$, $p=0.058$). For the between-module connectivity in PFC+ module, however, we did not find significant Age-by-Memory interaction ($F(1,39)=0.27$, $p=0.61$).

Reconfiguration: We found a similar pattern of Age-by-Module interaction for the two modules ($F(1,39)=8.53$, $p=0.0058$), where YAs showed higher reconfiguration in MTL+ than in PFC+ ($t(20)=6.18$, $p=4.89e-6$), but no difference was found in OAs ($t(19)=1.93$, $p=0.069$). OAs showed a higher PFC+ reconfiguration comparing with YAs ($t(39)=4.77$, $p=2.59e-5$). Importantly, the PFC reconfiguration is negatively correlated with the MTL reconfiguration ($r=-0.43$, $p=0.0054$), and this relationship also existed when controlling for the age difference ($r=-0.37$, $p=0.019$).

Appendix B: Supplementary Information of Chapter 3

Table 7: Whole-brain Searchlight Analysis of Sensory and Categorical Model-brain Fit.

Cluster	Hem	BA	MNI Coordinates (mm)			*t*-value	Size (voxels)
			x	*y*	*z*		
YA>0							
Sensory Model							
Calcarine Cortex		17	-23	-64	15	6.70	1452
		17	19	-68	11	6.25	
		23	26	-60	11	5.76	
Categorical Model							
Occipitotemporal Cortex		17	-26	-71	4	12.81	2171
		17	-15	-68	8	9.99	
		23	26	-56	11	8.87	
Midline		8	23	11	30	4.34	54
		-	23	-4	15	3.36	
Cerebellum		-	-4	-60	-30	4.10	21
OA>0							
Sensory Model							
Inferior Lateral Occipital Cortex		19	41	-71	11	6.61	324
		19	41	-75	4	5.98	
		19	45	-68	-4	5.09	
Inferior Lateral Occipital Cortex, Calcarine Cortex		18	-34	-75	8	4.49	149
		17	-15	-68	15	3.72	
		18	4	-74	23	3.15	

Categorical Model						
Inferior Lateral Occipital Cortex	19	-45	-64	8	6.22	1123
	39	45	-60	11	5.34	
	19	45	-64	0	5.18	
Dorsal, Ventral Medial PFC	9	-26	30	27	5.86	833
	10	23	53	4	5.25	
	10	26	45	8	5.06	
Midline	-	30	-11	30	4.35	106
	4	38	-15	42	3.94	
	24	11	-11	42	3.30	
Anterior Parahippocampal Gyrus	36	-34	-15	-27	4.17	29
Midline	8	-15	19	46	3.95	90
	-	-19	4	38	3.36	
	6	-15	-15	42	3.28	
Temporal Pole	21	-60	-8	-23	3.64	20
	21	-53	-11	-27	3.27	
	20	-45	-8	-30	3.24	
	8	26	23	38	3.45	13

Note: The table above shows coordinates of peaks and subpeaks within clusters (thresholded at $p<.005$, k=12; determined by 3dClust-Sim in AFNI version 17.0; only positive-values are shown). BA = Brodmann area; Hem = Hemisphere; L = Left; R = Right

Table 8: Scenes Used in the Experiment, and their Average Retrieval-scan Vividness Ratings, Post-scan Hit Rates, and Confidence Ratings.

Scene	**vividness**	(SD)	**hit rate**	(SD)	**confidence**	(SD)
airport	2.59	1.09	0.76	0.43	3.10	1.20
amphitheater	3.25	0.97	0.88	0.33	3.46	1.03
arcade	2.39	1.07	0.61	0.49	2.44	1.14
arch	3.07	1.29	0.80	0.40	3.51	0.84
ATM	2.54	1.12	0.68	0.47	2.66	1.13

bakery	2.38	1.04	0.63	0.49	2.95	1.12
balcony	2.13	1.05	0.78	0.42	2.93	1.06
bar	2.42	1.10	0.49	0.51	2.76	0.97
barn	2.63	1.02	0.76	0.43	2.90	1.04
bathroom	2.61	1.03	0.78	0.42	2.98	1.11
beach	2.66	1.13	0.80	0.40	3.17	1.09
bedroom	2.90	1.00	0.59	0.50	2.80	1.17
bike rack	2.15	1.06	0.73	0.45	2.82	1.16
bridge	3.34	1.04	0.37	0.49	2.59	0.87
buffet	2.74	1.05	0.51	0.51	2.71	1.19
bus	1.98	1.04	0.68	0.47	2.88	0.93
bus stop	1.96	1.00	0.85	0.36	3.56	0.81
canal	2.26	0.98	0.59	0.50	2.85	1.22
canyon	3.20	1.03	0.66	0.48	2.80	1.08
inside of a car	2.11	1.16	0.73	0.45	3.32	1.04
casino	2.46	1.03	0.46	0.50	2.44	0.90
castle	3.00	1.14	0.85	0.36	3.37	1.13
cemetery	2.93	1.06	0.63	0.49	2.71	1.01
church	2.81	0.94	0.63	0.49	2.56	1.00
circus	2.29	1.03	0.88	0.33	3.02	1.21
classroom	2.19	0.87	0.63	0.49	2.71	1.05
climbing wall	2.76	0.86	0.85	0.36	3.34	1.09
coast	2.74	1.04	0.49	0.51	2.20	1.17
coffee shop	2.16	1.13	0.80	0.40	2.98	1.11
conference room	2.68	0.99	0.34	0.48	2.56	1.07
construction site	2.34	1.13	0.73	0.45	2.73	1.05
country road	2.65	1.11	0.68	0.47	3.00	1.12
court room	2.71	0.90	0.68	0.47	2.93	1.15
deli	2.56	0.92	0.71	0.46	2.76	1.14
desert	2.93	1.11	0.56	0.50	2.71	1.10
door	2.03	1.06	0.76	0.43	2.90	1.26
driveway	2.60	1.02	0.88	0.33	3.51	0.90
dump	2.88	0.90	0.90	0.30	3.27	0.95
Eiffel Tower	3.78	0.47	0.56	0.50	2.78	1.01
empty room	2.63	1.18	0.76	0.43	3.00	0.95
escalator	2.49	1.10	0.73	0.45	2.78	1.31
fire station	2.60	1.12	0.63	0.49	2.57	1.21
flower shop	2.68	0.88	0.61	0.49	2.63	1.22
football field	2.88	1.05	0.88	0.33	3.02	0.99
game room	2.17	0.91	0.46	0.50	2.61	1.00
garage	2.28	1.19	0.90	0.30	3.27	1.12
garden	2.16	0.76	0.71	0.46	2.10	1.04
gas station	2.32	0.96	0.51	0.51	2.54	1.07
grocery store	2.33	0.98	0.85	0.36	3.00	1.12
hair salon	2.18	1.07	0.83	0.38	3.15	0.91
home office	2.36	0.99	0.59	0.50	2.31	1.03
house	2.37	1.20	0.90	0.30	3.05	1.05
iceberg	3.44	0.84	0.88	0.33	3.63	0.86
ice stadium	2.85	0.96	0.54	0.50	2.32	1.08

igloo	3.48	0.72	0.98	0.16	3.85	0.36
island	2.76	1.13	0.44	0.50	2.28	0.99
lab	2.56	1.03	0.83	0.38	3.22	1.04
laundry room	2.27	1.02	0.83	0.38	2.88	1.05
mall	2.85	1.02	0.88	0.33	3.07	1.10
market	1.85	0.91	0.59	0.50	2.88	1.17
McDonald's	3.27	0.95	0.93	0.26	3.20	1.05
monster truck	2.71	1.10	0.68	0.47	2.63	1.13
movie set	2.70	0.93	0.83	0.38	3.51	0.87
movie theater	2.80	1.27	0.59	0.50	2.85	1.04
museum	2.26	1.00	0.39	0.49	2.51	1.19
music studio	2.57	1.16	0.63	0.49	2.93	1.25
NASCAR	3.27	0.74	0.85	0.36	3.32	0.93
nursery	2.27	1.19	0.71	0.46	2.83	1.14
office copier	2.98	0.96	0.83	0.38	3.34	1.15
orchestra	2.80	1.00	0.78	0.42	3.20	1.05
outer space	3.65	0.75	0.95	0.22	3.76	0.49
playground	2.31	0.96	0.78	0.42	2.76	1.16
post office	2.44	1.21	0.85	0.36	3.29	0.84
pyramid	3.68	0.57	0.68	0.47	2.83	1.07
racetrack	2.47	1.20	0.73	0.45	2.95	1.14
restaurant	2.20	1.01	0.56	0.50	2.59	1.16
restroom stall	3.00	1.07	0.80	0.40	3.20	1.05
roller rink	2.66	1.04	0.85	0.36	3.39	0.95
sauna	3.34	0.94	0.90	0.30	3.47	0.92
seaport	2.24	1.09	0.83	0.38	3.46	0.90
sewing room	2.49	0.93	0.78	0.42	2.90	1.04
shop front	2.21	1.04	0.88	0.33	3.49	0.90
skyscraper	2.90	1.11	0.46	0.50	2.98	0.99
snow mountain	3.04	1.02	0.56	0.50	2.44	1.07
soccer field	2.51	0.93	0.71	0.46	2.98	1.23
swamp	2.52	0.89	0.63	0.49	2.86	1.33
swimming pool	2.06	1.03	0.76	0.43	2.76	1.20
temple	2.51	1.20	0.71	0.46	2.56	1.05
tennis court	2.68	1.01	0.88	0.33	3.05	1.05
train	2.07	1.01	0.71	0.46	2.85	1.15
tree house	2.88	1.00	0.85	0.36	3.02	1.04
volcano	3.33	0.92	0.88	0.33	2.78	1.06
volleyball court	2.61	1.16	0.56	0.50	2.56	1.16
waterfall	3.34	0.82	0.37	0.49	2.68	0.93
waves	3.32	0.85	0.49	0.51	2.80	1.05
woods	2.41	1.14	0.78	0.42	3.00	1.05

Table 9: Correlations between Post-scan Hit Rate and Sensory and Categorical Model-brain Fits across Participants.

Region & Model	YA	OA	All	All (age controlled)
EVC sensory	**r=0.45, p=0.041**	r=0.04, p=0.87	**r=0.46, p=0.0023**	r=0.31, p=0.051
EVC HMAX	**r=0.51, p=0.017**	r=-0.029, p=0.90	**r=0.47, p=0.0019**	**r=0.32, p=0.042**
EVC categorical	r=0.14, p=0.55	r=0.09, p=0.70	r=0.24, p=0.12	r=0.11, p=0.50
ATL sensory	r=-0.072, p=0.76	r=0.036, p=0.88	r=-0.12, p=0.47	r=-0.022, p=0.89
ATL categorical	r=0.14, p=0.54	r=0.053, p=0.83	r=-0.092, p=0.57	r=0.083, p=0.61
ATL in/outdoor	r=0.074, p=0.75	r=0.24, p=0.31	r=-0.022, p=0.89	r=0.15, p=0.37

Note: in the 4th column, partial correlation was used to control for the factor of age.

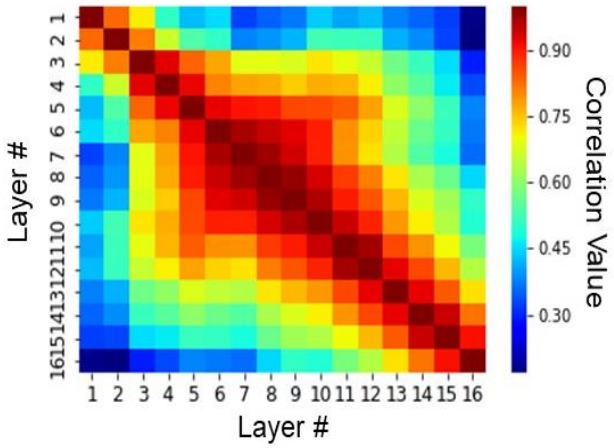

Figure 23: Correlation Matrix of DNN Stimuli Models. The figure shows the correlation matrix of stimuli models derived from every layer of the VGG16.

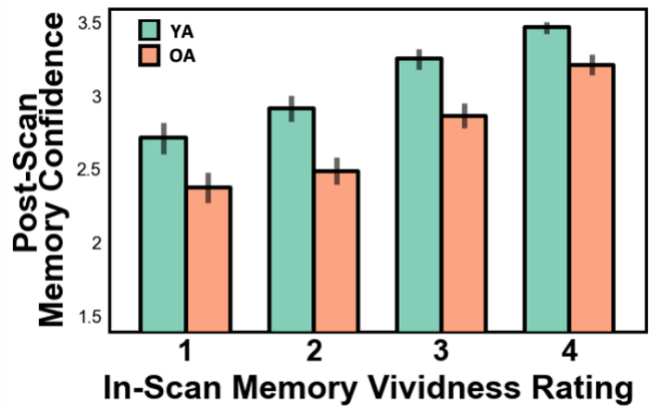

Figure 24: Association between Vividness Rating during Retrieval Scan and Post-scan Recognition Confidence.

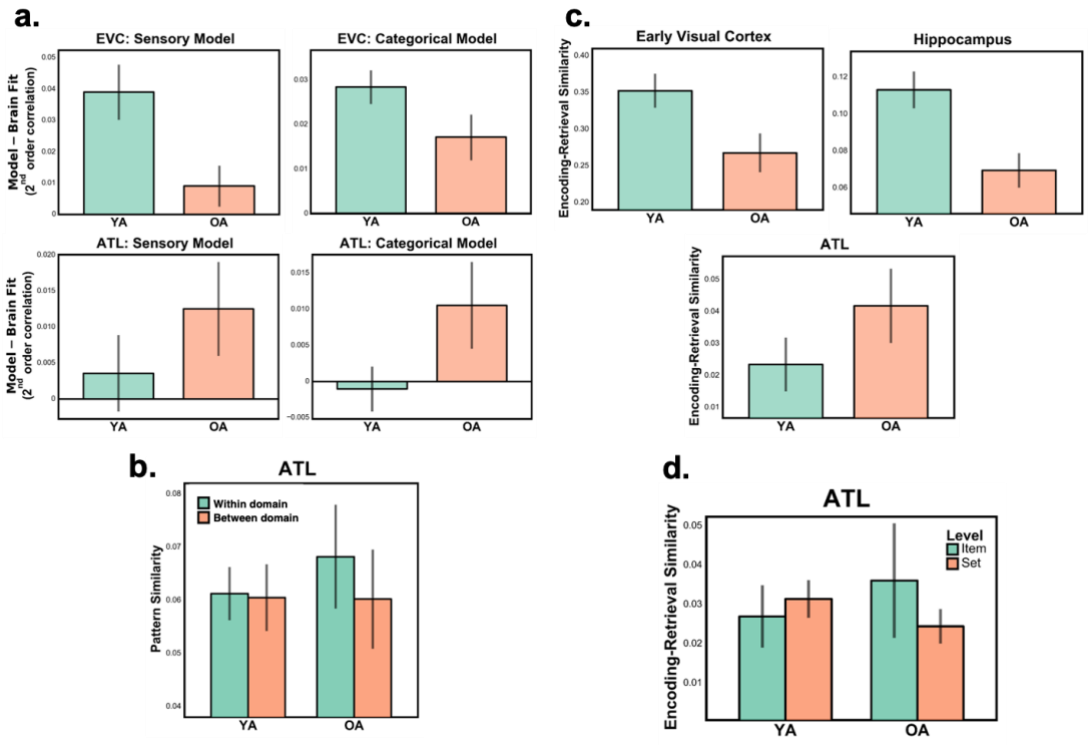

Figure 25: Model-brain Fit and ERS Raw Values. Panel a shows within the early visual cortex and anterior temporal lobe the raw values of the image model (sensory and categorical)-brain fit. Panel b shows the brain activation pattern similarity for within and between domains (domains = indoor vs. outdoor scenes) in the ATL. Panel c shows in the early visual cortex, hippocampus and ATL raw encoding-retrieval similarity values. Panel d shows in the ATL raw encoding-retrieval similarity values for trials that were subsequently remembered on the post-scan memory recognition task separately for item- and set-level encoding-retrieval similarity. Error bars represent the standard error of the mean. ATL = anterior temporal lobe; ERS = encoding-retrieval similarity; EVC = early visual cortex; OA = older adults; YA = younger adults.

References

Abdulrahman, H., Fletcher, P. C., Bullmore, E., & Morcom, A. M. (2017). Dopamine and memory dedifferentiation in aging. *NeuroImage*, *153*, 211–220. https://doi.org/10.1016/j.neuroimage.2015.03.031

Abraham, A., Pedregosa, F., Eickenberg, M., Gervais, P., Mueller, A., Kossaifi, J., … Varoquaux, G. (2014). Machine learning for neuroimaging with scikit-learn. *Frontiers in Neuroinformatics*, *8*(FEB), 1–10. https://doi.org/10.3389/fninf.2014.00014

Alvarez, P., & Squire, L. R. (1994). Memory consolidation and the medial temporal lobe: a simple network model. *Proceedings of the National Academy of Sciences*, *91*(15), 7041–7045. https://doi.org/10.1073/pnas.91.15.7041

Ashburner, J. (2007). A fast diffeomorphic image registration algorithm. *NeuroImage*, *38*(1), 95–113. https://doi.org/10.1016/j.neuroimage.2007.07.007

Avants, B. B., Epstein, C. L., Grossman, M., & Gee, J. C. (2008). Symmetric diffeomorphic image registration with cross-correlation: Evaluating automated labeling of elderly and neurodegenerative brain. *Medical Image Analysis*, *12*(1), 26–41. https://doi.org/https://doi.org/10.1016/j.media.2007.06.004

Baltes, P. B., & Lindenberger, U. (1997). Emergence of a powerful connection between sensory and cognitive functions across the adult life span: A new window to the study of cognitive aging? *Psychology and Aging*, *12*(1), 12–21. https://doi.org/10.1037/0882-7974.12.1.12

Bankson, B. B., Hebart, M. N., Groen, I. I. A., & Baker, C. I. (2018). The temporal evolution of conceptual object representations revealed through models of behavior, semantics and deep neural networks. *NeuroImage*, *178*(November 2017), 172–182. https://doi.org/10.1016/j.neuroimage.2018.05.037

Beck, A. T., Ward, C., Mendelson, M., Mock, J., & Erbaugh, J. (1961). Beck depression inventory (BDI).

Behzadi, Y., Restom, K., Liau, J., & Liu, T. T. (2007). A component based noise correction method (CompCor) for BOLD and perfusion based fMRI. *NeuroImage*, *37*(1), 90–101. https://doi.org/https://doi.org/10.1016/j.neuroimage.2007.04.042

Benjamini, Y., & Hochberg, Y. (1995). Controlling the False Discovery Rate: A Practical and Powerful Approach to Multiple Testing on JSTOR. *Journal of the Royal Statistical Society. Series B (Methodological)*, *57*(1), 289–300. Retrieved from

http://www.jstor.org/stable/2346101?seq=1#page_scan_tab_contents

Bertolero, M. A., Yeo, B. T. T., & D'Esposito, M. (2015). The modular and integrative functional architecture of the human brain. *Proceedings of the National Academy of Sciences*, *112*(49), E6798–E6807. https://doi.org/10.1073/pnas.1510619112

Betzel, R. F., Byrge, L., He, Y., Goñi, J., Zuo, X. N., & Sporns, O. (2014). Changes in structural and functional connectivity among resting-state networks across the human lifespan. *NeuroImage*, *102*(P2), 345–357. https://doi.org/10.1016/j.neuroimage.2014.07.067

Beynel, L., Deng, L., Crowell, C. A., Dannhauer, M., Palmer, H., Hilbig, S., … Davis, S. W. (2020). Structural controllability predicts functional patterns and brain stimulation benefits associated with working memory. *The Journal of Neuroscience*, *40*(35), JN-RM-0531-20. https://doi.org/10.1523/jneurosci.0531-20.2020

Binder, J. R., Frost, J. A., Hammeke, T. A., Bellgowan, P. S. F., Rao, S. M., & Cox, R. W. (1999). Conceptual processing during the conscious resting state: A functional MRI study. *Journal of Cognitive Neuroscience*, *11*(1), 80–93. https://doi.org/10.1162/089892999563265

Blondel, V. D., Guillaume, J. L., Lambiotte, R., & Lefebvre, E. (2008). Fast unfolding of communities in large networks. *Journal of Statistical Mechanics*, *2008*(10), P10008. https://doi.org/10.1088/1742-5468/2008/10/P10008

Bonasia, K., Sekeres, M. J., Gilboa, A., Grady, C. L., Winocur, G., & Moscovitch, M. (2018). Prior knowledge modulates the neural substrates of encoding and retrieving naturalistic events at short and long delays. *Neurobiology of Learning and Memory*, *153*(January), 26–39. https://doi.org/10.1016/j.nlm.2018.02.017

Bowman, C. R., Chamberlain, J. D., & Dennis, N. A. (2019). Sensory representations supporting memory specificity: Age effects on behavioral and neural discriminability. *Journal of Neuroscience*, *39*(12), 2265–2275. https://doi.org/10.1523/JNEUROSCI.2022-18.2019

Brashier, N. M., Umanath, S., Cabeza, R., & Marsh, E. J. (2017). Competing cues: Older adults rely on knowledge in the face of fluency. *Psychology and Aging*, *32*(4), 331–337. https://doi.org/10.1037/pag0000156

Bressler, S. L., & Menon, V. (2010). Large-scale brain networks in cognition: emerging methods and principles. *Trends in Cognitive Sciences*, *14*(6), 277–290. https://doi.org/10.1016/j.tics.2010.04.004

Bullmore, E., & Sporns, O. (2009). Complex brain networks: graph theoretical analysis of structural and functional systems. *Nat Rev Neurosci*, *10*(3), 186–198. https://doi.org/10.1038/nrn2575

Bullmore, E. T., & Bassett, D. S. (2011). Brain graphs: graphical models of the human brain connectome. *Annual Review of Clinical Psychology*, *7*, 113–140. https://doi.org/10.1146/annurev-clinpsy-040510-143934

Bussey, T. J., Saksida, L. M., & Murray, E. A. (2005). The perceptual-mnemonic/feature conjunction model of perirhinal cortex function. *Quarterly Journal of Experimental Psychology Section B: Comparative and Physiological Psychology*, *58*(3–4), 269–282. https://doi.org/10.1080/02724990544000004

Cabeza, R. (2002). Hemispheric asymmetry reduction in older adults: The HAROLD model. *Psychology and Aging*, *17*(1), 85–100. https://doi.org/10.1037/0882-7974.17.1.85

Cabeza, R. (2008). Role of parietal regions in episodic memory retrieval: The dual attentional processes hypothesis. *Neuropsychologia*, *46*(7), 1813–1827. https://doi.org/10.1016/j.neuropsychologia.2008.03.019

Cabeza, R., Albert, M., Belleville, S., Craik, F. I. M., Duarte, A., Grady, C. L., … Rajah, M. N. (2018). Maintenance, reserve and compensation: the cognitive neuroscience of healthy ageing. *Nature Reviews Neuroscience*, *19*(11), 701–710. https://doi.org/10.1038/s41583-018-0068-2

Cabeza, R., & Dennis, N. (2012). *FRONTAL LOBES AND AGING*. (D. Stuss & R. Knight, Eds.), *Principles of Frontal Lobe Function* (2nd ed.). New York: Oxford University Press. https://doi.org/10.1093/acprof:oso/9780195134971.001.0001

Cabeza, R., Kapur, S., Craik, F. I. M., McIntosh, A. R., Houle, S., & Tulving, E. (1997). Functional Neuroanatomy of Recall and Recognition: A PET Study of Episodic Memory. *Journal of Cognitive Neuroscience*, *9*(2), 254–265. https://doi.org/10.1162/jocn.1997.9.2.254

Cabeza, R., & Nyberg, L. (2000). Imaging Cognition II: An Empirical Review of 275 PET and fMRI Studies. *Journal of Cognitive Neuroscience*, *12*(1), 1–47. https://doi.org/10.1162/08989290051137585

Cabeza, R., Stanley, M. L., & Moscovitch, M. (2018, November). Process-Specific Alliances (PSAs) in Cognitive Neuroscience. *Trends in Cognitive Sciences*. Elsevier Ltd. https://doi.org/10.1016/j.tics.2018.08.005

Cadieu, C. F., Hong, H., Yamins, D. L. K., Pinto, N., Ardila, D., Solomon, E. A., … DiCarlo, J. J. (2014). Deep Neural Networks Rival the Representation of Primate IT Cortex for Core Visual Object Recognition. *PLoS Computational Biology*, *10*(12). https://doi.org/10.1371/journal.pcbi.1003963

Cao, M., Wang, J. H., Dai, Z. J., Cao, X. Y., Jiang, L. L., Fan, F. M., … He, Y. (2014). Topological organization of the human brain functional connectome across the lifespan. *Developmental Cognitive Neuroscience*, *7*(16), 76–93. https://doi.org/10.1016/j.dcn.2013.11.004

Carp, J., Park, J., Hebrank, A., Park, D. C., & Polk, T. A. (2011). Age-related neural dedifferentiation in the motor system. *PLoS ONE*, *6*(12), 1–6. https://doi.org/10.1371/journal.pone.0029411

Carp, J., Park, J., Polk, T. A., & Park, D. C. (2011). Age differences in neural distinctiveness revealed by multi-voxel pattern analysis. *NeuroImage*, *56*(2), 736–743. https://doi.org/10.1016/j.neuroimage.2010.04.267

Chan, M. Y., Alhazmi, F. H., Park, D. C., Savalia, N. K., & Wig, G. S. (2017). Resting-State Network Topology Differentiates Task Signals across the Adult Life Span. *The Journal of Neuroscience*, *37*(10), 2734–2745. https://doi.org/10.1523/JNEUROSCI.2406-16.2017

Chan, M. Y., Park, D. C., Savalia, N. K., Petersen, S. E., & Wig, G. S. (2014). Decreased segregation of brain systems across the healthy adult lifespan. *Proceedings of the National Academy of Sciences*, *111*(46), E4997–E5006. https://doi.org/10.1073/pnas.1415122111

Chee, M. W. L., Goh, J. O. S., Venkatraman, V., Jiat, C. T., Gutchess, A., Sutton, B., … Park, D. (2006). Age-related changes in object processing and contextual binding revealed using fMR adaptation. *Journal of Cognitive Neuroscience*, *18*(4), 495–507. https://doi.org/10.1162/jocn.2006.18.4.495

Cherry, K. E., Silva Brown, J., Jackson Walker, E., Smitherman, E. A., Boudreaux, E. O., Volaufova, J., & Michal Jazwinski, S. (2012). Semantic encoding enhances the pictorial superiority effect in the oldest-old. *Aging, Neuropsychology, and Cognition*, *19*(1–2), 319–337. https://doi.org/10.1080/13825585.2011.619645

Clarke, A., Pell, P. J., Ranganath, C., & Tyler, L. K. (2016). Learning Warps Object Representations in the Ventral Temporal Cortex. *Journal of Cognitive Neuroscience*, *28*(7), 1010–1023. https://doi.org/10.1162/jocn_a_00951

Clarke, A., & Tyler, L. K. (2014). Object-Specific Semantic Coding in Human Perirhinal Cortex. *Journal of Neuroscience*, *34*(14), 4766–4775. https://doi.org/10.1523/JNEUROSCI.2828-13.2014

Cole, M. W., Bassett, D. S., Power, J. D., Braver, T. S., & Petersen, S. E. (2014). Intrinsic and Task-Evoked Network Architectures of the Human Brain. *Neuron*, *83*(1), 238–251. https://doi.org/10.1016/j.neuron.2014.05.014

Cole, M. W., Ito, T., Bassett, D. S., & Schultz, D. H. (2016). Activity flow over resting-state networks shapes cognitive task activations. *Nature Neuroscience*, *19*(12), 1718–1726. https://doi.org/10.1038/nn.4406

Cole, M. W., Reynolds, J. R., Power, J. D., Repovs, G., Anticevic, A., & Braver, T. S. (2013). Multi-task connectivity reveals flexible hubs for adaptive task control. *Nature Neuroscience*, *16*(9), 1348–1355. https://doi.org/10.1038/nn.3470

Cowell, R. A., Barense, M. D., & Sadil, P. S. (2019). A roadmap for understanding memory: Decomposing cognitive processes into operations and representations. *ENeuro*, *6*(4), 1–19. https://doi.org/10.1523/ENEURO.0122-19.2019

Cox, R. W., & Hyde, J. S. (1997). Software tools for analysis and visualization of fMRI data. *NMR in Biomedicine*, *10*(4–5), 171–178. https://doi.org/https://doi.org/10.1002/(SICI)1099-1492(199706/08)10:4/5<171::AID-NBM453>3.0.CO;2-L

Crowell, C. A., Davis, S. W., Beynel, L., Deng, L., Lakhlani, D., Hilbig, S. A., … Cabeza, R. (2020). Older adults benefit from more widespread brain network integration during working memory. *NeuroImage*, *218*(May), 116959. https://doi.org/10.1016/j.neuroimage.2020.116959

Çukur, T., Nishimoto, S., Huth, A. G., & Gallant, J. L. (2013). Attention during natural vision warps semantic representation across the human brain. *Nature Neuroscience*, *16*(6), 763–770. https://doi.org/10.1038/nn.3381

Curran, T., Schacter, D. L., Norman, K. A., & Galluccio, L. (1997). False recognition after a right frontal lobe infarction: Memory for general and specific information. *Neuropsychologia*, *35*(7), 1035–1049. https://doi.org/10.1016/S0028-3932(97)00029-8

Dale, A. M., Fischl, B., & Sereno, M. I. (1999). Cortical Surface-Based Analysis: I. Segmentation and Surface Reconstruction. *NeuroImage*, *9*(2), 179–194. https://doi.org/https://doi.org/10.1006/nimg.1998.0395

Danker, J. F., & Anderson, J. R. (2010). The Ghosts of Brain States Past: Remembering Reactivates the Brain Regions Engaged During Encoding. *Psychological Bulletin*, *136*(1), 87–102. https://doi.org/10.1037/a0017937

Daselaar, S. M., Fleck, M. S., & Cabeza, R. (2006). Triple dissociation in the medial temporal lobes: Recollection, familiarity, and novelty. *Journal of Neurophysiology*, *96*(4), 1902–1911. https://doi.org/10.1152/jn.01029.2005

Daselaar, S. M., Fleck, M. S., Dobbins, I. G., Madden, D. J., & Cabeza, R. (2005). Effects of Healthy Aging on Hippocampal and Rhinal Memory Functions: An Event-Related fMRI Study. *Cerebral Cortex*, *16*(12), 1771–1782. https://doi.org/10.1093/cercor/bhj112

Davis, S. W., Crowell, C. A., Beynel, L., Deng, L., Lakhlani, D., Hilbig, S. A., … Cabeza, R. (2018). Complementary topology of maintenance and manipulation brain networks in working memory. *Scientific Reports*, *8*(1), 17827. https://doi.org/10.1038/s41598-018-35887-2

Davis, S. W., Dennis, N. A., Daselaar, S. M., Fleck, M. S., & Cabeza, R. (2008). Qué PASA? the posterior-anterior shift in aging. *Cerebral Cortex*, *18*(5), 1201–1209. https://doi.org/10.1093/cercor/bhm155

Davis, S. W., Geib, B. R., Wing, E. A., Wang, W.-C. C., Hovhannisyan, M., Monge, Z. A., & Cabeza, R. (2021). Visual and Semantic Representations Predict Subsequent Memory in Perceptual and Conceptual Memory Tests. *Cerebral Cortex*, *31*(2), 974–992. https://doi.org/10.1093/cercor/bhaa269

Davis, S. W., Luber, B., Murphy, D. L. K., Lisanby, S. H., & Cabeza, R. (2017). Frequency-specific neuromodulation of local and distant connectivity in aging and episodic memory function. *Human Brain Mapping*, *38*(12), 5987–6004. https://doi.org/10.1002/hbm.23803

Deng, L., Davis, S. W., Monge, Z. A., Wing, E. A., Geib, B. R., Raghunandan, A., & Cabeza, R. (2021). Age-related dedifferentiation and hyperdifferentiation of perceptual and mnemonic representations. *Neurobiology of Aging*, *106*(2021), 55–67. https://doi.org/10.1016/j.neurobiolaging.2021.05.021

Deng, L., Stanley, M. L., Monge, Z. A., Wing, E. A., Geib, B. R., Davis, S. W., & Cabeza, R. (2021). Age-Related Compensatory Reconfiguration of PFC Connections during Episodic Memory Retrieval. *Cerebral Cortex*, *31*(2), 717–730. https://doi.org/10.1093/cercor/bhaa192

Dennis, N. A., Daselaar, S. M., & Cabeza, R. (2007). Effects of aging on transient and

sustained successful memory encoding activity. *Neurobiology of Aging*, *28*(11), 1749–1758. https://doi.org/10.1016/j.neurobiolaging.2006.07.006

Dennis, N. A., Gutchess, A., & Thomas, A. K. (2020). Overview of Models of Cognitive Aging. In *The Cambridge Handbook of Cognitive Aging* (pp. 5–31). Cambridge University Press. https://doi.org/10.1017/9781108552684.002

Dennis, N. A., Hayes, S. M., Prince, S. E., Madden, D. J., Huettel, S. A., & Cabeza, R. (2008). Effects of Aging on the Neural Correlates of Successful Item and Source Memory Encoding. *Journal of Experimental Psychology: Learning Memory and Cognition*, *34*(4), 791–808. https://doi.org/10.1037/0278-7393.34.4.791

Dennis, N. A., Kim, H., & Cabeza, R. (2007). Effects of aging on true and false memory formation: An fMRI study. *Neuropsychologia*, *45*(14), 3157–3166. https://doi.org/10.1016/j.neuropsychologia.2007.07.003

Dennis, N. A., Kim, H., & Cabeza, R. (2008). Age-related differences in brain activity during true and false memory retrieval. *Journal of Cognitive Neuroscience*, *20*(8), 1390–1402. https://doi.org/10.1162/jocn.2008.20096

Devereux, B. J., Clarke, A., & Tyler, L. K. (2018). Integrated deep visual and semantic attractor neural networks predict fMRI pattern-information along the ventral object processing pathway. *Scientific Reports*, *8*(1), 1–12. https://doi.org/10.1038/s41598-018-28865-1

Dew, I. T. Z., Buchler, N., Dobbins, I. G., & Cabeza, R. (2012). Where is ELSA? the early to late shift in aging. *Cerebral Cortex*, *22*(11), 2542–2553. https://doi.org/10.1093/cercor/bhr334

Dickerson, B. C., & Sperling, R. A. (2008). Functional abnormalities of the medial temporal lobe memory system in mild cognitive impairment and Alzheimer's disease: Insights from functional MRI studies. *Neuropsychologia*, *46*(6), 1624–1635. https://doi.org/10.1016/j.neuropsychologia.2007.11.030

Driscoll, I., Hamilton, D. A., Petropoulos, H., Yeo, R. A., Brooks, W. M., Baumgartner, R. N., & Sutherland, R. J. (2003). The Aging Hippocampus: Cognitive, Biochemical and Structural Findings. *Cerebral Cortex*, *13*(12), 1344–1351. https://doi.org/10.1093/cercor/bhg081

Driscoll, I., & Sutherland, R. J. (2005). The aging hippocampus: Navigating between rat and human experiments. *Reviews in the Neurosciences*, *16*(2), 87–121. https://doi.org/10.1515/REVNEURO.2005.16.2.87

Eichenbaum, H. (2017). Prefrontal-hippocampal interactions in episodic memory. *Nature Reviews Neuroscience*, *18*(9), 547–558. https://doi.org/10.1038/nrn.2017.74

Eickenberg, M., Gramfort, A., Varoquaux, G., & Thirion, B. (2017). Seeing it all: Convolutional network layers map the function of the human visual system. *NeuroImage*, *152*(October 2016), 184–194. https://doi.org/10.1016/j.neuroimage.2016.10.001

Esteban, O., Blair, R. W., Nielson, D. M., Varada, J. C., Marrett, S., Thomas, A. G., … Gorgolewski, K. J. (2019). Crowdsourced MRI quality metrics and expert quality annotations for training of humans and machines. *Scientific Data*, *6*(1), 30.

Esteban, O., Markiewicz, C. J., Blair, R. W., Moodie, C. A., Isik, A. I., Erramuzpe, A., … Snyder, M. (2019). fMRIPrep: a robust preprocessing pipeline for functional MRI. *Nature Methods*, *16*(1), 111–116.

Fan, L., Li, H., Zhuo, J., Zhang, Y., Wang, J., Chen, L., … Jiang, T. (2016). The Human Brainnetome Atlas: A New Brain Atlas Based on Connectional Architecture. *Cerebral Cortex*, *26*(8), 3508–3526. https://doi.org/10.1093/cercor/bhw157

Fleck, M. S., Daselaar, S. M., Dobbins, I. G., & Cabeza, R. (2006). Role of prefrontal and anterior cingulate regions in decision-making processes shared by memory and nonmemory tasks. *Cerebral Cortex*, *16*(11), 1623–1630. https://doi.org/10.1093/cercor/bhj097

Folstein, M. F., Folstein, S. E., & McHugh, P. R. (1975). "Mini-mental state". A practical method for grading the cognitive state of patients for the clinician. *Journal of Psychiatric Research*, *12*(3), 189—198. https://doi.org/10.1016/0022-3956(75)90026-6

Fonov, V. S., Evans, A. C., McKinstry, R. C., Almli, C. R., & Collins, D. L. (2009). Unbiased nonlinear average age-appropriate brain templates from birth to adulthood. *NeuroImage*, *47*, S102. https://doi.org/https://doi.org/10.1016/S1053-8119(09)70884-5

Frisoni, G. B., Fox, N. C., Jack, C. R., Scheltens, P., & Thompson, P. M. (2010). The clinical use of structural MRI in Alzheimer disease. *Nature Reviews Neurology*, *6*(2), 67–77. https://doi.org/10.1038/nrneurol.2009.215

Gallen, C. L., Turner, G. R., Adnan, A., & D'Esposito, M. (2016). Reconfiguration of brain network architecture to support executive control in aging. *Neurobiology of Aging*, *44*, 42–52. https://doi.org/10.1016/j.neurobiolaging.2016.04.003

Geerligs, L., Renken, R. J., Saliasi, E., Maurits, N. M., & Lorist, M. M. (2015). A Brain-Wide Study of Age-Related Changes in Functional Connectivity. *Cerebral Cortex*, *25*(7), 1987–1999. https://doi.org/10.1093/cercor/bhu012

Geib, B. R., Stanley, M. L., Dennis, N. A., Woldorff, M. G., & Cabeza, R. (2017). From hippocampus to whole-brain: The role of integrative processing in episodic memory retrieval. *Human Brain Mapping*, *38*(4), 2242–2259. https://doi.org/10.1002/hbm.23518

Geib, B. R., Stanley, M. L., Wing, E. A., Laurienti, P. J., & Cabeza, R. (2017). Hippocampal Contributions to the Large-Scale Episodic Memory Network Predict Vivid Visual Memories. *Cerebral Cortex*, *27*(1), 680–693. https://doi.org/10.1093/cercor/bhv272

Ghosh, V. E., Moscovitch, M., Melo Colella, B., & Gilboa, A. (2014). Schema Representation in Patients with Ventromedial PFC Lesions. *Journal of Neuroscience*, *34*(36), 12057–12070. https://doi.org/10.1523/JNEUROSCI.0740-14.2014

Gilboa, A., & Moscovitch, M. (2017). Ventromedial prefrontal cortex generates pre-stimulus theta coherence desynchronization: A schema instantiation hypothesis. *Cortex*, *87*, 16–30. https://doi.org/10.1016/j.cortex.2016.10.008

Gilmore, G. C., Spinks, R. A., & Thomas, C. W. (2006). Age effects in coding tasks: Componential analysis and test of the sensory deficit hypothesis. *Psychology and Aging*, *21*(1), 7–18. https://doi.org/10.1037/0882-7974.21.1.7

Goh, J. O., Suzuki, A., & Park, D. C. (2010). Reduced neural selectivity increases fMRI adaptation with age during face discrimination. *NeuroImage*, *51*(1), 336–344. https://doi.org/10.1016/j.neuroimage.2010.01.107

Goñi, J., van den Heuvel, M. P., Avena-Koenigsberger, A., Velez de Mendizabal, N., Betzel, R. F., Griffa, A., … Sporns, O. (2014). Resting-brain functional connectivity predicted by analytic measures of network communication. *Proceedings of the National Academy of Sciences of the United States of America*, *111*(2), 833–838. https://doi.org/10.1073/pnas.1315529111

Gordon, E. M., Laumann, T. O., Adeyemo, B., Huckins, J. F., Kelley, W. M., & Petersen, S. E. (2014). Generation and Evaluation of a Cortical Area Parcellation from Resting-State Correlations. *Cerebral Cortex*, (January), bhu239-. https://doi.org/10.1093/cercor/bhu239

Gorgolewski, K. J., Burns, C. D., Madison, C., Clark, D., Halchenko, Y. O., Waskom, M. L., & Ghosh, S. S. (2011). Nipype: a flexible, lightweight and extensible

neuroimaging data processing framework in python. *Frontiers in Neuroinformatics*, 13.

Gorgolewski, K. J., Esteban, O., Markiewicz, C. J., Ziegler, E., Ellis, D. G., Notter, M. P., … Manhães-Savio, A. (2018). Nipype. *Software*. Zenodo.

Grady, C. L. (2008). Cognitive neuroscience of aging. *Annals of the New York Academy of Sciences*. https://doi.org/10.1196/annals.1440.009

Grady, C. L. (2012). The cognitive neuroscience of ageing. *Nature Reviews Neuroscience*, *13*(7), 491–505. https://doi.org/10.1038/nrn3256

Grady, C. L., McIntosh, A. R., Horwitz, B., Maisog, J. M., Ungerleider, L. G., Mentis, M. J., … Haxby, J. V. (1995). Age-related reductions in human recognition memory due to impaired encoding. *Science*, *269*(5221), 218–221.

Grady, C. L., Sarraf, S., Saverino, C., & Campbell, K. (2016). Age differences in the functional interactions among the default, frontoparietal control, and dorsal attention networks. *Neurobiology of Aging*, *41*, 159–172. https://doi.org/10.1016/j.neurobiolaging.2016.02.020

Greicius, M. D., Supekar, K., Menon, V., & Dougherty, R. F. (2009). Resting-state functional connectivity reflects structural connectivity in the default mode network. *Cerebral Cortex*, *19*(1), 72–78. https://doi.org/10.1093/cercor/bhn059

Greve, A., Cooper, E., Tibon, R., & Henson, R. N. (2019). Knowledge is power: Prior knowledge aids memory for both congruent and incongruent events, but in different ways. *Journal of Experimental Psychology: General*, *148*(2), 325–341. https://doi.org/10.1037/xge0000498

Greve, D. N., & Fischl, B. (2009). Accurate and robust brain image alignment using boundary-based registration. *NeuroImage*, *48*(1), 63–72. https://doi.org/https://doi.org/10.1016/j.neuroimage.2009.06.060

Groen, I. I. A., Greene, M. R., Baldassano, C., Fei-Fei, L., Beck, D. M., & Baker, C. I. (2018). Distinct contributions of functional and deep neural network features to representational similarity of scenes in human brain and behavior. *ELife*, *7*, 1–26. https://doi.org/10.7554/eLife.32962

Gronau, N., & Shachar, M. (2015). Contextual consistency facilitates long-term memory of perceptual detail in barely seen images. *Journal of Experimental Psychology: Human Perception and Performance*, *41*(4), 1095–1111. https://doi.org/10.1037/xhp0000071

Güçlü, U., & van Gerven, M. A. J. (2015). Deep neural networks reveal a gradient in the complexity of neural representations across the ventral stream. *Journal of Neuroscience*, *35*(27), 10005–10014. https://doi.org/10.1523/JNEUROSCI.5023-14.2015

Guimerà, R., & Amaral, L. A. N. (2005). Cartography of complex networks: modules and universal roles. *Journal of Statistical Mechanics: Theory and Experiment*, *2005*(02), P02001. https://doi.org/10.1088/1742-5468/2005/02/P02001

Guo, D., & Yang, J. (2022). Reactivation of schema representation in lateral occipital cortex supports successful memory encoding. *Cerebral Cortex*, (2018), 1–13. https://doi.org/10.1093/cercor/bhac475

Gusnard, D. A., Akbudak, E., Shulman, G. L., & Raichle, M. E. (2001). Medial prefrontal cortex and self-referential mental activity: Relation to a default mode of brain function. *Proceedings of the National Academy of Sciences of the United States of America*, *98*(7), 4259–4264. https://doi.org/10.1073/pnas.071043098

Gutchess, A. H., Welsh, R. C., Hedden, T., Bangert, A., Minear, M., Liu, L. L., & Park, D. C. (2005). Aging and the Neural Correlates of Successful Picture Encoding: Frontal Activations Compensate for Decreased Medial-Temporal Activity. *Journal of Cognitive Neuroscience*, *17*(1), 84–96. https://doi.org/10.1162/0898929052880048

Habib, R., Nyberg, L., & Nilsson, L. G. (2007). Cognitive and non-cognitive factors contributing to the longitudinal identification of successful older adults in the Betula study. *Aging, Neuropsychology, and Cognition*, *14*(3), 257–273. https://doi.org/10.1080/13825580600582412

Haxby, J. V., Gobbini, M. I., Furey, M. L., Ishai, A., Schouten, J. L., & Pietrini, P. (2001). Distributed and Overlapping Representations of Faces and Objects in Ventral Temporal Cortex. *Science*, *293*(5539), 2425–2430. https://doi.org/10.1126/science.1063736

Hearne, L. J., Cocchi, L., Zalesky, A., & Mattingley, J. B. (2017). Reconfiguration of brain network architectures between resting state and complexity-dependent cognitive reasoning. *The Journal of Neuroscience*, *37*(35), 0485–17. https://doi.org/10.1523/JNEUROSCI.0485-17.2017

Hebscher, M., & Gilboa, A. (2016). A boost of confidence: The role of the ventromedial prefrontal cortex in memory, decision-making, and schemas. *Neuropsychologia*, *90*, 46–58. https://doi.org/10.1016/j.neuropsychologia.2016.05.003

Henson, R. N. A., Shallice, T., & Dolan, R. J. (1999). Right prefrontal cortex and episodic

memory retrieval: A functional MRI test of the monitoring hypothesis. *Brain*, *122*(7), 1367–1381. https://doi.org/10.1093/brain/122.7.1367

Heuvel, M. P. Van Den, Kahn, R. S., Goñi, J., Sporns, O., & van den Heuvel, M. P. (2012). High-cost, high-capacity backbone for global brain communication. *Proceedings of the National Academy of Sciences of the United States of America*, *109*, 11372–11377. https://doi.org/10.1073/pnas.1203593109/-/DCSupplemental.www.pnas.org/cgi/doi/10.1073/pnas.1203593109

Hodges, J. R., Patterson, K., Oxbury, S., & Funnell, E. (1992). Semantic dementia: progressive fluent aphasia with temporal lobe atrophy. *Brain*, *115*(6), 1783–1806. https://doi.org/10.1093/brain/115.6.1783

Hovhannisyan, M., Clarke, A., Geib, B. R., Cicchinelli, R., Monge, Z. A., Worth, T., … Davis, S. W. (2021). The visual and semantic features that predict object memory: Concept property norms for 1,000 object images. *Memory and Cognition*. https://doi.org/10.3758/s13421-020-01130-5

Huijbers, W., Pennartz, C. M. A., Cabeza, R., & Daselaar, S. M. (2011). The hippocampus is coupled with the default network during memory retrieval but not during memory encoding. *PLoS ONE*, *6*(4). https://doi.org/10.1371/journal.pone.0017463

Inman, C. S., James, G. A., Vytal, K., & Hamann, S. (2018). Dynamic changes in large-scale functional network organization during autobiographical memory retrieval. *Neuropsychologia*, *110*(February 2017), 208–224. https://doi.org/10.1016/j.neuropsychologia.2017.09.020

Jacoby, L. L., Shimizu, Y., Daniels, K. A., & Rhodes, M. G. (2005). Modes of cognitive control in recognition and source memory: Depth of retrieval. *Psychonomic Bulletin and Review*, *12*(5), 852–857. https://doi.org/10.3758/BF03196776

Jacoby, L. L., Shimizu, Y., Velanova, K., & Rhodes, M. G. (2005). Age differences in depth of retrieval: Memory for foils. *Journal of Memory and Language*, *52*(4), 493–504. https://doi.org/10.1016/j.jml.2005.01.007

Jenkinson, M., Bannister, P., Brady, M., & Smith, S. (2002). Improved optimization for the robust and accurate linear registration and motion correction of brain images. *NeuroImage*, *17*(2), 825–841. Retrieved from http://www.ncbi.nlm.nih.gov/pubmed/12377157

Johnson, M. K., Kuhl, B. A., Mitchell, K. J., Ankudowich, E., & Durbin, K. A. (2015). Age-related differences in the neural basis of the subjective vividness of memories:

evidence from multivoxel pattern classification. *Cognitive, Affective and Behavioral Neuroscience*, *15*(3), 644–661. https://doi.org/10.3758/s13415-015-0352-9

Josephs, E. L., & Konkle, T. (2019). Perceptual dissociations among views of objects, scenes, and reachable spaces. *Journal of Experimental Psychology: Human Perception and Performance*, *45*(6), 715–728. https://doi.org/10.1037/xhp0000626

Kausler, D. H. (1994). *Learning and memory in normal aging*. Academic Press San Diego, CA:

Kennedy, K. M., Rodrigue, K. M., Bischof, G. N., Hebrank, A. C., Reuter-Lorenz, P. a., & Park, D. C. (2015). Age trajectories of functional activation under conditions of low and high processing demands: An adult lifespan fMRI study of the aging brain. *NeuroImage*, *104*, 21–34. https://doi.org/10.1016/j.neuroimage.2014.09.056

Khaligh-Razavi, S. M., & Kriegeskorte, N. (2014). Deep Supervised, but Not Unsupervised, Models May Explain IT Cortical Representation. *PLoS Computational Biology*, *10*(11). https://doi.org/10.1371/journal.pcbi.1003915

Kim, H., & Cabeza, R. (2007). Trusting our memories: Dissociating the neural correlates of confidence in veridical versus illusory memories. *Journal of Neuroscience*, *27*(45), 12190–12197. https://doi.org/10.1523/JNEUROSCI.3408-07.2007

Klein, A., Ghosh, S. S., Bao, F. S., Giard, J., Häme, Y., Stavsky, E., … Keshavan, A. (2017). Mindboggling morphometry of human brains. *PLOS Computational Biology*, *13*(2), e1005350. Retrieved from https://doi.org/10.1371/journal.pcbi.1005350

Koen, J. D., Hauck, N., & Rugg, M. D. (2019). The relationship between age, neural differentiation, and memory performance. *Journal of Neuroscience*, *39*(1), 149–162. https://doi.org/10.1523/JNEUROSCI.1498-18.2018

Koen, J. D., & Rugg, M. D. (2019). Neural Dedifferentiation in the Aging Brain. *Trends in Cognitive Sciences*, *23*(7), 547–559. https://doi.org/10.1016/j.tics.2019.04.012

Koen, J. D., Srokova, S., & Rugg, M. D. (2020). Age-related neural dedifferentiation and cognition. *Current Opinion in Behavioral Sciences*, *32*(Figure 1), 7–14. https://doi.org/10.1016/j.cobeha.2020.01.006

Krakauer, J. W., Ghazanfar, A. A., Gomez-Marin, A., MacIver, M. A., & Poeppel, D. (2017). Neuroscience Needs Behavior: Correcting a Reductionist Bias. *Neuron*, *93*(3), 480–490. https://doi.org/10.1016/j.neuron.2016.12.041

Kriegeskorte, N. (2008). Representational similarity analysis – connecting the branches of systems neuroscience. *Frontiers in Systems Neuroscience*, *2*(November), 1–28. https://doi.org/10.3389/neuro.06.004.2008

Kriegeskorte, N. (2015). Deep Neural Networks: A New Framework for Modeling Biological Vision and Brain Information Processing. *Annual Review of Vision Science*, *1*(1), 417–446. https://doi.org/10.1146/annurev-vision-082114-035447

Kriegeskorte, N., & Douglas, P. K. (2018). Cognitive computational neuroscience. *Nature Neuroscience*, *21*(9), 1148–1160. https://doi.org/10.1038/s41593-018-0210-5

Kriegeskorte, N., Goebel, R., & Bandettini, P. (2006). Information-based functional brain mapping. *Proceedings of the National Academy of Sciences of the United States of America*, *103*(10), 3863–3868. https://doi.org/10.1073/pnas.0600244103

Kriegeskorte, N., & Kievit, R. A. (2013). Representational geometry: Integrating cognition, computation, and the brain. *Trends in Cognitive Sciences*, *17*(8), 401–412. https://doi.org/10.1016/j.tics.2013.06.007

Kriegeskorte, N., Mur, M., Ruff, D. A., Kiani, R., Bodurka, J., Esteky, H., … Bandettini, P. A. (2008). Matching Categorical Object Representations in Inferior Temporal Cortex of Man and Monkey. *Neuron*, *60*(6), 1126–1141. https://doi.org/10.1016/j.neuron.2008.10.043

Krizhevsky, A., Sutskever, I., & Hinton, G. E. (2017). ImageNet classification with deep convolutional neural networks. *Communications of the ACM*, *60*(6), 84–90. https://doi.org/10.1145/3065386

Lanczos, C. (1964). Evaluation of Noisy Data. *Journal of the Society for Industrial and Applied Mathematics Series B Numerical Analysis*, *1*(1), 76–85. https://doi.org/10.1137/0701007

Laumann Long, L., & Shaw, R. J. (2000). Adult age differences in vocabulary acquisition. *Educational Gerontology*, *26*(7), 651–664. https://doi.org/10.1080/03601270050200644

Leal, S. L., & Yassa, M. A. (2015). Neurocognitive Aging and the Hippocampus across Species. *Trends in Neurosciences*, *38*(12), 800–812. https://doi.org/10.1016/j.tins.2015.10.003

Lecun, Y., Bengio, Y., & Hinton, G. (2015). Deep learning. *Nature*, *521*(7553), 436–444. https://doi.org/10.1038/nature14539

Leeds, D. D., Seibert, D. A., Pyles, J. A., & Tarr, M. J. (2013). Comparing visual representations across human fMRI and computational vision. *Journal of Vision*, *13*(13), 1–27. https://doi.org/10.1167/13.13.25

Li, H. J., Hou, X. H., Liu, H. H., Yue, C. L., Lu, G. M., & Zuo, X. N. (2015). Putting age-related task activation into large-scale brain networks: A meta-analysis of 114 fMRI studies on healthy aging. *Neuroscience and Biobehavioral Reviews*, *57*(16), 156–174. https://doi.org/10.1016/j.neubiorev.2015.08.013

Lighthall, N. R., Huettel, S. A., & Cabeza, R. (2014). Functional Compensation in the Ventromedial Prefrontal Cortex Improves Memory-Dependent Decisions in Older Adults. *Journal of Neuroscience*, *34*(47), 15648–15657. https://doi.org/10.1523/JNEUROSCI.2888-14.2014

Lindenberger, U., & Baltes, P. B. (1994). Sensory functioning and intelligence in old age: A strong connection. *Psychology and Aging*, *9*(3), 339–355. https://doi.org/10.1037/0882-7974.9.3.339

Martin, C. B., Douglas, D., Newsome, R. N., Man, L. L., & Barense, M. D. (2018). Integrative and distinctive coding of visual and conceptual object features in the ventral visual stream. *ELife*, *7*, 1–29. https://doi.org/10.7554/eLife.31873

Masís-Obando, R., Norman, K. A., & Baldassano, C. (2022). Schema representations in distinct brain networks support narrative memory during encoding and retrieval. *ELife*, *11*, 1–25. https://doi.org/10.7554/eLife.70445

Mather, M., Johnson, M. K., & De Leonardis, D. M. (1999). Stereotype reliance in source monitoring: Age differences and neuropsychological test correlates. *Cognitive Neuropsychology*, *16*(3–5), 437–458. https://doi.org/10.1080/026432999380870

Maximilian Riesenhuber, & Tomaso Poggio. (1999). Hierarchical models of object recognition in cortex. *Nature Neuroscience*, *2*(11), 1019–1025.

McClelland, J. L., McNaughton, B. L., & O'Reilly, R. C. (1995). Why there are complementary learning systems in the hippocampus and neocortex: Insights from the successes and failures of connectionist models of learning and memory. *Psychological Review*, *102*(3), 419–457. https://doi.org/10.1037/0033-295X.102.3.419

McRae, K., Cree, G. S., Seidenberg, M. S., & McNorgan, C. (2005). Semantic feature production norms for a large set of living and nonliving things. *Behavior Research Methods*, *37*(4), 547–559. https://doi.org/10.3758/BF03192726

Medaglia, J. D., Lynall, M. E., & Bassett, D. S. (2015). Cognitive network neuroscience. *Journal of Cognitive Neuroscience*, *27*(8), 1471–1491. https://doi.org/10.1162/jocn_a_00810

Meilă, M. (2007). Comparing clusterings—an information based distance. *Journal of Multivariate Analysis*, *98*(5), 873–895.

Meunier, D., Lambiotte, R., & Bullmore, E. T. (2010). Modular and hierarchically modular organization of brain networks. *Frontiers in Neuroscience*, *4*(DEC), 1–11. https://doi.org/10.3389/fnins.2010.00200

Mikolov, T., Chen, K., Corrado, G., & Dean, J. (2013). Efficient estimation of word representations in vector space. *1st International Conference on Learning Representations, ICLR 2013 - Workshop Track Proceedings*, 1–12.

Mohanty, P. P., Naveh-Benjamin, M., & Ratneshwar, S. (2016). Beneficial effects of semantic memory support on older adults' episodic memory: Differential patterns of support of item and associative information. *Psychology and Aging*, *31*(1), 25–36. https://doi.org/10.1037/pag0000059

Monge, Z. A., Geib, B. R., Siciliano, R. E., Packard, L. E., Tallman, C. W., & Madden, D. J. (2017). Functional modular architecture underlying attentional control in aging. *NeuroImage*, *155*(May), 257–270. https://doi.org/10.1016/j.neuroimage.2017.05.002

Monge, Z. A., & Madden, D. J. (2016). Linking cognitive and visual perceptual decline in healthy aging: The information degradation hypothesis. *Neuroscience and Biobehavioral Reviews*, *69*, 166–173. https://doi.org/10.1016/j.neubiorev.2016.07.031

Monge, Z. A., Stanley, M. L., Geib, B. R., Davis, S. W., & Cabeza, R. (2018). Functional networks underlying item and source memory: shared and distinct network components and age-related differences. *Neurobiology of Aging*, *69*, 140–150. https://doi.org/10.1016/j.neurobiolaging.2018.05.016

Morcom, A. M., & Henson, R. N. A. (2018). Increased Prefrontal Activity with Aging Reflects Nonspecific Neural Responses Rather than Compensation. *The Journal of Neuroscience*, *38*(33), 7303–7313. https://doi.org/10.1523/jneurosci.1701-17.2018

Morris, R. G. M. (2006). Elements of a neurobiological theory of hippocampal function: The role of synaptic plasticity, synaptic tagging and schemas. *European Journal of Neuroscience*, *23*(11), 2829–2846. https://doi.org/10.1111/j.1460-9568.2006.04888.x

Moscovitch, M., Cabeza, R., Winocur, G., & Nadel, L. (2016). Episodic Memory and

Beyond: The Hippocampus and Neocortex in Transformation. *Annual Review of Psychology*, *67*(1), 105–134. https://doi.org/10.1146/annurev-psych-113011-143733

Moscovitch, M., & Melo, B. (1997). Strategic retrieval and the frontal lobes: Evidence from confabulation and amnesia. *Neuropsychologia*, *35*(7), 1017–1034. https://doi.org/10.1016/S0028-3932(97)00028-6

Mumford, J. A., Turner, B. O., Ashby, F. G., & Poldrack, R. A. (2012). Deconvolving BOLD activation in event-related designs for multivoxel pattern classification analyses. *NeuroImage*, *59*(3), 2636–2643. https://doi.org/10.1016/j.neuroimage.2011.08.076

Murphy, D. R., Craik, F. I. M., Li, K. Z. H., & Schneider, B. A. (2000). Comparing the effects of aging and background noise on short-term memory performance. *Psychology and Aging*, *15*(2), 323–334. https://doi.org/10.1037/0882-7974.15.2.323

Naspi, L., Hoffman, P., Devereux, B., & Morcom, A. M. (2021). Perceptual and semantic representations at encoding contribute to true and false recognition of objects. *Journal of Neuroscience*, *41*(41), 8375–8389. https://doi.org/10.1523/JNEUROSCI.0677-21.2021

Naspi, L., Stensholt, C., Karlsson, A. E., Monge, Z. A., & Cabeza, R. (2022). Effects of aging on successful object encoding : Enhanced semantic representations compensate for impaired visual representations. *Biorxiv*. https://doi.org/10.1101/2022.12.10.519871

Nasreddine, Z. S., Phillips, N. A., Bédirian, V., Charbonneau, S., Whitehead, V., Collin, I., … Chertkow, H. (2005). The Montreal Cognitive Assessment, MoCA: a brief screening tool for mild cognitive impairment. *Journal of the American Geriatrics Society*, *53*(4), 695–699.

Nastase, S. A., Connolly, A. C., Oosterhof, N. N., Halchenko, Y. O., Guntupalli, J. S., Di Oleggio Castello, M. V., … Haxby, J. V. (2017). Attention selectively reshapes the geometry of distributed semantic representation. *Cerebral Cortex*, *27*(8), 4277–4291. https://doi.org/10.1093/cercor/bhx138

Naveh-Benjamin, M. (2000). Adult age differences in memory performance: tests of an associative deficit hypothesis. *Journal of Experimental Psychology: Learning, Memory, and Cognition*, *26*(5), 1170.

Newman, M. E. J. (2006). Modularity and community structure in networks. *Proceedings of the National Academy of Sciences*, *103*(23), 8577–8582.

https://doi.org/10.1073/pnas.0601602103

Norman, K. A., Polyn, S. M., Detre, G. J., & Haxby, J. V. (2006). Beyond mind-reading: multi-voxel pattern analysis of fMRI data. *Trends in Cognitive Sciences*, *10*(9), 424–430. https://doi.org/10.1016/j.tics.2006.07.005

Nyberg, L. (2017). Functional brain imaging of episodic memory decline in ageing. *Journal of Internal Medicine*, *281*(1), 65–74. https://doi.org/https://doi.org/10.1111/joim.12533

Nyberg, L., Lövdén, M., Riklund, K., Lindenberger, U., & Bäckman, L. (2012). Memory aging and brain maintenance. *Trends in Cognitive Sciences*, *16*(5), 292–305. https://doi.org/10.1016/j.tics.2012.04.005

Oldham, S., & Fornito, A. (2019). The development of brain network hubs. *Developmental Cognitive Neuroscience*, *36*(October 2018), 100607. https://doi.org/10.1016/j.dcn.2018.12.005

Owsley, C. (2011). Aging and vision. *Vision Research*, *51*(13), 1610–1622. https://doi.org/10.1016/j.visres.2010.10.020

Park, D. C., Lautenschlager, G., Hedden, T., Davidson, N. S., Smith, A. D., & Smith, P. K. (2002). Models of visuospatial and verbal memory across the adult life span. *Psychology and Aging*, *17*(2), 299–320. Retrieved from http://www.ncbi.nlm.nih.gov/pubmed/12061414

Park, D. C., Polk, T. A., Mikels, J. A., Taylor, S. F., & Marshuetz, C. (2001). Cerebral aging: integration of brain and behavioral models of cognitive function. *Dialogues in Clinical Neuroscience*, *3*(3), 151.

Park, D. C., Polk, T. A., Park, R., Minear, M., Savage, A., & Smith, M. R. (2004). Aging reduces neural specialization in ventral visual cortex. *Proceedings of the National Academy of Sciences of the United States of America*, *101*(35), 13091–13095. https://doi.org/10.1073/pnas.0405148101

Park, D. C., & Reuter-Lorenz, P. (2009). The Adaptive Brain: Aging and Neurocognitive Scaffolding. *Annual Review of Psychology*, *60*(1), 173–196. https://doi.org/10.1146/annurev.psych.59.103006.093656

Park, J., Carp, J., Hebrank, A., Park, D. C., & Polk, T. A. (2010). Neural specificity predicts fluid processing ability in older adults. *Journal of Neuroscience*, *30*(27), 9253–9259. https://doi.org/10.1523/JNEUROSCI.0853-10.2010

Payer, D., Marshuetz, C., Sutton, B., Hebrank, A., Welsh, R. C., & Park, D. C. (2006). Decreased neural specialization in old adults on a working memory task. *NeuroReport*, *17*(5), 487–491. https://doi.org/10.1097/01.wnr.0000209005.40481.31

Peters, A., Moss, M. B., & Sethares, C. (2001). The effects of aging on layer 1 of primary visual cortex in the rhesus monkey. *Cerebral Cortex*, *11*(2), 93–103.

Pichora-Fuller, M. K., Schneider, B. A., & Daneman, M. (1995). How young and old adults listen to and remember speech in noise. *The Journal of the Acoustical Society of America*, *97*(1), 593–608.

Poldrack, R. A., Mumford, J. A., & Nichols, T. E. (2011). *Handbook of Functional MRI Data Analysis*. Cambridge University Press. https://doi.org/10.1017/CBO9780511895029

Power, J. D., Mitra, A., Laumann, T. O., Snyder, A. Z., Schlaggar, B. L., & Petersen, S. E. (2014). Methods to detect, characterize, and remove motion artifact in resting state fMRI. *NeuroImage*, *84*, 320–341. https://doi.org/10.1016/j.neuroimage.2013.08.048

Power, J. D., Schlaggar, B. L., & Petersen, S. E. (2014). Studying Brain Organization via Spontaneous fMRI Signal. *Neuron*, *84*(4), 681–696. https://doi.org/10.1016/j.neuron.2014.09.007

Preston, A. R., & Eichenbaum, H. (2013). Interplay of hippocampus and prefrontal cortex in memory. *Current Biology*, *23*(17), R764–R773. https://doi.org/10.1016/j.cub.2013.05.041

Prull, M. W., Dawes, L. L. C., Martin, A. M. L., Rosenberg, H. F., & Light, L. L. (2006). Recollection and familiarity in recognition memory: Adult age differences and neuropsychological test correlates. *Psychology and Aging*, *21*(1), 107–118. https://doi.org/10.1037/0882-7974.21.1.107

Ralph, M. A. L., Jefferies, E., Patterson, K., & Rogers, T. T. (2016). The neural and computational bases of semantic cognition. *Nature Reviews Neuroscience*, *18*(1), 42–55. https://doi.org/10.1038/nrn.2016.150

Ranganath, C., Heller, A., Cohen, M. X., Brozinsky, C. J., & Rissman, J. (2005). Functional connectivity with the hippocampus during successful memory formation. *Hippocampus*, *15*(8), 997–1005. https://doi.org/10.1002/hipo.20141

Rathore, S., Habes, M., Iftikhar, M. A., Shacklett, A., & Davatzikos, C. (2017). A review on neuroimaging-based classification studies and associated feature extraction methods for Alzheimer's disease and its prodromal stages. *NeuroImage*, *155*(March),

530–548. https://doi.org/10.1016/j.neuroimage.2017.03.057

Raz, N., Lindenberger, U., Rodrigue, K. M., Kennedy, K. M., Head, D., Williamson, A., … Acker, J. D. (2005). Regional brain changes in aging healthy adults: General trends, individual differences and modifiers. *Cerebral Cortex*, *15*(11), 1676–1689. https://doi.org/10.1093/cercor/bhi044

Reagh, Z. M., Delarazan, A. I., Garber, A., & Ranganath, C. (2020). Aging alters neural activity at event boundaries in the hippocampus and Posterior Medial network. *Nature Communications*, *11*(1), 1–12. https://doi.org/10.1038/s41467-020-17713-4

Reichardt, J., & Bornholdt, S. (2006). Statistical mechanics of community detection. *Physical Review E - Statistical, Nonlinear, and Soft Matter Physics*, *74*(1), 1–14. https://doi.org/10.1103/PhysRevE.74.016110

Reuter-Lorenz, P. A., & Cappell, K. A. (2008). Neurocognitive Aging and the Compensation Hypothesis. *Current Directions in Psychological Science*, *17*(3), 177–182. https://doi.org/10.1111/j.1467-8721.2008.00570.x

Rissman, J., Gazzaley, A., & D'Esposito, M. (2004). Measuring functional connectivity during distinct stages of a cognitive task. *NeuroImage*, *23*(2), 752–763. https://doi.org/10.1016/j.neuroimage.2004.06.035

Ritchey, M., Wing, E. A., LaBar, K. S., & Cabeza, R. (2013). Neural Similarity Between Encoding and Retrieval is Related to Memory Via Hippocampal Interactions. *Cerebral Cortex*, *23*(12), 2818–2828. https://doi.org/10.1093/cercor/bhs258

Robin, J., & Moscovitch, M. (2017). Details, gist and schema: hippocampal–neocortical interactions underlying recent and remote episodic and spatial memory. *Current Opinion in Behavioral Sciences*, *17*, 114–123. https://doi.org/10.1016/j.cobeha.2017.07.016

Rolls, E. T. (2000). Hippocampo-Cortical and Cortico-Cortical Backprojections. *Hippocampus*, *388*(May), 380–388. Retrieved from https://onlinelibrary.wiley.com/doi/10.1002/1098-1063(2000)10:4%3C380::AID-HIPO4%3E3.0.CO;2-0

Rubinov, M., & Sporns, O. (2010). Complex network measures of brain connectivity: uses and interpretations. *NeuroImage*, *52*(3), 1059–1069. https://doi.org/10.1016/j.neuroimage.2009.10.003

Rugg, M. D., & Vilberg, K. L. (2013). Brain networks underlying episodic memory

retrieval. *Current Opinion in Neurobiology*, *23*(2), 255–260. https://doi.org/10.1016/j.conb.2012.11.005

Sala-Llonch, R., Bartrés-Faz, D., & Junque, C. (2015). Reorganization of brain networks in aging: a review of functional connectivity studies. *Frontiers in Psychology*, *6*(May), 1–11. https://doi.org/10.3389/fpsyg.2015.00663

Salthouse, T. A. (2004). What and When of Cognitive Aging Percentile of Population Z-Score. *Aging And Cognition*, *13*(4), 140–144.

Samanez-Larkin, G. R., & D'Esposito, M. (2008). Group comparisons: Imaging the aging brain. *Social Cognitive and Affective Neuroscience*, *3*(3), 290–297. https://doi.org/10.1093/scan/nsn029

Särkkä, S., Solin, A., Nummenmaa, A., Vehtari, A., Auranen, T., Vanni, S., & Lin, F.-H. (2012). Dynamic retrospective filtering of physiological noise in BOLD fMRI: DRIFTER. *NeuroImage*, *60*(2), 1517–1527. https://doi.org/https://doi.org/10.1016/j.neuroimage.2012.01.067

Satterthwaite, T. D., Elliott, M. A., Gerraty, R. T., Ruparel, K., Loughead, J., Calkins, M. E., … Wolf, D. H. (2013). An improved framework for confound regression and filtering for control of motion artifact in the preprocessing of resting-state functional connectivity data. *NeuroImage*, *64*, 240–256. https://doi.org/https://doi.org/10.1016/j.neuroimage.2012.08.052

Schaefer, A., Kong, R., Gordon, E. M., Laumann, T. O., Zuo, X.-N., Holmes, A. J., … Yeo, B. T. T. (2018). Local-Global Parcellation of the Human Cerebral Cortex from Intrinsic Functional Connectivity MRI. *Cerebral Cortex*, *28*(9), 3095–3114. https://doi.org/10.1093/cercor/bhx179

Schlichting, M. L., Mumford, J. A., & Preston, A. R. (2015). Learning-related representational changes reveal dissociable integration and separation signatures in the hippocampus and prefrontal cortex. *Nature Communications*, *6*. https://doi.org/10.1038/ncomms9151

Seabold, S., & Perktold, J. (2010). Statsmodels: Econometric and statistical modeling with python. In *Proceedings of the 9th Python in Science Conference* (Vol. 57, pp. 10–25080). Austin, TX.

Sekuler, R., & Sekuler, A. B. (2000). Vision and aging. *Encyclopedia of Psychology*, *8*, 180–183.

Serre, T., Wolf, L., Bileschi, S., Riesenhuber, M., & Poggio, T. (2007). Robust object recognition with cortex-like mechanisms. *IEEE Transactions on Pattern Analysis and Machine Intelligence*, *29*(3), 411–426. https://doi.org/10.1109/TPAMI.2007.56

Simony, E., Honey, C. J., Chen, J., Lositsky, O., Yeshurun, Y., Wiesel, A., & Hasson, U. (2016). Dynamic reconfiguration of the default mode network during narrative comprehension. *Nature Communications*, *7*(1), 12141. https://doi.org/10.1038/ncomms12141

Simonyan, K., & Zisserman, A. (2015). Very deep convolutional networks for large-scale image recognition. *3rd International Conference on Learning Representations, ICLR 2015 - Conference Track Proceedings*, 1–14.

Spalding, K. N., Jones, S. H., Duff, M. C., Tranel, D., & Warren, D. E. (2015). Investigating the neural correlates of schemas: Ventromedial prefrontal cortex is necessary for normal schematic influence on memory. *Journal of Neuroscience*, *35*(47), 15746–15751. https://doi.org/10.1523/JNEUROSCI.2767-15.2015

Spaniol, J., Davidson, P. S. R., Kim, A. S. N., Han, H., Moscovitch, M., & Grady, C. L. (2009). Event-related fMRI studies of episodic encoding and retrieval: Meta-analyses using activation likelihood estimation. *Neuropsychologia*, *47*(8–9), 1765–1779. https://doi.org/10.1016/j.neuropsychologia.2009.02.028

Spencer, W. D., & Raz, N. (1995). Differential effects of aging on memory for content and context: A meta-analysis. *Psychology and Aging*, *10*(4), 527–539. https://doi.org/10.1037/0882-7974.10.4.527

Spielberg, J. M., Miller, G. A., Heller, W., & Banich, M. T. (2015). Flexible brain network reconfiguration supporting inhibitory control. *Proceedings of the National Academy of Sciences*, *112*(32), 10020–10025. https://doi.org/10.1073/pnas.1500048112

Sporns, O. (2014). Contributions and challenges for network models in cognitive neuroscience. *Nature Neuroscience*, *17*(5), 652–660. https://doi.org/10.1038/nn.3690

Spreng, R. N., Stevens, W. D., Viviano, J. D., & Schacter, D. L. (2016). Attenuated anticorrelation between the default and dorsal attention networks with aging: evidence from task and rest. *Neurobiology of Aging*, *45*, 149–160. https://doi.org/10.1016/j.neurobiolaging.2016.05.020

Spreng, R. N., & Turner, G. R. (2019). The Shifting Architecture of Cognition and Brain Function in Older Adulthood. *Perspectives on Psychological Science*, *14*(4), 523–542. https://doi.org/10.1177/1745691619827511

St-Laurent, M., Abdi, H., Bondad, A., & Buchsbaum, B. R. (2014). Memory reactivation in healthy aging: Evidence of stimulus-specific dedifferentiation. *Journal of Neuroscience*, *34*(12), 4175–4186. https://doi.org/10.1523/JNEUROSCI.3054-13.2014

St. Jacques, P. L., Dolcos, F., & Cabeza, R. (2009). Effects of Aging on Functional Connectivity of the Amygdala for Subsequent Memory of Negative Pictures. *Psychological Science*, *20*(1), 74–84. https://doi.org/10.1111/j.1467-9280.2008.02258.x

St. Jacques, P. L., Rubin, D. C., & Cabeza, R. (2012). Age-related effects on the neural correlates of autobiographical memory retrieval. *Neurobiology of Aging*, *33*(7), 1298–1310. https://doi.org/10.1016/j.neurobiolaging.2010.11.007

Stanley, M. L., Gessell, B., & De Brigard, F. (2019). Network Modularity as a Foundation for Neural Reuse. *Philosophy of Science*, *86*(1), 23–46. https://doi.org/10.1086/701037

Stanley, M. L., Moussa, M. N., Paolini, B. M., Lyday, R. G., Burdette, J. H., & Laurienti, P. J. (2013). Defining nodes in complex brain networks. *Frontiers in Computational Neuroscience*, *7*, 169. https://doi.org/10.3389/fncom.2013.00169

Stanley, M. L., Simpson, S. L., Dagenbach, D., Lyday, R. G., Burdette, J. H., & Laurienti, P. J. (2015). Changes in brain network efficiency and working memory performance in aging. *PLoS ONE*, *10*(4), e0123950. https://doi.org/10.1371/journal.pone.0123950

Stawarczyk, D., Bezdek, M. A., & Zacks, J. M. (2021). Event Representations and Predictive Processing: The Role of the Midline Default Network Core. *Topics in Cognitive Science*, *13*(1), 164–186. https://doi.org/10.1111/tops.12450

Stern, Y., Albert, M., Barnes, C. A., Cabeza, R., Pascual-Leone, A., & Rapp, P. R. (2023, December). A framework for concepts of reserve and resilience in aging. *Neurobiology of Aging*. Elsevier Inc. https://doi.org/10.1016/j.neurobiolaging.2022.10.015

Teyler, T. J., & Rudy, J. W. (2007). The hippocampal indexing theory and episodic memory: Updating the index. *Hippocampus*, *17*(12), 1158–1169. https://doi.org/10.1002/hipo.20350

Thakral, P. P., Madore, K. P., & Schacter, D. L. (2017). A role for the left angular gyrus in episodic simulation and memory. *The Journal of Neuroscience*, *37*(34), 1319–17. https://doi.org/10.1523/JNEUROSCI.1319-17.2017

Thakral, P. P., Wang, T. H., & Rugg, M. D. (2019). Effects of age on across-participant variability of cortical reinstatement effects. *NeuroImage*, *191*(August 2018), 162–175.

https://doi.org/10.1016/j.neuroimage.2019.02.005

Tomasi, D., & Volkow, N. D. (2012). Aging and functional brain networks. *Molecular Psychiatry*, *17*(5), 549–558. https://doi.org/10.1038/mp.2011.81

Trelle, A. N., Henson, R. N., & Simons, J. S. (2019). Neural evidence for age-related differences in representational quality and strategic retrieval processes. *Neurobiology of Aging*, *84*, 50–60. https://doi.org/10.1016/j.neurobiolaging.2019.07.012

Turner, G. R., & Spreng, R. N. (2012). Executive functions and neurocognitive aging: dissociable patterns of brain activity. *Neurobiology of Aging*, *33*(4), 826.e1-826.e13. https://doi.org/10.1016/j.neurobiolaging.2011.06.005

Tustison, N. J., Avants, B. B., Cook, P. A., Zheng, Y., Egan, A., Yushkevich, P. A., & Gee, J. C. (2010). N4ITK: Improved N3 Bias Correction. *IEEE Transactions on Medical Imaging*, *29*(6), 1310–1320. https://doi.org/10.1109/TMI.2010.2046908

Tyler, L. K., Stamatakis, E. A., Bright, P., Acres, K., Abdallah, S., Rodd, J. M., & Moss, H. E. (2004). Processing objects at different levels of specificity. *Journal of Cognitive Neuroscience*, *16*(3), 351–362. https://doi.org/10.1162/089892904322926692

Tzourio-Mazoyer, N., Landeau, B., Papathanassiou, D., Crivello, F., Etard, O., Delcroix, N., … Joliot, M. (2002). Automated anatomical labeling of activations in SPM using a macroscopic anatomical parcellation of the MNI MRI single-subject brain. *NeuroImage*, *15*(1), 273–289. https://doi.org/10.1006/nimg.2001.0978

Umanath, S., & Marsh, E. J. (2014). Understanding How Prior Knowledge Influences Memory in Older Adults. *Perspectives on Psychological Science*, *9*(4), 408–426. https://doi.org/10.1177/1745691614535933

van den Heuvel, M. P., & Hulshoff Pol, H. E. (2010). Exploring the brain network: a review on resting-state fMRI functional connectivity. *European Neuropsychopharmacology : The Journal of the European College of Neuropsychopharmacology*, *20*(8), 519–534. https://doi.org/10.1016/j.euroneuro.2010.03.008

van Kesteren, M. T. R., Beul, S. F., Takashima, A., Henson, R. N., Ruiter, D. J., & Fernández, G. (2013). Differential roles for medial prefrontal and medial temporal cortices in schema-dependent encoding: From congruent to incongruent. *Neuropsychologia*, *51*(12), 2352–2359. https://doi.org/10.1016/j.neuropsychologia.2013.05.027

van Kesteren, M. T. R., Fernandez, G., Norris, D. G., & Hermans, E. J. (2010). Persistent schema-dependent hippocampal-neocortical connectivity during memory encoding and postencoding rest in humans. *Proceedings of the National Academy of Sciences*, *107*(16), 7550–7555. https://doi.org/10.1073/pnas.0914892107

Van Kesteren, M. T. R., Rijpkema, M., Ruiter, D. J., & Fernández, G. (2010). Retrieval of associative information congruent with prior knowledge is related to increased medial prefrontal activity and connectivity. *Journal of Neuroscience*, *30*(47), 15888–15894. https://doi.org/10.1523/JNEUROSCI.2674-10.2010

Van Kesteren, M. T. R., Ruiter, D. J., Fernández, G., & Henson, R. N. (2012). How schema and novelty augment memory formation. *Trends in Neurosciences*, *35*(4), 211–219. https://doi.org/10.1016/j.tins.2012.02.001

Verhaeghen, P. (2003). Aging and vocabulary scores: A meta-analysis. *Psychology and Aging*, *18*(2), 332–339. https://doi.org/10.1037/0882-7974.18.2.332

Voss, M. W., Erickson, K. I., Chaddock, L., Prakash, R. S., Colcombe, S. J., Morris, K. S., … Kramer, A. F. (2008). Dedifferentiation in the visual cortex: An fMRI investigation of individual differences in older adults. *Brain Research*, *1244*(0), 121–131. https://doi.org/10.1016/j.brainres.2008.09.051

Wagner, A. D., Shannon, B. J., Kahn, I., & Buckner, R. L. (2005). Parietal lobe contributions to episodic memory retrieval. *Trends in Cognitive Sciences*, *9*(9), 445–453. https://doi.org/10.1016/j.tics.2005.07.001

Wang, L., Zang, Y., He, Y., Liang, M., Zhang, X., Tian, L., … Li, K. (2006). Changes in hippocampal connectivity in the early stages of Alzheimer's disease: Evidence from resting state fMRI. *NeuroImage*, *31*(2), 496–504. https://doi.org/10.1016/j.neuroimage.2005.12.033

Wang, T. H., Johnson, J. D., de Chastelaine, M., Donley, B. E., & Rugg, M. D. (2016). The Effects of Age on the Neural Correlates of Recollection Success, Recollection-Related Cortical Reinstatement, and Post-Retrieval Monitoring. *Cerebral Cortex*, *26*(4), 1698–1714. https://doi.org/10.1093/cercor/bhu333

Wang, W. C., Brashier, N. M., Wing, E. A., Marsh, E. J., & Cabeza, R. (2018). Neural basis of goal-driven changes in knowledge activation. *European Journal of Neuroscience*, *48*(11), 3389–3396. https://doi.org/10.1111/ejn.14196

Warrington, E. K., & McCarthy, R. (1983). Category specific access dysphasia. *Brain*, *106*(4), 859–878. https://doi.org/10.1093/brain/106.4.859

Webb, C. E., Turney, I. C., & Dennis, N. A. (2016). What's the gist? The influence of schemas on the neural correlates underlying true and false memories. *Neuropsychologia*, *93*(September), 61–75. https://doi.org/10.1016/j.neuropsychologia.2016.09.023

Welvaert, M., & Rosseel, Y. (2013). On the definition of signal-to-noise ratio and contrast-to-noise ratio for fMRI data. *PLoS ONE*, *8*(11). https://doi.org/10.1371/journal.pone.0077089

Wen, H., Shi, J., Zhang, Y., Lu, K. H., Cao, J., & Liu, Z. (2018). Neural encoding and decoding with deep learning for dynamic natural vision. *Cerebral Cortex*, *28*(12), 4136–4160. https://doi.org/10.1093/cercor/bhx268

Westphal, A. J., Wang, S., & Rissman, J. (2017). Episodic Memory Retrieval Benefits from a Less Modular Brain Network Organization. *The Journal of Neuroscience : The Official Journal of the Society for Neuroscience*, *37*(13), 3523–3531. https://doi.org/10.1523/JNEUROSCI.2509-16.2017

Wing, E. A., Marsh, E. J., & Cabeza, R. (2013). Neural correlates of retrieval-based memory enhancement: An fMRI study of the testing effect. *Neuropsychologia*, *51*(12), 2360–2370. https://doi.org/10.1016/j.neuropsychologia.2013.04.004

Wing, E. A., Ritchey, M., & Cabeza, R. (2015). Reinstatement of Individual Past Events Revealed by the Similarity of Distributed Activation Patterns during Encoding and Retrieval. *Journal of Cognitive Neuroscience*, *27*(4), 679–691. https://doi.org/10.1162/jocn

Wright, M. E., & Wise, R. G. (2018). Can Blood Oxygenation Level Dependent Functional Magnetic Resonance Imaging Be Used Accurately to Compare Older and Younger Populations? A Mini Literature Review. *Frontiers in Aging Neuroscience*, *10*(November), 1–7. https://doi.org/10.3389/fnagi.2018.00371

Xia, M., Wang, J., & He, Y. (2013). BrainNet Viewer: A Network Visualization Tool for Human Brain Connectomics. *PLOS ONE*, *8*(7), e68910. Retrieved from https://doi.org/10.1371/journal.pone.0068910

Yeo, B. T. T., Krienen, F. M. F., Sepulcre, J., Sabuncu, M. R., Lashkari, D., Hollinshead, M., … Buckner, R. L. (2011). The organization of the human cerebral cortex estimated by intrinsic functional connectivity. *Journal of Neurophysiology*, *106*(3), 1125–1165. https://doi.org/10.1152/jn.00338.2011

Yuste, R. (2015). From the neuron doctrine to neural networks. *Nature Reviews*

Neuroscience, *16*(8), 487–497. https://doi.org/10.1038/nrn3962

Zacks, J. M., Speer, N. K., Swallow, K. M., Braver, T. S., & Reynolds, J. R. (2007). Event perception: A mind-brain perspective. *Psychological Bulletin*, *133*(2), 273–293. https://doi.org/10.1037/0033-2909.133.2.273

Zeiler, M. D., & Fergus, R. (2014). Visualizing and Understanding Convolutional Networks. In *Analytical Chemistry Research* (Vol. 12, pp. 818–833). https://doi.org/10.1007/978-3-319-10590-1_53

Zhang, Y., Brady, M., & Smith, S. (2001). Segmentation of brain MR images through a hidden Markov random field model and the expectation-maximization algorithm. *IEEE Transactions on Medical Imaging*, *20*(1), 45–57. https://doi.org/10.1109/42.906424

Zhao, Y., Song, L., Ding, J., Lin, N., Wang, Q., Du, X., … Han, Z. (2017). Left anterior temporal lobe and bilateral anterior cingulate cortex are semantic hub regions: Evidence from behavior-nodal degree mapping in brain-damaged patients. *Journal of Neuroscience*, *37*(1), 141–151. https://doi.org/10.1523/JNEUROSCI.1946-16.2016

Zheng, L., Gao, Z., Xiao, X., Ye, Z., Chen, C., & Xue, G. (2018). Reduced Fidelity of Neural Representation Underlies Episodic Memory Decline in Normal Aging. *Cerebral Cortex*, *28*(7), 2283–2296. https://doi.org/10.1093/cercor/bhx130

Zhou, B., Lapedriza, A., Khosla, A., Oliva, A., & Torralba, A. (2018). Places: A 10 Million Image Database for Scene Recognition. *IEEE Transactions on Pattern Analysis and Machine Intelligence*, *40*(6), 1452–1464. https://doi.org/10.1109/TPAMI.2017.2723009

Biography

Lifu Deng obtained his B.Sc. degrees in Biomedical Engineering and Mathematics in Shanghai Jiao Tong University (SJTU) in 2014. He then continued his graduate study in SJTU and was awarded the National Scholarship in 2016, and he obtained his M.Sc. degree in Biomedical Engineering in 2017. Between March and May 2017, he worked briefly as an intern R&D engineer at Philips in the company's Shanghai campus. Starting Fall 2017, Lifu was a PhD student in the Cognitive Neuroscience Admitting Program and then the Department of Psychology and Neuroscience at Duke University, where he worked under the supervision of his advisor, Dr. Roberto Cabeza, and co-advisor, Dr. Simon W. Davis. His PhD work is primarily focused on aging and episodic memory, but he also worked on several side projects involving transcranial magnetic stimulation (TMS). Lifu has published studies as first author or co-author on multiple journals, including Journal of Neuroscience, Cerebral Cortex, Neurobiology of Aging, NeuroImage, and Scientific Reports.